







EX LIBRIS  
UNIVERSITATIS  
ALBERTENSIS

---

The Bruce Peel  
Special Collections  
Library













Digitized by the Internet Archive  
in 2025 with funding from  
University of Alberta Library

<https://archive.org/details/0162014920407>



University of Alberta

Library Release Form

**Name of Author:** Trevor Carnelley

**Title of Thesis:** Synthesis of a benzo[a]pyrene diol epoxide – DNA damage standard and applications to DNA adduct analysis

**Degree:** Master of Science

**Year this Degree Granted:** 2001

Permission is hereby granted to the University of Alberta Library to reproduce single copies of this thesis and to lend or sell such copies for private, scholarly or scientific research purposes only.

The author reserves all other publication and other rights in association with the copyright in the thesis, and except as herein before provided, neither the thesis nor any substantial portion thereof may be printed or otherwise reproduced in any material form whatever without the author's prior written permission.







**University of Alberta**

Synthesis of a benzo[*a*]pyrene diol epoxide – DNA damage standard and applications to  
DNA adduct analysis

by

Trevor Carnelley



A thesis submitted to the Faculty of Graduate Studies and Research in partial fulfillment  
of the requirements for the degree of Master of Science

in

Medical Sciences – Public Health Sciences

Edmonton, Alberta

Fall 2001





**University of Alberta**

**Faculty of Graduate Studies and Research**

The undersigned certify that they have read, and recommend to the Faculty of Graduate Studies and Research for acceptance, a thesis entitled **Synthesis of a benzo[*a*]pyrene diol epoxide – DNA damage standard and applications to DNA adduct analysis** by **Trevor Carnelley** in partial fulfillment of the requirements for the degree of Master of Science in Medical Sciences – Public Health Sciences.





*To Mom, Dad, and Tracy,*

*For your love and encouragement throughout my program*





## **Abstract**

The long-term objective of this research was to develop a biomarker of exposure to benzo[*a*]pyrene, an environmental carcinogen. DNA damage induced by benzo[*a*]pyrene-diol-epoxide (BPDE) was detected using a technique combining immunorecognition, capillary electrophoresis (CE), and laser-induced fluorescence. Inconclusive results from preliminary experiments suggested that synthesis of a fluorescent DNA damage standard was necessary for improved assay development. A 90 base-pair double-stranded oligonucleotide was synthesized with a single BPDE adduct and fluorescent dye on the same strand. Experiments using this oligonucleotide provided useful information about antibody binding characteristics and optimization of sample preparation, incubation parameters, and CE conditions. Additional applications of this standard included CE instrument calibration and comparison of different BPDE-DNA antibodies. It has successfully been used as a probe for BPDE adduct analysis using competitive immunoassay approaches and for binding stoichiometry studies. The design also enables easy substitution of different DNA damage types for future research.





## **Acknowledgements**

I would like to sincerely thank my supervisor, Dr. X. Chris Le, for his guidance and support throughout my program, and for encouraging me to broaden my knowledge and skills by participating in projects beyond the normal scope of graduate training. His efforts made my graduate studies a positive experience, and were greatly appreciated. I would also like to thank Dr. Michael Weinfeld for his advice and input throughout my program, and Dr. Kenneth Froese and Dr. Monica Palcic for taking the time to participate in my thesis defense.

Several people provided valuable input and technical support during my thesis research. I would particularly like to thank Dr. Mingsheng Ma and Dr. Michael Lam for being the “go-to guys” for a seemingly endless number of questions about computers, instrumentation, and theory. Other important contributors to my research that I would like to thank include: Dr James Xing for his advice about the DNA damage assay; Dr. Qianhong Wan for our discussions on a range on topics; Jane Lee for cell incubations and DNA isolation; Sharon Barker for her help with the DNA standard synthesis and purification; Dr. Woei Tan for his support during the final stages of my research; and Dianne Sergy and Mary Tweedie for their endless help with all the “little things”.

Financial support during my degree was provided by Alberta Heritage Foundation for Medical Research, University of Alberta, Department of Public Health Sciences, Environmental Health Sciences program, and Dr. Le and was greatly appreciated.

The nature of scientific research in a university setting is that people are often in a position for only a short time. However, the bond that was shared between us enabled me to make some valuable friends. I would particularly like to thank Mike Lam, Karina Bodo, Cindy Jardine, Mingsheng Ma, Victor Pavski, Irene Wenger, Jeff Rose, Woei Tan, and Dianne Sergy for their friendship and support throughout my degree. The entire EHS program was like family, and made the past few years that much more enjoyable.

Most importantly, I would like to thank my parents for their constant love and support, and for always being there to lend a hand when they were needed. Finally, I want to thank my loving wife Tracy for her endless encouragement and patience, particularly during the final stages of my thesis preparation. She was one person I could always count on for support during hard times or to share in my successes.



## Table of Contents

<b>Chapter 1 Literature Review</b>	<b>Page</b>
1.1 Introduction.....	1
1.2 Human biomonitoring.....	2
1.3 DNA damage and human cancer risk.....	6
1.4 Benzo[a]pyrene adducts and oxidative DNA damage.....	8
1.5 Methods of detecting DNA damage.....	12
1.6 Issues associated with using DNA adducts in human biomonitoring.....	17
1.7 New techniques and implications.....	19
1.8 Objectives.....	22
1.9 References.....	23
 <b>Chapter 2 Preliminary experiments on detection of BPDE-DNA adducts using capillary electrophoresis with laser-induced fluorescence</b>	
2.1 Introduction.....	29
2.2 Materials and Methods.....	31
2.2.1 Reagents.....	31
2.2.2 Antibody preparation and characterization.....	31
2.2.3 BPDE-DNA samples.....	34
2.2.4 Capillary electrophoresis instrumentation and methods.....	35
2.3 Results.....	38
2.3.1 Measurement of protein concentration.....	38
2.3.2 Antibody purification.....	44
2.3.3 Interaction between primary and fluorescent secondary antibodies.....	49
2.3.3.1 Preliminary experiments with anti-BPDE-DNA antibody E5.....	49
2.3.3.2 Comparison of anti-BPDE DNA antibodies.....	56
2.3.4 Analysis of BPDE-modified DNA samples.....	59
2.3.4.1 Experiments using E5 antibody.....	59
2.3.4.2 Interaction between BPDE-DNA and antibodies 8E11 and 5D11...	67
2.4 Discussion and Conclusions.....	72





2.5	References.....	77
-----	-----------------	----

### **Chapter 3 Synthesis and characterization of a fluorescent BPDE-DNA damage standard**

3.1	Introduction.....	80
3.2	Materials and Methods.....	80
3.2.1	Reagents.....	80
3.2.2	Design of standard.....	81
3.2.3	Synthesis of damaged oligonucleotide.....	84
3.2.4	Purification of BPDE-oligonucleotide.....	84
3.2.5	Synthesis and purification of 90-mer oligonucleotides.....	85
3.2.6	Instrumentation for analysis of ligation products.....	87
3.2.7	Characterization of BPDE and control 90-mers.....	87
3.3	Results.....	88
3.3.1	Purification of BPDE-16-mer oligonucleotide.....	88
3.3.2	Synthesis and purification of 90-mer ligation products.....	93
3.3.3	Characterization of the 90-mer ligation products.....	94
3.3.4	Interaction between 90-mers and BPDE-DNA antibodies.....	97
3.3.4.1	Interaction of 90-mers with monoclonal antibody 8E11.....	97
3.3.4.2	Comparison of anti-BPDE-DNA antibodies.....	106
3.4	Discussion and Conclusions.....	109
3.5	References.....	121

### **Chapter 4 Conclusions and Future Research**

4.1	Discussion and Conclusions.....	124
4.2	Future Research.....	126
4.3	References.....	127



## List of Tables

Table	Page
1-1. Methods for detecting benzo[ <i>a</i> ]pyrene / PAH DNA adducts.....	14
2-1. Absorbance of buffers at 210 nm and 280 nm.....	41
2-2. Comparison of mouse IgG and BSA absorbance at 280 nm.....	42
3-1. Reactivity of antibody 8E11 with native and denatured BPDE 90-mer.....	102





## List of Figures

Figure	Page
1-1. Linearized multistage model of cancer risk assessment.....	3
1-2. Mechanism of BPDE-DNA adduct formation.....	10
1-3. Fluorescent species in mixtures of antibodies and damaged DNA.....	20
2-1. Schematic of CE-LIF instrument.....	36
2-2. Standard curve for protein determination at 280 nm.....	39
2-3. Standard curve for protein determination using BCA method.....	43
2-4. Polyacrylamide gel electrophoresis of antibody preparations.....	45
2-5. Profile of antibody elution from a Protein G column.....	47
2-6. Polyacrylamide gel electrophoresis of elution fractions from a Protein G column.....	48
2-7. Interaction between E5 antibody and fluorescent secondary antibodies.....	51
2-8. Effect of separation voltage during capillary electrophoresis.....	52
2-9. Specificity of TMR-labeled secondary antibody.....	54
2-10. Effect of E5 concentration on complex formation.....	55
2-11. Effect of pH on separation of antibody peaks.....	57
2-12. Comparison of BPDE-DNA antibodies.....	58
2-13. Analysis of BPDE-damaged mouse skin DNA.....	60
2-14. Binding of E5 and TMR-labeled secondary antibody to mouse skin DNA..	63
2-15. Analysis of different BPDE-DNA samples using E5 antibody.....	64
2-16. Comparison of BPDE-treated and control A549 DNA samples.....	66
2-17. Analysis of BPDE-treated A549 DNA digested by EcoRI.....	68
2-18. Comparison of E5 and 8E11 antibodies with A549 DNA.....	69
2-19. Interaction between 5D11 antibody and A549 DNA.....	70
2-20. Relationship between A549 DNA concentration and migration time of complex peak.....	71
3-1. Schematic representation of the DNA damage standard design.....	83
3-2. Preliminary reversed-phase HPLC characterization of products from a reaction involving ( $\pm$ )-anti-BPDE and a 16-mer oligonucleotide.....	89



3-3.	First step in the HPLC purification of BPDE-modified 16-mers from a reaction involving ( $\pm$ )- <i>anti</i> -BPDE and a 16-mer oligonucleotide.....	91
3-4.	Second step in the HPLC purification of BPDE-modified 16-mers.....	92
3-5.	Effect of heat denaturation on BPDE-modified and control 90-mers.....	95
3-6.	Interaction between antibody 8E11 and BPDE 90-mer.....	98
3-7.	Effect of incubation time and temperature on complex formation.....	100
3-8.	Effect of overnight incubation for BPDE 90-mer and 8E11 antibody.....	101
3-9.	Incubation of BPDE 90-mer ( $5 \times 10^{-9}$ M) with varying concentrations of antibody 8E11.....	104
3-10.	Incubation of 8E11 (1 $\mu$ g/ml) with varying concentrations of BPDE 90-mer.....	105
3-11.	Comparison between BPDE-DNA antibodies using the BPDE 90-mer standard.....	107
3-12.	Comparison of BPDE-DNA antibody electrophoretic mobility.....	108
3-13.	Schematic representation of the effect of incomplete 5'-phosphorylation of the BPDE 16-mer prior to the ligation step.....	112
3-14.	Denaturing urea-PAGE of gel-purified BPDE and control double-stranded 90-mer samples.....	113
3-15.	Stereochemistry of BPDE adduct formation.....	116





## List of Abbreviations

1°	primary
2°	secondary
B[a]P	benzo[a]pyrene
BCA	bicinchoninic acid
BPDE	benzo[a]pyrene-7,8-diol-9,10-epoxide
BSA	bovine serum albumin
CE	capillary electrophoresis
dG	deoxyguanosine
D.L.	detection limit
DNA	deoxyribonucleic acid
ELISA	enzyme-linked immunosorbent assay
GC	gas chromatography
HPLC	high performance liquid chromatography
IgG	immunoglobulin G
LIF	laser-induced fluorescence
MS	mass spectrometry
oligo	oligonucleotide
PAGE	polyacrylamide gel electrophoresis
PAH	polycyclic aromatic hydrocarbon
PBS	phosphate buffered saline
PCR	polymerase chain reaction
PNK	T4 polynucleotide kinase
RIA	radioimmunoassay
SDS	sodium dodecyl sulfate
SFS	synchronous fluorescence spectroscopy
TEMED	<i>N,N,N',N'</i> -tetramethylethylenediamine
TMR	tetramethylrhodamine
UV	ultraviolet



## Chapter 1: Literature Review

### 1.1 Introduction

The effect of the environment on human health has become an increasing concern in today's society. Reasons for this concern include greater public awareness of environmental issues and advances in scientific knowledge regarding detection of contaminants and their health effects. New analytical technologies have permitted identification of chemical contaminants in air, soil, water, and food samples at extremely low levels that had previously been undetectable. Furthermore, studies are constantly associating a wide range of environmental contaminants to a variety of health outcomes in humans. One example is the suggested link between the increasing incidence of cancer and carcinogens present in environmental media. However, this observed increase is more accurately attributed to longer life expectancies (cancer incidence correlates with increasing age) and lifestyle factors such as smoking and diet. Regulatory agencies therefore need to assess the degree of risk that environmental compounds represent to exposed populations in order to create appropriate regulatory guidelines.

Current methods for estimating human cancer risk from environmental sources have been established for several years. These methods are primarily based on carcinogenicity data from animal experiments and incorporate a variety of assumptions to estimate the potential effects in humans. A significant source of uncertainty in this process is extrapolation between species, from experimental animals such as rats or mice to humans. Although a comparative effect can be estimated, unique differences exist in anatomy, physiology, and metabolism. In the case of environmental contaminants, the rate of absorption of a chemical from the environment as well as its metabolic transformation in the body to a less toxic (detoxification) or more toxic (toxification) form are important factors in the biological effect of the chemical. Because these rates can vary significantly between animals and humans, the addition of an uncertainty factor in human risk calculations is necessary. An additional problem associated with quantitative risk estimates based on animal studies is the need for extrapolation from high





experimental doses down to levels encountered by humans in environmental settings. The prohibitive cost associated with animal studies requires that only a few doses of the suspected carcinogen are tested. To ensure a measurable outcome of cancer in the test subjects, these doses must be close to the maximum dose tolerated by the animals without causing acute toxic effects. The results are then extrapolated down to levels typical of human environmental exposures, often by several orders of magnitude. This extrapolation is based on the linearized multistage model, which assumes a linear extrapolation through the origin (US EPA, 1986) (Figure 1-1). This assumption has been subjected to considerable debate (Abelson, 1994), as it implies the absence of any thresholds in the complex process of cancer development.

Even when the hazard presented by a carcinogen is assessed using the above method, human exposure to the chemical must be characterized. Environmental concentrations of many contaminants are usually very low, making exposure assessment a difficult process. Inadequate exposure assessments are a common problem in epidemiological studies attempting to link environmental agents with cancer occurrence; data is often obtained indirectly in the form of personal interviews (Hulka and Wilcosky, 1988). Because of the relatively low risks associated with these exposure levels, these studies are often not sensitive enough to evaluate the nature of the association. A pertinent example is the proposed causal link between environmental tobacco smoke and lung cancer, where the uncertainty associated with confounding and bias in exposure assessments of nonsmokers usually outweighs the consistently small increased risk. When environmental monitoring data is available it is only able to estimate the external dose, and numerous assumptions must be made to determine individual exposure, including duration of exposure and rates of absorption, metabolism (toxification or detoxification), and excretion of the compound.

## **1.2 Human biomonitoring**

In an attempt to address some of these problems, considerable research has been undertaken to develop methods of human biomonitoring. Biomarkers have been defined



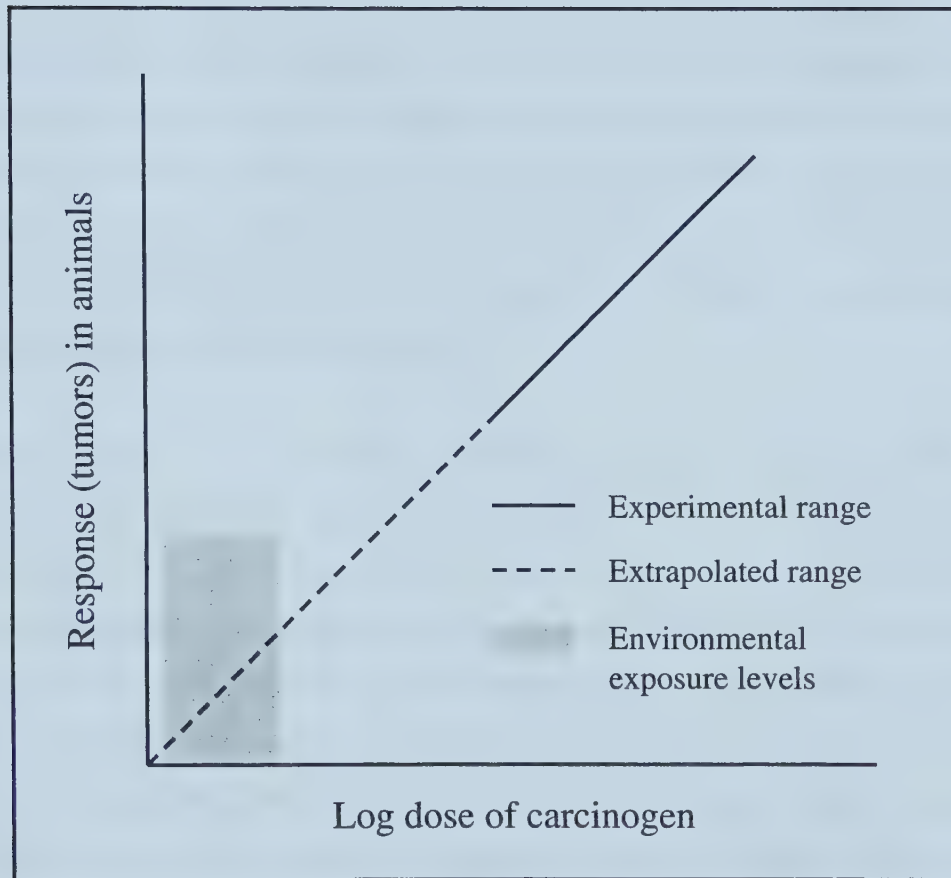


**Figure 1-1. Linearized multistage model of cancer risk assessment.** Schematic representation of extrapolation of high dose animal carcinogenicity studies to low doses typical of human environmental exposures.





as measures of a contaminant in the body. Valid techniques would contribute to a more accurate estimate of human cancer risk. Three general classes of biomarkers have been described: exposure, effect, and susceptibility.

Biomarkers of exposure are measures of a toxic substance or its metabolites in breath, blood, urine, or other body fluids or tissues (internal dose), or of products of the chemical's interaction with target macromolecules in the body (biologically effective dose). Biomarkers of exposure integrate cumulative uptake of a contaminant through all exposure routes. Some examples of biomarkers of exposure are blood lead levels and concentrations of different arsenic compounds in the urine. While contaminants such as heavy metals and dioxins reside in the body for extended periods of time, others such as arsenic are excreted more quickly. This residence time influences the conclusions that may be reached when using these biomarkers.

Biomarkers of effect are pre-clinical alterations in organs, tissue structure, cells, macromolecules or functional capacity that are directly associated with an adverse health outcome. These abnormal characteristics are caused by interaction with the environmental contaminant being monitored. There is a progression from exposure to effect in the body, with markers of effect being closer to the presentation of disease. Examples of biomarkers of effect relevant to cancer include cytogenetic abnormalities, chromosomal aberrations, and enhanced expression of oncogene products in affected cells. While the association between a contaminant, biological effect, and adverse health outcome may be evident, effect markers are not usually unique to a specific agent or exposure situation.

Biomarkers of susceptibility are indicators of an individual or population's inherent or acquired limitations that affect its response to the toxic effects of a chemical. Varying degrees of sensitivity may result from differences in absorption, metabolism, age, sex, genetic makeup, lifestyle (physical activity and diet), health status, physiological state (e.g. pregnancy), and prior chemical exposures. Markers of susceptibility may exist between any of the stages on the exposure-disease continuum: exposure; internal dose;



biologically effective dose; early biological effect; altered structure or function; adverse health outcome. There is usually overlap between these three classes of biomarkers, with a given technique providing information on, for example, both exposure and susceptibility of humans to a toxic agent.

The use of biomarkers combined with ambient environmental monitoring, animal data and epidemiological studies has important potential implications for human cancer risk assessment. However, existing techniques suffer from a variety of limitations (Ward Jr. and Henderson, 1996). Several methods are useful for monitoring higher exposures typical of occupational settings, but are not sensitive enough for routine use at lower environmental doses. Lack of specificity for a given agent or route of exposure also limits the applicability of some techniques. As mentioned above this is usually the case for biomarkers of effect, since they measure an altered state in the body that may result from a variety of causes. Markers of exposure and susceptibility may also suffer from confounding by other factors. For example, urinary phenol levels are sometimes measured to assess exposure to benzene, but phenol may also be the metabolic end-product for other compounds. The amount of biological material available for analysis may be limited, therefore a technique capable of detecting the contaminant of interest in small samples is more desirable. Many current methods require relatively large amounts of blood or other tissues in order to detect the desired chemical. Complexity of the analytical process may be a problem if specialized equipment or analysts are required for routine use. The time required per sample is another factor which is important from a practical viewpoint; if biomarkers are to be used in monitoring exposure of the general population to environmental carcinogens, the techniques must be able to process large numbers of samples quickly. Associated with this concept of practical ease is the suitability of the method for automation; this would increase efficiency while reducing the chance of human error in the analysis. Finally, the cost of equipment needed for analysis as well as the cost per sample are important considerations. To adequately characterize exposure in a population, more than one method would likely be necessary. Several methods currently being developed would be unsuitable because of cost





restrictions. These limitations will be discussed further by considering methods of detecting DNA adducts in human cells.

### **1.3 DNA damage and human cancer risk**

Measurement of DNA damage induced by exposure to environmental agents has been an active area of research since the early 1980's. Methods that detect DNA adducts or other forms of damage in human samples possess characteristics of all three biomarker classes identified above. Adducts are bulky structures resulting from a chemical reaction between a mutagenic compound and the phosphate backbone structure of DNA or one of the four bases that make up the DNA sequence: adenine (A), guanine (G), cytosine (C), or thymine (T). DNA adducts are markers of biologically effective dose, since they are products resulting from the interaction of a contaminant with cellular DNA. DNA adducts, particularly in blood lymphocytes, measure cumulative uptake of carcinogens from different sources through all exposure routes. This effect has been observed by the lack of correlation between ambient air pollution levels and DNA adducts in exposed individuals, indicating that other sources such as diet are also significant (Hemminki et al., 1990). Since DNA damage is thought to be the initial step in cancer development, it is also a marker of early biological effect. This will be discussed further below. Furthermore, because adduct formation is dependent on a variety of factors including rate of absorption, metabolism, excretion, and DNA repair capacity, individuals will exhibit different adduct levels for a given exposure. This is particularly important for chemicals that must undergo metabolic conversion into a more toxic form capable of reacting with DNA. Therefore, DNA adducts may be used to determine interindividual susceptibility to the effects of environmental carcinogens.

The importance of DNA adduct determination to human cancer risk is due to the currently accepted paradigm of tumor development. This states that DNA must first be damaged by some causative factor, such as UV damage or interaction with reactive endogenous or environmental compounds (Friedberg et al., 1995). This DNA damage can take the form of bulky adduct structures, DNA strand breaks, cross-links, and other



conformational changes. The human body constantly repairs damaged DNA through a variety of mechanisms including routine surveillance and base pair correction during DNA replication and cell division. This repair network is extremely efficient; nevertheless, mistakes are made due to the constant barrage of damaging events. These errors may involve substitution of an incorrect base in the DNA sequence (missense or nonsense mutations) or deletion of a base pair or section of the DNA. In human cells, genes are transcribed and then translated by a series of biochemical mechanisms into their corresponding protein products. Because each amino acid in a protein is encoded by a codon of three bases, a deletion mutation results in a shift of the translational "reading frame", causing incorrect or incomplete protein structure. If these genetic mutations occur in a replicating cell, they may be preserved in subsequent daughter generations. These cells may undergo further changes that cause a failure of the body's mechanism for suppressing abnormal cell growth, resulting in the progression of a malignant tumor. These stages will not be discussed in detail, but include: bypassing programmed cell death in response to DNA damage, becoming independent of cellular growth factors, escape from immunological mechanisms for detecting cancerous cells, acquisition of a blood supply, invasion of surrounding tissues, and ultimately entering the circulation and spreading throughout the body (metastasis) (Alberts et al., 1994).

Mutation induced by DNA adducts and other damage is not always sufficient for initiation of this series of events, depending on the location of the mutations within the DNA. DNA structure is highly redundant, and genes comprise only a small portion of the total sequence. Because of this, mutations occurring in the extraneous DNA (introns) are not likely to have any effect on the cell. Even when a mutation occurs within a gene it may be a "silent mutation"; the resulting codon sequence may incorporate the same amino acid into the protein, another example of protective redundancy in the cell. Furthermore, only certain genes that may become mutated have been linked to the development of cancer. These critical genes include oncogenes and tumor suppressor genes. Oncogenes are mutated forms of genes normally expressed in the cell, which encode a variety of cellular proteins involved in cell growth and replication. These include transcription factors involved in regulation of gene expression (myc, fos, jun),



growth factors (PDGF, EGF), growth factor receptors, GTP-binding proteins (ras), and protein kinases (src) (Alberts et al., 1994). Mutation of these genes may result in unregulated expression of their proteins, increased activity of the proteins, or loss of control of the proteins by other mechanisms. All of these potential effects may result in uncontrolled cell growth and replication. Tumor suppressors are related to cell growth in an inhibitory manner. The most characterized tumor suppressor gene is p53, which is involved in the mechanism of programmed cell death, or apoptosis, in response to DNA damage. Mutations in p53 have been found in some cancer subjects, for example in lung tissue from smokers with lung cancer (Denissenko et al., 1996). The mutated form of p53 is unable to control cells that have been transformed, allowing them to proliferate and advance toward later stages of tumor development. Human cells have two copies of DNA, one from each parent. Mutations often are necessary in both copies of p53 to exhibit an effect. Despite these numerous protective measures against DNA damage caused by environmental agents, the use of DNA adducts as markers of human cancer risk is well supported by this theory of tumor development. The presence of elevated levels of adducts may precede initiation of mutation events. Consequently, they may be used as a biomarker of early effect to identify highly exposed or susceptible individuals or populations.

#### **1.4 Benzo[a]pyrene adducts and oxidative DNA damage**

Numerous methods for detection of DNA adducts have been developed over the past two decades. Chemical and radiation exposures of clinical, occupational, and more recently environmental importance have been studied. DNA damaging agents include UV light (Friedberg et al., 1995), aflatoxins (Wang and Groopman, 1999), nitrosamines (Hecht, 1998), polycyclic aromatic hydrocarbons (Szeliga and Dipple, 1998), aromatic and heterocyclic amines (Eisenbrand and Tang, 1993), anticancer drugs such as cisplatin (Poirier and Weston, 1996), as well as radiation (Weinfeld and Soderlind, 1991) and free radicals (Moller and Wallin, 1998) that induce a range of oxidative damage. A variety of analytical chemistry and molecular biology techniques have been assessed for their utility in detecting DNA adducts and their potential relevance in biomonitoring. Some of these





methods will be reviewed by considering the disadvantages of biomarkers listed above, using benzo[*a*]pyrene DNA adducts and oxidative DNA damage as examples.

Benzo[*a*]pyrene is a polycyclic aromatic hydrocarbon (PAH) commonly found at low levels in the environment. PAHs are byproducts of combustion and usually occur as mixtures including benzo[*a*]pyrene. Major sources of human exposure include cigarette smoke, vehicle exhaust, fossil fuel or wood combustion, organic mixtures such as coal tar and creosote, and consumption of smoked or charbroiled meat and fish. It is a concern in human cancer risk because of its ubiquitous presence in the environment combined with its high mutagenic potential. Many occupational studies have shown increased cancer risk for workers exposed to benzo[*a*]pyrene in industrial settings such as coke oven emissions in steel and aluminum plants. Extensive research has been conducted in animals and humans in an attempt to assess the magnitude of risk benzo[*a*]pyrene presents to the general population (ATSDR, 1990; Butler et al., 1993). Several biomarker methods for assessing exposure to benzo[*a*]pyrene and other PAHs have been developed, including protein adducts (Hemminki et al., 1995), 1-hydroxypyrene (Jongeneelen, 1997) and other metabolites (Strickland et al., 1996) in the urine, and DNA adducts. Of these, DNA adducts are the most direct indicator of cancer risk.

The mechanism of benzo[*a*]pyrene and other PAHs in formation of DNA adducts has been well characterized. A recent review summarized the chemistry of PAH-DNA adduct formation (Szeliga and Dipple, 1998). After absorption into the body, benzo[*a*]pyrene must first be metabolized to a more reactive form. This occurs via the mixed function oxidase (MFO) pathways, including the enzymes cytochrome P450 and epoxide hydrolase. Although several forms of benzo[*a*]pyrene have been shown to react with more than one DNA base, the most important species is the diol-epoxide, benzo[*a*]pyrene-7,8-diol-9,10-epoxide (BPDE) (Figure 1-2). BPDE may exist in different stereochemical configurations, but the most important isomer, (+)-*anti*-BPDE, is shown in Figure 1-2. The diol-epoxide structure is a common theme for the most mutagenic PAH compounds. BPDE intercalates into the DNA helix structure and the reactive epoxide binds primarily to the N<sup>2</sup> position of guanine bases. This reaction forms a bulky



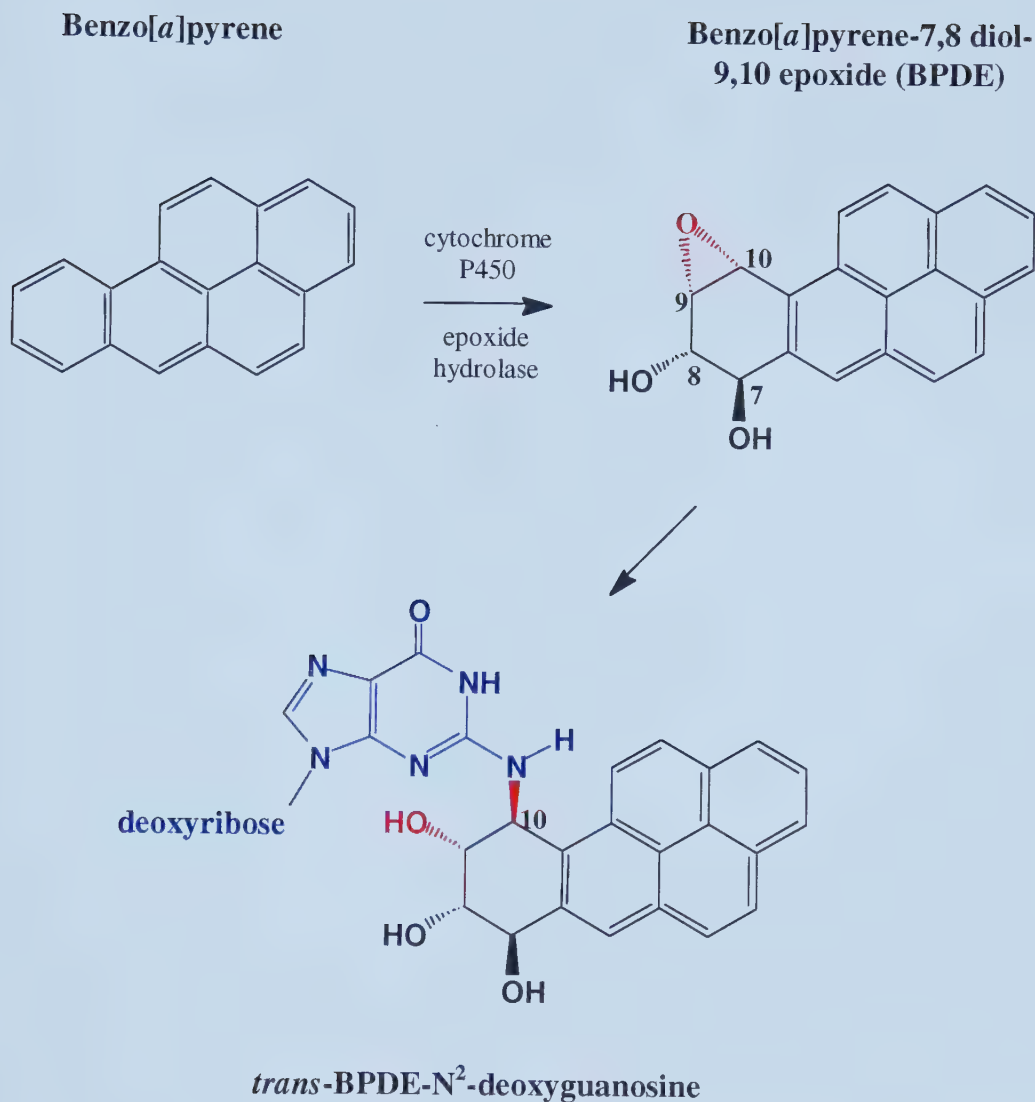


**Figure 1-2. Mechanism of BPDE-DNA adduct formation.** Benzo[*a*]pyrene is metabolically activated by cytochrome P450 and epoxide hydrolase to its mutagenic form, benzo[*a*]pyrene-7,8 diol 9,10 epoxide (BPDE). The reactive epoxide moiety (shown in red) binds to the N<sup>2</sup> position of guanine bases in DNA (shown in blue), resulting in predominantly *trans*-BPDE-N<sup>2</sup>-deoxyguanosine adducts (BPDE-N<sup>2</sup>-dG).





adduct structure (BPDE-N<sup>2</sup>-dG) within the double helix, breaking the hydrogen bonding between guanine and cytosine and distorting the overall structure of DNA in the adducted region. This distortion of the helix can disrupt biological processes including DNA repair, DNA replication, and transcription (Hess et al., 1997; Choi et al., 1994; Thrall et al., 1992) which may result in mutations. Increased levels of benzo[a]pyrene adducts have been found in cancer patients, including in exfoliated or surgically removed cells from smokers with lung cancer (Weston and Bowman, 1991; van Schooten et al., 1990). A recent study has determined preferential BPDE-DNA adduct formation in the p53 gene of smokers (Denissenko et al., 1996), supporting the proposed association between adducts and cancer through mutation of tumor suppressors. For these reasons, BPDE-DNA adducts could potentially be an important indicator of cancer risk for human populations.

Oxidative DNA damage is another modification that has received considerable attention. Oxidation may result from a variety of agents including radiation and reactive oxygen species, and has been implicated in the aging process and cancer risk. Oxidative damage may occur from environmental exposures or via endogenous reactions in human cells. Because oxidation damage from exposure to sunlight has been associated with the increase in skin cancer over the past few years, methods of detecting elevated DNA damage levels might be useful as a possible preventive measure. The mechanisms of UV and other forms of radiation in damaging DNA have been well studied. UV light induces various oxidation products of thymine residues as well as photochemical reactions between adjacent thymine bases in DNA, resulting in thymine dimer products. These adducts and other bulky structures such as BPDE-DNA adducts are usually repaired by the nucleotide excision repair pathway. This pathway has been extensively studied in *E. coli* bacteria. Distortion in the DNA helix caused by a large adduct is recognized by the uvrABC protein complex, which removes the adduct by cleaving the DNA backbone. DNA polymerase then regenerates the DNA sequence, and DNA ligase rejoins the backbone structure. A more complex nucleotide excision repair mechanism exists in human cells, involving several different proteins and enzymes (Friedberg et al., 1995). Despite these processes, damaged sections of DNA may be incorrectly repaired resulting in mutation. Another important oxidation product is thymine glycol, a hydroxylated form



of thymine which can be induced by UV light and clinical radiation doses (Le et al., 1998; Weinfeld and Soderlind, 1991). Thymine glycols may also be induced by any chemical or process that generates free radicals. In fact, it has been shown that benzo[*a*]pyrene is capable of producing thymine glycol bases in human cells exposed *in vitro* (Leadon, 1987). Other types of DNA damage induced by radiation include single-strand breaks, DNA-protein cross-links, and inter- and intrastrand DNA cross-links. All of these structural modifications are indicators of oxidative stress and may be useful for assessing overall exposures of humans to a range of environmental contaminants.

### 1.5 Methods of detecting DNA damage

Many of the same methods have been used to detect different types of DNA damage including oxidation products such as thymine glycols and BPDE-DNA adducts. These techniques use a combination of analytical chemistry, immunology and molecular biology. Immunological methods used to measure BPDE-DNA adducts include radioimmunoassays (RIA) (Harris et al., 1985; Haugen et al., 1986; Poirier et al., 1980), enzyme-linked immunosorbent assays (ELISA) (Dickey et al., 1997; Hemminki et al., 1990; Kang et al., 1995; Perera et al., 1992; Perera et al., 1988; Perera et al., 1982; Rothman et al., 1990; Santella et al., 1995; van Schooten et al., 1990), and immunohistochemical approaches (Santella, 1999). The most common molecular biology techniques include  $^{32}\text{P}$ -postlabeling assays (Baan et al., 1997; Hemminki et al., 1990; Kato et al., 1995; Perera et al., 1992; van Schooten et al., 1990; Godschalk et al., 1997), single cell gel electrophoresis (Comet) assays (Sauvaigo et al., 1998; Hanelt et al., 1997), and PCR-based approaches (Pfeifer et al., 1998; Denissenko et al., 1996). Typical analytical chemistry methods used for BPDE adducts are synchronous fluorescence spectroscopy (SFS) (Harris et al., 1985; Haugen et al., 1986), gas chromatography-mass spectrometry (GC-MS, Melikian et al., 1999) immunoaffinity chromatography-HPLC-SFS (Weston and Bowman, 1991), and HPLC combined with fluorescence detection (Pavanello et al., 1999; Godschalk et al., 1997) or  $^{32}\text{P}$ -postlabeling (Zeisig and Moller, 1995). HPLC, CE and CEC (capillary electrochromatography) coupled with electrospray-MS have also been reported for analysis of BPDE- or PAH-DNA adducts (Andrews et



al., 1999; Ding and Vouros, 1997; Barry et al., 1996). Characteristics of some of these methods are summarized in Table 1-1. Each of these techniques has advantages and disadvantages, which will be reviewed below.

Immunoassays are one of the most common methods used to detect BPDE-DNA adducts (Santella, 1999). However, these assays have three main limitations. First, they are typically not sensitive enough for reliable detection of adducts in humans exposed to environmental levels of carcinogens, with a detection limit of 2-3 adducts in  $10^8$  normal nucleotides for ELISA and higher for RIA (Table 1-1). One reason for these relatively poor detection limits is the amount of background signal created during the procedure due to non-specific binding of antibodies on the assay media. These techniques also require large amounts of DNA, usually 50  $\mu\text{g}$  / well or 100-200  $\mu\text{g}$  in total per sample for replicate analysis. This can be inconvenient when analyzing blood lymphocytes in humans, as it requires collection of between 30 and 40 ml of blood per individual (Santella et al., 1995). Immunoassays may also lack specificity because of antibody cross-reactivity with other adduct structures or, to a lesser extent, undamaged DNA (Booth et al., 1994; Poirier, 1997; Santella et al., 1988). Monoclonal antibodies can be used to detect individual adduct structures such as BPDE-guanine, and are generally very specific for one type of damage. Nevertheless, some cross-reactivity with other PAH-DNA adducts may be observed (Booth et al., 1994). Polyclonal antibodies are designed to detect a range of related adduct structures, such as several related PAH adducts. This may be beneficial for assessing overall exposure since PAHs are usually present as mixtures in the environment. An additional advantage of immunoassays is the ability to use intact DNA samples. The lack of an enzymatic digestion step decreases the time of analysis and the possibility of artifacts in the assay.

$^{32}\text{P}$ -postlabeling methods have also been used extensively in the literature for detecting DNA damage. They have a better detection limit than immunoassays, generally between 1-2 adducts in  $10^9$  nucleotides (Table 1-1), or about  $10^{-15}$  moles of adducts. An additional advantage is the requirement of only 2-10  $\mu\text{g}$  of DNA (Table 1-1, Poirier and Weston, 1996) for analysis. However, it is difficult to identify specific adducts with this method





**Table 1-1.** Methods for detecting benzo[a]pyrene/PAH DNA adducts.

Method of Detection and Reference	DNA Source (human unless noted)	Amount of DNA ( $\mu$ g) Required	Detection Limit (adducts/normal bases)	Range of Adduct Levels Detected (per normal bases)
<sup>32</sup> P-postlabeling				
Baan et al. 1997	lymphocytes	-	1 / 10 <sup>9</sup>	10 - 90 / 10 <sup>8</sup> (DRZ)
Hemminki et al. 1990	lymphocytes	-	-	4.4 - 24.5 / 10 <sup>8</sup> (mean values for groups)
Kato et al. 1995	lung tissue	-	-	-
Perera et al. 1992	lymphocytes	-	-	0.3 - 18 / 10 <sup>8</sup> (DRZ)
van Schooten et al. 1990	lung tissue	-	2 / 10 <sup>9</sup>	0.2 - 8.0 / 10 <sup>8</sup> (BPDE)
				1.9 - 34 / 10 <sup>8</sup> (DRZ)
Godschalk et al. 1997	rat tissues	10	1 / 10 <sup>9</sup>	0.5 - 30 / 10 <sup>8</sup> (BPDE)
Radioimmunoassay (RIA)				
Harris et al. 1985	lymphocytes	10	2 / 10 <sup>8</sup>	13 - 1100 / 10 <sup>8</sup>
Haugen et al. 1986	lymphocytes	-	3 / 10 <sup>8</sup>	3 - 450 / 10 <sup>8</sup>
Poirier et al. 1980	CT-DNA	2-20	1 / 10 <sup>5</sup>	-
Enzyme-linked immunosorbent assay (ELISA)				
Dickey et al. 1997	lymphocytes		2 / 10 <sup>8</sup>	*1 - 26 / 10 <sup>8</sup>
Hemminki et al. 1990	lymphocytes	-	-	2.3 - 15.3 / 10 <sup>8</sup> (mean values for groups)
Kang et al. 1995	lymphocytes	-	1.3 / 10 <sup>8</sup>	*0.7 - 17 / 10 <sup>8</sup>
Perera et al. 1992	lymphocytes	-	2 / 10 <sup>8</sup>	*1 - 73 / 10 <sup>8</sup>
Perera et al. 1988	lymphocytes	50 / well	2 / 10 <sup>8</sup>	*1 - 90 / 10 <sup>8</sup>
Perera et al. 1982	lung tissue, lymphocytes	50 / well	3 / 10 <sup>8</sup>	*1.5 - 6.0 / 10 <sup>8</sup>
Rothman et al. 1990	lymphocytes	-	1.3 / 10 <sup>8</sup>	*0.7 - 16 / 10 <sup>8</sup>
Santella et al. 1995	lymphocytes	50 / well	2 / 10 <sup>8</sup>	*1 - 26 / 10 <sup>8</sup>
van Schooten et al. 1990	lung tissue	-	3 / 10 <sup>8</sup>	*2 - 134 / 10 <sup>8</sup>
Synchronous fluorescence spectroscopy (SFS)				
Harris et al. 1985	lymphocytes	-	-	-
Haugen et al. 1986	lymphocytes	100	1.3 / 10 <sup>7</sup>	13 - 72 / 10 <sup>8</sup>
IAC-HPLC-SFS				
Weston and Bowman 1991	lung tissue	-	1 / 10 <sup>8</sup>	1 - 40 / 10 <sup>8</sup>
<sup>32</sup> P-postlabeling-HPLC				
Zeisig and Moller 1995	CT-DNA	10	5 / 10 <sup>9</sup>	-
HPLC-fluorescence detection				
Godschalk et al. 1997	rat tissues	60-100	0.5 - 7.4 / 10 <sup>8</sup>	0.5 - 8.0 / 10 <sup>8</sup>
Pavanello et al. 1999	lymphocytes	100	2 / 10 <sup>8</sup>	ND - 48.2 / 10 <sup>8</sup>

\* Samples that were below the detection limit were assigned a value of one-half the D.L.

ND – non-detectable

DRZ – diagonal radioactive zone, a region containing PAH-DNA adducts

BPDE – specific analysis for BPDE-DNA adducts

CT-DNA – calf thymus DNA



(Poirier, 1997). Several possibilities exist for introduction of "phantom" spots or false positives in the autoradiography process (Beach and Gupta, 1992). The procedure is also complex, requiring skilled personnel to achieve reproducible results. Because of this, interlaboratory comparisons of the  $^{32}\text{P}$ -postlabeling technique have generated inconsistent results (Baan et al., 1997; Hemminki et al., 1990). In addition to this difficulty with reproducibility is the amount of time required for sample analysis. The procedure involves several steps (Beach and Gupta, 1992) (times are approximate):

- complete enzymatic digestion of DNA (5 hours);
- adduct enrichment by butanol extraction (1 hour) and nuclease P1 (1 hour) methods;
- labeling of enriched adducted nucleotides and total nucleotides with  $^{32}\text{P}$ -ATP (1 hour);
- adduct separation by thin-layer chromatography in 5 stages (>20 hours);
- detection of adducts by autoradiography (>15 hours for 1 adduct /  $10^8$ - $10^9$ );
- quantitation in a scintillation counter (10 minutes per sample).

Although several samples may be processed simultaneously through to the autoradiography step, the total time required for the procedure would likely be a major disadvantage for routine use in biomonitoring of large populations. A further problem with the method is the use of large amounts of radioactivity, which is cost prohibitive as well as a potential safety hazard.

Other techniques based on molecular biology have been developed in recent years. The single cell gel electrophoresis (or comet) assay measures damaged DNA in individual cells (Hanelt et al., 1997). Cell samples are embedded in agarose gel on a slide, lysed and subjected to electrophoresis. Damaged DNA migrates more quickly than intact DNA, resulting in a comet-shaped tail. This assay may be used to detect strand breaks or alkali-labile lesions by using an alkaline buffer, but cannot usually detect specific types of damage or identify the damaging agents. Some groups have attempted to combine the comet assay with immunological detection of specific damage types (Sauvaigo et al., 1998). Methods based on the polymerase chain reaction (PCR) have been used to study adduct distributions within gene sequences such as p53 (Denissenko et al., 1996). These



techniques use specific enzymes involved in DNA repair or chemicals to create DNA strand breaks at damaged sites. The DNA fragments are then analyzed using a form of PCR to generate "maps" of adduct locations in the gene of interest (Pfeifer et al., 1998). Both of these approaches may provide useful information about human exposures to environmental carcinogens. One disadvantage of these techniques is that they are still relatively new and have not been fully validated. However, they may provide useful information about human exposures to carcinogens and potential risk when used in combination with more established methods.

Analytical techniques such as SFS, GC-MS or HPLC with different detection methods have also been used to quantify DNA adducts. Sensitivity of these methods is usually comparable with immunoassays (1 adduct /  $10^8$  nucleotides), with the exception of SFS (Table 1-1). One major advantage of GC-MS is the ability to chemically characterize a range of adducted nucleotides in a DNA sample. However, this method requires chemical derivatization of the DNA samples to achieve sufficient volatility for GC analysis, a procedure which may alter adduct levels and introduce artifactual results. HPLC does not require derivatization, but does need a hydrolysis step in order to separate adducted DNA from normal DNA, and generally requires more than 30  $\mu\text{g}$  of DNA per analysis (Godschalk et al., 1997; Cadet and Weinfeld, 1993). The requirement of 100  $\mu\text{g}$  or more of DNA and a relatively poor detection limit are also problems associated with synchronous fluorescence spectroscopy (Table 1-1). An additional drawback of these analytical techniques is the cost of the equipment used, particularly high quality mass spectrometers.

Many of the above methods have also been applied to the detection of oxidative DNA damage, and have been summarized previously (Cadet and Weinfeld, 1993; Melamede et al., 1996). These include RIA, ELISA, GC-MS (Dizdaroglu, 1993; Naritsin and Markey, 1996), and  $^{32}\text{P}$ -postlabeling. The difficulties associated with these methods for BPDE-DNA adducts are similar for detection of thymine glycol and other oxidative damage. Some additional problems have also been observed in oxidative damage studies. For techniques such as GC-MS and  $^{32}\text{P}$ -postlabeling, significant levels of artifacts may be





formed by oxidation of DNA residues during the hydrolysis and derivatization steps (Cadet et al., 1997), which may invalidate measurements. Furthermore, cross-reactivity can be a major problem in immunoassays, because damage such as thymine glycol is very similar in structure to normal thymine residues. This cross-reactivity significantly increases background in the assay (Melamed et al., 1996). Other techniques used to detect oxidative damage are HPLC combined with electrochemical, fluorescence, or MS detection, and HPLC with  $^{32}\text{P}$  or fluorescence postlabeling. Generally speaking, these techniques have the same limitations as HPLC methods described above.

A common problem in the studies cited in this paper is the lack of sensitivity for analysis of human samples. For all methods, excluding  $^{32}\text{P}$ -postlabeling, the adduct levels in people exposed to low levels of environmental benzo[*a*]pyrene were at or near the detection limit of the assay. For many of the references, more than half of the values were reported as "not detected". Most studies using the ELISA technique (shown in Table 1-1) estimated adduct levels for those subjects below the D.L. by assigning a value of one-half the D.L. Considering the possible range of adduct levels below the limit of detection, this estimation is questionable at best, and may greatly underestimate interindividual variation in adduct levels. Even for  $^{32}\text{P}$ -postlabeling, if quantitation of individual adducts like BPDE-guanine is achieved, non-detectable levels may result (van Schooten et al., 1990). This lack of sensitivity combined with the other limitations discussed above suggest that improvements would be necessary for monitoring DNA damage levels in human populations.

## **1.6 Issues associated with using DNA adducts in human biomonitoring**

As shown in Table 1-1, studies assessing human DNA adduct levels have generally used either blood lymphocytes or lung tissue obtained from hospitalized lung cancer patients or at autopsy. In addition, determination of adducts in pancreas (Wang et al., 1998), exfoliated urothelial cells (Talaska et al., 1996), and other tissues have been described. It is obvious that measurements performed on internal tissues such as lung are beneficial in determining the association of DNA adducts with cancer risk, but would not be



applicable in routine biomonitoring of the population. Consequently, DNA from lymphocytes is most commonly analyzed. However, the use of lymphocytes to estimate human cancer risk raises some issues. First, the strength of the relationship between adduct levels in blood cells and lung tissue, a common site of cancer risk for exposure to carcinogens like benzo[*a*]pyrene, must be proven. Second, the importance of the short half-life of blood cells in relation to rates of adduct removal by DNA repair mechanisms and how can this be extrapolated to the target tissue remains unclear. Further studies combining DNA adduct measurements with epidemiological results may validate the use of surrogate tissues such as lymphocytes as biomarkers of cancer risk.

Although most studies on DNA adduct levels in response to PAH exposure have been in occupational settings, some have assessed exposure to environmental PAHs. Sources of exposure examined include environmental tobacco smoke (Perera et al., 1982), ambient air pollution (Hemminki et al., 1990; Perera et al., 1992), charbroiled beef consumption (Kang et al., 1995; Rothman et al., 1990), and total exposure (Dickey et al., 1997), as well as clinical application of coal tar in psoriasis patients (Santella et al., 1995). These studies have recorded significant variation in adduct levels among participants, which may be a result of lack of reproducibility in the method, measurement of adducts near the detection limit, or true interindividual variability in adduct levels. Dickey et al. (1997) attempted to determine true variability among individuals, by averaging DNA adduct measurements taken over a period of several weeks. They found a 24-fold variation in DNA damage, although several samples were below the detection limit and were assigned values as described previously (one-half the detection limit). Therefore, the true variability was likely underestimated. New methods with better detection limits would more accurately assess this variability and provide valuable information on individual risk.

The application of DNA adduct methods to routine biomonitoring requires additional research. Concepts that must be addressed include intra- and interlaboratory comparisons to determine reproducibility and validity, elucidation of the relationship between DNA adducts and cancer risk, and improvements in the methodologies. These include





improved sensitivity and specificity, more efficient use of biological material, faster, less complex procedures, and reduced cost of analysis. Validated methods may potentially be used in conjunction with epidemiological study designs to improve exposure assessments. An appealing prospect for DNA adducts in epidemiology is their potential use as markers of early biological effect in prospective cohort studies. Instead of having to wait for a latency period of several years to record the number of deaths from cancer, adduct levels could be used to predict incidence rates (Hattis, 1996).

### **1.7 New techniques and implications**

In an attempt to improve on the problems of current techniques described above, our research group has developed a new method for detection of DNA adducts caused by environmental sources, including radiation and chemicals such as benzo[*a*]pyrene. Damaged DNA is mixed with a primary (1°) monoclonal antibody specific for the DNA lesion and an excess of secondary (2°) antibody that is labeled with a fluorescent dye, typically fluorescein or tetramethylrhodamine (TMR). The resulting mixture contains three different species (Figure 1-3), all of which are fluorescent. These species are separated using free-zone capillary electrophoresis and the DNA-antibody complex is quantified by measuring fluorescence induced by the dye-specific laser. The technique has been used to detect thymine glycol induced by clinically relevant levels of radiation (Le et al., 1998). The technique was found to have a detection limit of  $3 \times 10^{-21}$  moles of thymine glycol, which is  $10^4$ - $10^5$  times more sensitive than the best available technologies. Other advantages of the technique are the speed of analysis, the lack of any enzyme digestion or chemical derivatization steps, low cost per sample analyzed, and the requirement of only nanogram amounts of DNA. The technique also has the potential for automation, an important factor in processing large numbers of samples.

The improved sensitivity of this method has numerous potential implications in human cancer assessment. Le et al. (1998) were able to demonstrate a dose-response relationship between amount of radiation exposure and thymine glycol formation; this is an important component of quantitative risk assessment. As well, they were able to detect repair of the





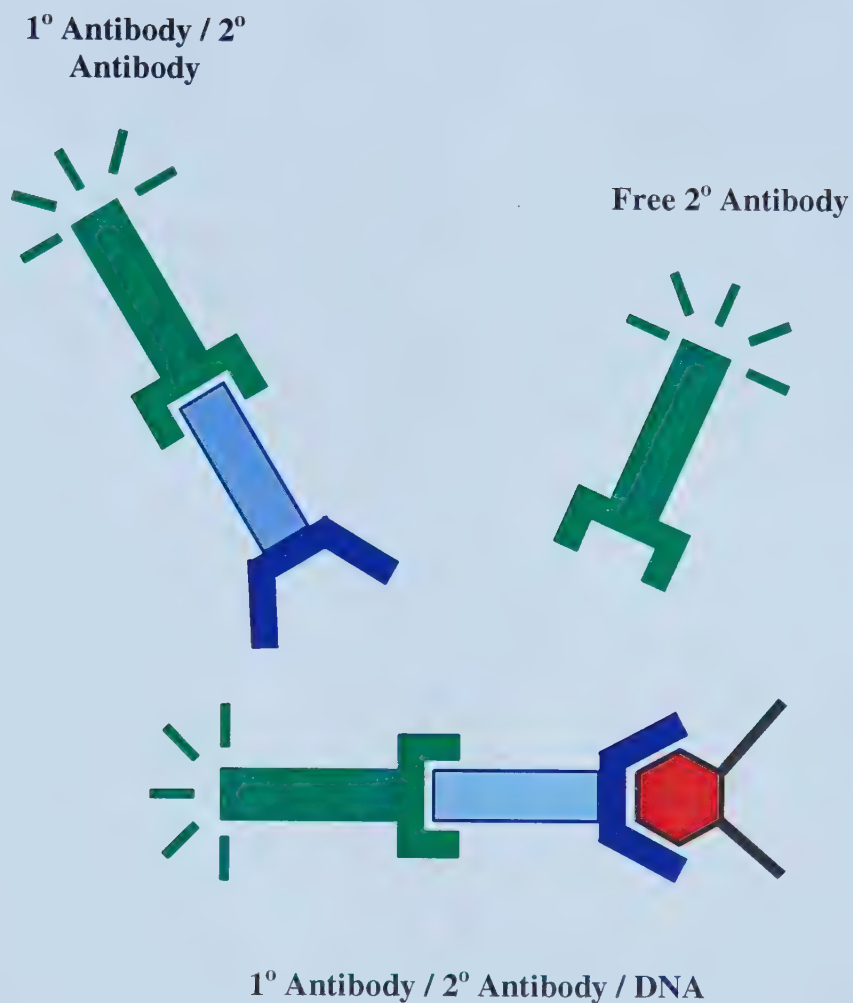


**Figure 1-3. Fluorescent species in mixtures of antibodies and damaged DNA.** The fluorescent secondary (2°) antibody is added in excess of the primary (1°) antibody and damaged DNA, resulting in three fluorescent species in solution. These species are separated by capillary electrophoresis and the DNA/antibody complex is detected by laser-induced fluorescence.



damaged DNA. Because DNA repair is an important mechanism in defense against cancer development, the ability to detect its activity at clinically and environmentally relevant levels of exposure will help to clarify some questions that remain about low level effects. Currently, it is assumed that molecular mechanisms such as DNA repair behave similarly at high or low level exposures to carcinogens. This assumes the absence of any practical thresholds of effect in these processes. By analyzing these processes directly in human samples, this debate may potentially be resolved. The sensitivity of this new method may also allow better understanding of interindividual susceptibility to DNA adduct formation. Finally, this method has several advantages over other DNA damage detection methods that suggest it may be suitable for use in human biomonitoring efforts.



## 1.8 Objectives

The long-term objectives of this research were to develop capillary electrophoresis / laser-induced fluorescence DNA damage assays and to adapt them for biomarker research. With respect to biomonitoring of BPDE-DNA adducts, the necessary studies to achieve this long-term goal include:

1. To identify appropriate antibodies specific for BPDE-damaged DNA and characterize their behavior in the capillary electrophoresis system.
2. To design and synthesize a DNA standard containing BPDE adducts. This would be used to study antibody binding and optimize and calibrate DNA damage assays.
3. To develop an assay for BPDE adducts in a human cell line treated with a range of doses of BPDE. This would assess the performance of the assay prior to testing actual human samples.
4. To establish and validate DNA adduct measurements as biomarkers.

This thesis focuses on the first two aspects. Chapter 2 describes preliminary results on developing an assay for DNA adducts of BPDE. It was realized that several parameters need to be considered including antibody affinity, formation and separation of complexes, and the generation of BPDE adducts. Without a standard containing BPDE adducts of known concentration, it was difficult to optimize these parameters. Therefore, the majority of effort was given to the design, synthesis, and characterization of a DNA standard containing a single BPDE adduct. Details are discussed in Chapter 3. This standard has subsequently been used for competitive assay of BPDE-DNA adducts (Tan et al., 2001) and studies of binding stoichiometry (Wang et al., 2001).





## 1.9 References

- Abelson, P.H. Risk assessments of low-level exposures (Editorial). *Science* 265:1507 (1994).
- Alberts, B., Bray, D., Lewis, J., Raff, M., Roberts, K., and Watson, J.D. *Molecular Biology of the Cell*. New York: Garland Publishing Inc, 1994.
- Andrews, C.L., Vouros, P., and Harsch, A. Analysis of DNA adducts using high-performance separation techniques coupled to electrospray ionization mass spectrometry. *J Chromatogr A* 856:515-526 (1999).
- ATSDR (Agency for Toxic Substances and Disease Registry). Toxicological profile for benzo[a]pyrene. U.S. Dept. of Health & Human Services, Public Health Service, Atlanta, GA. 125 pp (1990).
- Baan, R.A., Steenwinkel, M.J.S.T., van Asten, S., Roggeband, R., and van Delft, J.H.M. The use of benzo(a)pyrene dilepoxide-modified DNA standards for adduct quantification in <sup>32</sup>P-postlabeling to assess exposure to polycyclic aromatic hydrocarbons: application in a biomonitoring study. *Mutat Res* 378:41-50 (1997).
- Barry, J.P., Norwood, C., and Vouros, P. Detection and identification of benzo[a]pyrene diol epoxide adducts to DNA utilizing capillary electrophoresis-electrospray mass spectrometry. *Anal Chem* 68:1432-1438 (1996).
- Beach, A.C. and Gupta, R.C. Human biomonitoring and the <sup>32</sup>P-postlabeling assay. *Carcinogenesis* 13:1053-1074 (1992).
- Booth, E.D., Aston, J.P., van den Berg, P.T.M., Baan, R.A., Riddick, D.A., Wade, L.T., Wright, A.S., and Watson, W.P. Class-specific immunoabsorption purification for polycyclic aromatic hydrocarbon-DNA adducts. *Carcinogenesis* 15:2099-2106 (1994).
- Butler, J.P., Post, G.B., Liroy, P.J., Waldman, J.M., and Greenberg, A. Assessment of carcinogenic risk from personal exposure to benzo(a)pyrene in the Total Human Environmental Exposure Study (THEES). *J Air Waste Manage Assoc* 43:970-977 (1993).
- Cadet, J., Douki, T., and Ravanat, J.L. Artifacts associated with the measurement of oxidized DNA bases. *Environ Health Perspect* 105:1034-1039 (1997).
- Cadet, J. and Weinfeld, M. Detecting DNA damage. *Anal Chem* 65:675A-682A (1993).



- Choi, D.J., Marino-Alessandri, D.J., Geactinov, N.E., and Scicchitano, D.A. Site-specific benzo[a]pyrene diol epoxide-DNA adducts inhibit transcription elongation by bacteriophage T7 RNA polymerase. *Biochemistry* 33:780-787 (1994).
- Denissenko, M.F., Pao, A., Tang, M., and Pfeifer, G.P. Preferential formation of benzo(a)pyrene adducts at lung cancer mutational hotspots in *P53*. *Science* 274:430-432 (1996).
- Dickey, C., Santella, R.M., Hattis, D., Tang, D., Hsu, Y., Cooper, T., Young, T.L., and Perera, F.P. Variability in PAH-DNA adduct measurements in peripheral mononuclear cells: implications for quantitative cancer risk assessment. *Risk Analysis* 17(5):649-656 (1997).
- Ding J. and Vouros P. Capillary electrochromatography and capillary electrochromatography-mass spectrometry for the analysis of DNA adduct mixtures. *Anal Chem* 69:379-384 (1997).
- Dizdaroglu, M. Quantitative determination of oxidative base damage in DNA by stable isotope-dilution mass spectrometry. *FEBS Letters* 315:1-6 (1993).
- Eisenbrand, G. and Tang, W. Food-borne heterocyclic amines. Chemistry, formation, occurrence and biological activities: a literature review. *Toxicology* 84:1-82 (1993).
- Friedberg, E.C., Walker, G.C., and Siede, W. DNA Repair and Mutagenesis. ASM Press, Washington, DC (1995).
- Godschalk, R.W.L., Vermeer, I.T.M., Kriek, E., Floot, B., Schilderman, P.A.E.L., Moonen, E.J.C., Kleinjans, J.C.S., and van Schooten, F.J. Comparison of <sup>32</sup>P-postlabeling and HPLC-FD analysis of DNA adducts in rats acutely exposed to benzo(a)pyrene. *Chem-Biol Interact* 104:41-54 (1997).
- Hanelt, S., Helbig, R., Hartmann, A., Lang, M., Seidel, A., and Speit, G. A comparative investigation of DNA adducts, DNA strand breaks and gene mutations induced by benzo[a]pyrene and (±)-anti-benzo[a]pyrene-7,8-diol 9,10-oxide in cultured human cells. *Mutat Res* 390:179-188 (1997).
- Harris, C.C., Vahakangas, K., Newman, M.J., Trivers, G.E., Shamsuddin, A., Sinopoli, N., Mann, D.L., and Wright, W.E. Detection of benzo(a)pyrene diol epoxide-DNA adducts in peripheral blood lymphocytes and antibodies to the adducts in serum from coke oven workers. *Proc Natl Acad Sci USA* 82:6672-6676 (1985).
- Hattis, D. Advances for epidemiology (Book review). *Science* 271:770 (1996).
- Haugen, A., Becher, G., Benestad, C., Vahakangas, K., Trivers, G.E., Newman, M.J., and Harris, C.C. Determination of polycyclic aromatic hydrocarbons in the urine,



- benzo(a)pyrene diol epoxide-DNA adducts in lymphocyte DNA, and antibodies to the adducts in sera from coke oven workers exposed to measured amounts of polycyclic aromatic hydrocarbons in the work atmosphere. *Cancer Res* 46:4178-4183 (1986).
- Hecht, S.S. Biochemistry, biology, and carcinogenicity of tobacco-specific *N*-nitrosamines. *Chem Res Toxicol* 11:560-603 (1998).
- Hemminki, K., Autrup, H., and Haugen, A. DNA and protein adducts. *Toxicology* 101:41-53 (1995).
- Hemminki, K., Grzybowska, E., Chorazy, M., Twardowska-Sauch, K., Sroczynski, J.W., Putman, K.L., Randerath, K., Phillips, D.H., Hewer, A., Santella, R.M., Young, T.L., and Perera, F.P. DNA adducts in humans environmentally exposed to aromatic compounds in an industrial area of Poland. *Carcinogenesis* 11:1229-1231 (1990).
- Hess, M.T., Gunz, D., Luneva, N., Geactinov, N.E., and Naegeli, H. Base pair conformation-dependent excision of benzo[a]pyrene diol epoxide-guanine adducts by human nucleotide excision repair enzymes. *Mol Cell Biol* 17:7069-7076 (1997).
- Hrudey, S.E. and Krewski, D. Is there a safe level of exposure to a carcinogen? *Environ Sci Tech* 29:370A-375A (1995).
- Hulka, B.S. and Wilcosky, T. Biological markers in epidemiologic research. *Arch Environ Health* 43:83-89 (1988).
- Jongeneelen, F.J. Methods for routine biological monitoring of carcinogenic PAH-mixtures. *Sci Total Environ* 199:141-149 (1997).
- Kang, D.H., Rothman, N., Poirier, M.C., Greenberg, A., Hsu, C.H., Schwartz, B.S., Baser, M.E., Groopman, J.D., Weston, A., and Strickland, P.T. Interindividual differences in the concentration of 1-hydroxypyrene-glucuronide in urine and polycyclic aromatic hydrocarbon-DNA adducts in peripheral white blood cells after charbroiled beef consumption. *Carcinogenesis* 16:1079-1085 (1995).
- Kato, S., Bowman, E.D., Harrington, A.M., Blomeke, B., and Shields, P.G. Human lung carcinogen-DNA adduct levels mediated by genetic polymorphisms in vivo. *J Natl Cancer Inst* 87:902-907 (1995).
- Le, X.C., Xing, J.Z., Lee, J., Leadon, S.A., and Weinfeld, M. Inducible repair of thymine glycol detected by an ultrasensitive assay for DNA damage. *Science* 280:1066-1069 (1998).





- Leadon, S.A. Production of thymine glycols in DNA by radiation and chemical carcinogens as detected by a monoclonal antibody. *Br J Cancer* 55 Suppl VIII:113-117 (1987).
- Melamede, R.J., Kow, Y.W., Bessalov, I.A., and Wallace, S.S. Detection of oxidative DNA base damages: immunochemical and electrochemical approaches. In: *Technologies for Detection of DNA Damage and Mutations* (Pfeifer GP, ed.). New York: Plenum Press, 1996;103-115.
- Melikian, A.A., Sun, P., Prokopczyk, B., El-Bayoumy, K., Hoffmann, D., Wang, X., and Waggoner, S. Identification of benzo[a]pyrene metabolites in cervical mucus and DNA adducts in cervical tissues in humans by gas chromatography-mass spectrometry. *Cancer Letters* 146:127-134 (1999).
- Moller, P. and Wallin, H. Adduct formation, mutagenesis and nucleotide excision repair of DNA damage produced by reactive oxygen species and lipid peroxidation products. *Mutat Res* 410:271-290 (1998).
- Naritsin, D.B. and Markey, S.P. Assessment of DNA oxidative damage by quantification of thymidine glycol residues using gas chromatography / electron capture negative ionization mass spectrometry. *Anal Biochem* 241:35-41 (1996).
- Pavanello, S., Favretto, D., Brugnone, F., Mastrangelo, G., Dal Pra, G., and Clonfero, E. HPLC/fluorescence determination of *anti*-BPDE-DNA adducts in mononuclear white blood cells from PAH-exposed humans. *Carcinogenesis* 20:431-435 (1999).
- Perera, F.P., Hemminki, K., Grzybowska, E., Motykiewicz, G., Michalska, J., Santella, R.M., Young, T.L., Dickey, C., Brandt-Rauf, P., DeVivo, I., Blaner, W., Tsai, W.Y., and Chorazy, M. Molecular and genetic damage in humans from environmental pollution in Poland. *Nature* 360:256-258 (1992).
- Perera, F.P., Hemminki, K., Young, T.L., Brenner, D., Kelly, G., and Santella, R.M. Detection of polycyclic aromatic hydrocarbon-DNA adducts in white blood cells of foundry workers. *Cancer Res* 48:2288-2291 (1988).
- Perera, F.P., Poirier, M.C., Yuspa, S.H., Nakayama, J., Jaretzki, A., Curnen, M.M., Knowles, D.M., and Weinstein, I.B. A pilot project in molecular cancer epidemiology: determination of benzo(a)pyrene-DNA adducts in animal and human tissues by immunoassays. *Carcinogenesis* 3:1405-1410 (1982).
- Pfeifer, G.P., Denissenko, M.F., and Tang, M. PCR-based approaches to adduct analysis. *Toxicol Letters* 102-103:447-451 (1998).
- Poirier, M.C. DNA adducts as exposure biomarkers and indicators of cancer risk. *Environ Health Perspect* 105(Suppl 4):907-912 (1997).



- Poirier, M.C. and Weston, A. Human DNA adduct measurements: State of the art. *Environ Health Perspect* 104(Suppl 5):883-893 (1996).
- Poirier, M.C., Santella, R., Weinstein, I.B., Grunberger, D., and Yuspa, S.H. Quantitation of benzo(a)pyrene-deoxyguanosine adducts by radioimmunoassay. *Cancer Res* 40:412-416 (1980).
- Rothman, N., Poirier, M.C., Baser, M.E., Hansen, J.A., Gentile, C., Bowman, E.D., and Strickland, P.T. Formation of polycyclic aromatic hydrocarbon-DNA adducts in peripheral white blood cells during consumption of charcoal-broiled beef. *Carcinogenesis* 11:1241-1243 (1990).
- Santella, R.M. Immunological methods for detection of carcinogen-DNA damage in humans. *Cancer Epidemiology Biomarkers & Prevention* 8:733-739 (1999).
- Santella, R.M., Perera, F.P., Young, T.L., Zhang, Y.J., Chiamprasert, S., Tang, D., Wang, L.W., Beachman, A., Lin, J.H., and DeLeo, V.A. Polycyclic aromatic hydrocarbon-DNA and protein adducts in coal tar treated patients and controls and their relationship to glutathione S-transferase genotype. *Mutat Res* 334:117-124 (1995).
- Santella, R.M., Weston, A., Perera, F.P., Trivers, G.T., Harris, C.C., Young, T.L., Nguyen, D., Lee, B.M., and Poirier, M.C. Interlaboratory comparison of antisera and immunoassays for benzo(a)pyrene-diol-epoxide-I-modified DNA. *Carcinogenesis* 9:1265-1269 (1988).
- Sauvaigo, S., Serres, C., Signorini, N., Emonet, N., Richard, M., and Cadet, J. Use of the single-cell gel electrophoresis assay for the immunofluorescent detection of specific DNA damage. *Anal Biochem* 259:1-7 (1998).
- Strickland, P., Kang, D., and Sithisarankul, P. Polycyclic aromatic hydrocarbon metabolites in urine as biomarkers of exposure and effect. *Environ Health Perspect* 104(Suppl 5):927-932 (1996).
- Szeliga, J. and Dipple, A. DNA adduct formation by polycyclic aromatic hydrocarbon dihydrodiol epoxides. *Chem Res Toxicol* 11(1):1-11 (1998).
- Talaska, G., Underwood, P., Maier, A., Lewtas, J., Rothman, N., and Jaeger, M. Polycyclic aromatic hydrocarbons (PAHs), Nitro-PAHs and related environmental compounds: biological markers of exposure and effects. *Environ Health Perspect* 104(Suppl 5):901-906 (1996).
- Tan, W.G., Carnelley, T.J., Murphy, P., Lee, J., Barker, S., Wang, H., Weinfeld, M., and Le, X.C. Detection of DNA adducts of benzo[a]pyrene using immunoelectrophoresis with laser-induced fluorescence – analysis of A549 cells. *J Chromatogr A*, in press (2001).



- Thrall, B.D., Mann, D.B., Smerdon, M.J., and Springer, D.L. DNA polymerase, RNA polymerase and exonuclease activities on a DNA sequence modified by benzo[a]pyrene diolepoxide. *Carcinogenesis* 13:1529-1534 (1992).
- US EPA. Guidelines for carcinogen risk assessment. Federal Register 51:33992-34003 (1986).
- van Schooten, F.J., Hillebrand, M.J.X., van Leeuwen, F.E., Lutgerink, J.T., van Zandwijk, N., Jansen, H.M., and Kriek, E. Polycyclic aromatic hydrocarbon-DNA adducts in lung tissue from lung cancer patients. *Carcinogenesis* 11:1677-1681 (1990).
- Wang, H., Xing, J., Tan, W., Lam, M., Carnelley, T., Weinfeld, M., and Le, X.C. Binding stoichiometry of DNA adducts with antibodies studied by capillary electrophoresis and laser-induced fluorescence. *Anal Chem*, submitted (2001).
- Wang, J.S. and Groopman, J.D. DNA damage by mycotoxins (Review). *Mutat Res* 424:167-181 (1999).
- Wang, M., Abbruzzese, J.L., Friess, H., Hittelman, W.N., Evans, D.B., Abbruzzese, M.C., Chiao, P., and Li, D. DNA adducts in human pancreatic tissues and their potential role in carcinogenesis. *Cancer Res* 58:38-41 (1998).
- Ward Jr., J.B. and Henderson, R.E. Identification of needs in biomarker research. *Environ Health Perspect* 104(Suppl 5):895-900 (1996).
- Weinfeld, M. and Soderlind, K.M.  $^{32}\text{P}$ -postlabeling detection of radiation-induced DNA damage: identification and estimation of thymine glycols and phosphoglycolate termini. *Biochemistry* 30:1091-1097 (1991).
- Weston, A. and Bowman, E.D. Fluorescence detection of benzo(a)pyrene-DNA adducts in human lung. *Carcinogenesis* 12:1445-1449 (1991).
- Zeisig, M. and Moller, L.  $^{32}\text{P}$ -HPLC suitable for characterization of DNA adducts formed *in vitro* by polycyclic aromatic hydrocarbons and derivatives. *Carcinogenesis* 16:1-9 (1995).





## Chapter 2: Preliminary experiments on detection of BPDE-DNA adducts using capillary electrophoresis with laser-induced fluorescence

### 2.1 Introduction

Structural damage to DNA is generally considered to be the initial step in the complex multistage model of cancer development (Friedberg et al., 1995). Our DNA is exposed to a variety of endogenous and environmental agents that may induce a wide range of damage. Environmental sources of DNA damage include ultraviolet light (Friedberg et al., 1995), ionizing radiation (Weinfeld and Soderlind, 1991), alkylating agents (Shuker and Farmer, 1992), nitrosamines (Hecht, 1998), mycotoxins (Wang and Groopman, 1999), heterocyclic amines (Eisenbrand and Tang, 1993), and polycyclic aromatic hydrocarbons (PAHs) (Szeliga and Dipple, 1998). Many of these agents, including PAHs, induce bulky lesions or adducts in the DNA structure. One of this class of compounds, benzo[*a*]pyrene, has been extensively studied due to its strong ability to react with DNA and cause mutation. Benzo[*a*]pyrene is metabolized *in vivo* by cytochrome P450 and epoxide hydrolase to form benzo[*a*]pyrene-7,8-diol 9,10-epoxide (BPDE), which is generally considered to be the ultimate carcinogenic species. The reactive epoxide moiety of BPDE binds primarily to the N<sup>2</sup> position of deoxyguanosine to form a bulky adduct structure (BPDE-N<sup>2</sup>-dG) (Szeliga and Dipple, 1998). This adduct causes changes in the conformation of the DNA helix surrounding the damaged site. This distortion can disrupt biological processes including DNA repair, DNA replication, and transcription (Hess et al., 1997; Choi et al., 1994; Thrall et al., 1992), during which mutations in the DNA sequence may occur. These mutations have been shown to affect genes critical to the development of cancer, including the tumor suppressor p53 (Denissenko et al., 1996). Consequently, the detection of DNA damage caused by compounds such as benzo[*a*]pyrene is an important issue regarding human exposures to these environmental chemicals.

An array of techniques has been developed to detect BPDE-DNA damage, including immunochemical methods (Santella, 1999), <sup>32</sup>P-postlabeling (Beach and Gupta, 1992),



gas chromatography-mass spectrometry (GC-MS) (Melikian et al., 1999), high performance liquid chromatography (HPLC) combined with fluorescence detection (Pavanello et al., 1999) or  $^{32}\text{P}$ -postlabeling (Zeisig and Moller, 1995), single cell gel electrophoresis (comet) assays (Hanelt et al., 1997), and PCR-based assays (Pfeifer et al., 1998). Of these techniques, one of the most popular and useful is the enzyme-linked immunosorbent assay (ELISA) using antibodies specific for the type of damage being investigated. Several groups have developed monoclonal antibodies that recognize BPDE-DNA damage (Baan et al., 1988; Santella et al., 1984; Poirier et al., 1980). This method has been used to determine BPDE adduct levels in samples from human subjects exposed to benzo[*a*]pyrene in a variety of environmental settings (Santella, 1999). While very useful, this technique does have some disadvantages including a requirement for relatively large amounts of DNA (200  $\mu\text{g}$  or more), a lack of sensitivity necessary for routine measurement of human samples, and a requirement for highly trained personnel to achieve consistent results for the assay.

In an attempt to address some of these limitations, an assay that combines immunological detection of damaged DNA with capillary electrophoresis separation and laser-induced fluorescence detection was developed (Le et al., 1998). In this technique, damaged DNA is mixed with a primary ( $1^\circ$ ) monoclonal antibody specific for the DNA lesion and an excess of secondary ( $2^\circ$ ) antibody that is labeled with a fluorescent dye, typically fluorescein or tetramethylrhodamine (TMR). The resulting mixture contains 1) excess  $2^\circ$  antibody, 2)  $2^\circ$  antibody +  $1^\circ$  antibody, and 3)  $2^\circ$  antibody +  $1^\circ$  antibody + damaged DNA, all of which are fluorescent. These species are separated using free-zone capillary electrophoresis and the DNA-antibody complex is quantified by measuring fluorescence induced by the dye-specific laser. Laser-induced fluorescence combined with the lack of a solid matrix allows for extremely sensitive detection of these molecules. This was demonstrated by measuring thymine glycol bases induced by ionizing radiation, with an observed detection limit of  $3 \times 10^{-21}$  moles of damaged bases (Le et al., 1998).

A series of experiments were required in order to apply this novel technique to the detection of BPDE-damaged DNA. It was necessary to first determine the reactivity



between BPDE-DNA primary antibodies and a fluorescent-labeled secondary antibody, and to determine the characteristics of the complex in capillary electrophoresis. Purification of the antibodies used in this research was carried out to improve the affinity reaction and the quality of the fluorescence profile in the electropherogram. Several electrophoretic parameters were also assessed to optimize the separation of the complex from the free secondary antibody. After these preliminary experiments, the assay was tested using BPDE-DNA samples from different sources. Results from these attempts will be presented, along with a discussion of some of the findings from this stage of the research project.

## **2.2 Materials and Methods**

### **2.2.1 Reagents**

Common chemicals and biochemicals used for these experiments were supplied by Sigma, Fisher Scientific or VWR Canlab. More specific reagents including antibodies and DNA are described in greater detail below.

### **2.2.2 Antibody Preparation and Characterization**

Tetramethylrhodamine (TMR) -conjugated polyclonal goat anti-mouse IgG (Calbiochem) was used as the secondary antibody for most of the experiments in this section. The crude preparation contained excess bovine serum albumin (confirmed by SDS-polyacrylamide gel electrophoresis as described below) and free TMR dye. It was therefore necessary to purify the antibody to improve its profile during capillary electrophoresis. Purification was achieved using Protein G affinity columns (Hi-Trap 1-ml, Amersham Pharmacia Biotech) and a syringe pump (Harvard Apparatus) to control the flow rate through the column. 100  $\mu$ l aliquots of stock TMR-anti-mouse IgG were stored at  $-20^{\circ}\text{C}$  and purified as needed. The manufacturer's suggested elution protocol for the Protein G column was used in these experiments. Antibodies were eluted from the column using 100 mM glycine-HCl, pH 2.7, and then immediately neutralized by collecting the fractions into





tubes containing 1 M Tris-HCl, pH 9.0. This resulted in the antibody being dissolved in a high-salt Tris-glycine buffer solution. The antibody was subsequently desalted by buffer exchange against water or phosphate-buffered saline (PBS) using 10,000 NMWL (nominal molecular weight limit) ultrafiltration units (Ultrafree-MC 400  $\mu$ l, Millipore). These were later replaced by 4-ml units containing a 10,000 NMWL high-flux membrane (Ultrafree-4 /Biomax, Millipore). The 4-ml filter units were centrifuged at 3500 rpm (3100g) for 10 minutes per run in a benchtop centrifuge (Beckman). Buffer exchange was achieved by rediluting the antibody sample to 4 ml with buffer or water followed by centrifugation for a total of three times. Purified, desalted TMR-anti-mouse IgG was stored in the dark at 4°C. For preliminary experiments an alternate secondary antibody, Cy3-anti-mouse IgG (Sigma), was also tested in the capillary electrophoresis system. Like the TMR-labeled secondary antibody, Cy3-anti-mouse IgG was suitable for detection by the laser-induced fluorescence instrumentation being used.

Three different primary antibodies specific for BPDE-damaged DNA were used in this study. Monoclonal antibodies 5D11 and 8E11 (Santella et al., 1984) were purchased from BD Pharmingen and stored at 4°C as indicated. The antigens they were raised against were full-length BPDE-DNA and BPDE-N<sup>2</sup>-dG mononucleotide adducts, respectively. Antibody E5 was raised as previously described (Booth et al., 1994; Baan et al., 1988), also against the BPDE-N<sup>2</sup>-dG adduct. This antibody was produced by the same monoclonal cell line (designated E4 in the above references), but was maintained in culture at a different time. The antibody was initially supplied in purified, concentrated form by Dr. William Watson and Dr. Ewan Booth, Shell Research and Technology Centre, Shell International Chemicals B.V., Amsterdam. An additional quantity of E5 was provided in the form of cell supernatant from the monoclonal cell culture. The antibody was purified from the supernatant using Protein G affinity columns. Elution of protein from the column was monitored by collecting fractions and measuring absorbance of the sample at 280 nm using flow injection analysis with either a Hewlett Packard Model 1040A diode array HPLC detector or a Waters 484 tunable absorbance detector. 50  $\mu$ l of an appropriate dilution of each protein sample was injected into a 20- $\mu$ l injection loop to ensure complete filling of the loop. The chromatogram data generated by the



detector was analyzed using Chemstation software to determine peak areas. Fractions containing material absorbing at this wavelength were subjected to SDS-polyacrylamide gel electrophoresis to confirm the identity of the eluted species. Gels were cast according to standard protocols (Ausubel 1992) using 37.5:1 acrylamide / bis-acrylamide solution. Electrophoresis was carried out at 120 V for 1-2 hours depending on the percentage composition of the gel. Proteins were visualized by overnight shaking in Coomassie Blue staining solution. The recovered antibody fractions were then desalted and concentrated using ultrafiltration units as described above. The final concentration of E5 antibody was determined by measuring absorbance at 280 nm or by using the BCA-200 Protein Assay Kit (Pierce, Rockford, IL). Absorbance of the BCA (bicinchoninic acid) reaction product at 562 nm was determined using the diode array detector and was compared to standard curves constructed with bovine serum albumin (Sigma) and polyclonal mouse IgG (Calbiochem, La Jolla, CA). Aliquots of E5 were then stored at  $-20^{\circ}\text{C}$  until needed.

To verify that the primary and secondary antibodies were binding to the BPDE-DNA samples, an alternate method to capillary electrophoresis was used. The procedure was a modification of dot blot assays normally used to measure hybridization of DNA or RNA probes to genomic DNA samples (Ausubel, 1992). A small piece of nitrocellulose membrane (Amersham Pharmacia Biotech) was soaked in 20X SSC (3 M sodium chloride, 0.3 M sodium citrate, adjusted to pH 7.0 with 1 M HCl) for 10 minutes. Mouse skin BPDE-DNA and control calf thymus DNA samples (1  $\mu\text{g}$  in 10  $\mu\text{l}$ ) were diluted in 20X SSC to a final volume of 30  $\mu\text{l}$ . The membrane was suspended over two glass pipettes and excess solution was removed. The DNA samples were then applied to the membrane in 2  $\mu\text{l}$  aliquots, with drying between applications using a gentle stream of air. After the entire sample was applied, the membrane was dried and baked between two sheets of Whatman 3MM filter paper in a vacuum oven at  $80^{\circ}\text{C}$  for 2 hours to immobilize the DNA. The remaining binding sites on the membrane were then blocked by gently shaking the membrane overnight in TTBS (100 mM Tris-HCl, pH 7.5, 0.9% NaCl, 0.1% Tween 20 detergent). The membrane was then shaken in a solution of 0.5  $\mu\text{g}/\text{ml}$  E5 antibody in TTBS for 1 hour followed by 4 X 15 minute washes in 50 ml of TTBS, changed after each wash. The secondary anti-mouse IgG antibody conjugated





with either TMR or alkaline phosphatase (Sigma) was then diluted 2000-4000X in TTBS and added to the membrane. The secondary incubation was carried out for 1-2 hours followed by 4 X 15 minute washes. Alkaline phosphatase activity was detected using the BCIP/NBT chromogenic substrate system (Sigma) which resulted in a blue color on affected areas of the membrane. Fluorescence emitted by membrane-bound TMR-anti-mouse IgG was visualized by laser confocal microscopy in the Department of Biological Sciences, University of Alberta.

### 2.2.3 BPDE-DNA samples

Two different sources of BPDE-damaged DNA were used for these experiments. DNA isolated from mouse skin was provided by Dr. William Watson and Dr. Ewan Booth, Shell Research and Technology Centre, Shell International Chemicals B.V., Amsterdam, and was prepared as described previously (Booth et al., 1994). 3 mice were each treated cutaneously with 100 µg of benzo[*a*]pyrene applied in 100 µl of acetone. After 24 hours the mice were killed and the treated area of skin was removed and stored frozen at -80°C. Whole skin samples were treated with depilatory cream to remove traces of hair, then washed with pre-chilled distilled water. The skin was finely minced with scissors and added to a mixture of 1 ml of proteinase K solution [1500 units dissolved in Tris-HCl (20 mM, pH 8.5, 12 ml)], 3 ml lysis buffer, 3 ml phosphate-buffered saline and 120 µl β-mercaptoethanol. The samples were incubated with brisk shaking in a 55°C water bath for 4 hours. After digestion, the samples were homogenized by hand using a mortar and pestle and transferred to an automated DNA extractor. DNA was isolated and purified by phenol/chloroform extraction and ethanol precipitation. The resulting pellets were combined by resuspending in ddH<sub>2</sub>O and dried using a centrifugal evaporator. Dried samples were dissolved in ddH<sub>2</sub>O prior to analysis. Adduct levels in the mouse skin DNA were estimated to be approximately 1 in 10<sup>5</sup> normal nucleotides using the <sup>32</sup>P-postlabeling assay.

The second series of DNA samples used for analysis were generated by treating a human cell line with (±)-*r*-7,*t*-8-dihydroxy-*t*-9,10-epoxy-7,8,9,10-tetrahydrobenzo[*a*]pyrene





(anti) [(±)-*anti*-BPDE], which was supplied by the National Cancer Institute Chemical Carcinogen Reference Standard Repository (Midwest Research Institute, Kansas City, MO). Several groups have measured BPDE adduct levels in cells after treatment with BPDE or benzo[*a*]pyrene (Hanelt et al., 1997; van Aagen et al., 1997; Shinozaki et al., 1998; Wu et al., 1998), and the treatment protocol used was adapted from these studies. (±)-*anti*-BPDE was dissolved in dimethylsulfoxide (DMSO) to a concentration of 3mM, and this stock solution was stored in the dark under argon at -20°C until required. A549 human lung adenocarcinoma cells (American Type Culture Collection, Rockville, MD) were cultured as monolayers in Dulbecco's modified Eagle's medium/Ham's F12 medium (1:1 v/v) supplemented with 10% fetal bovine serum at 37°C in a humidified (75-85%) atmosphere containing 5% CO<sub>2</sub>. About 7.5 X 10<sup>5</sup> cells were seeded in plastic Petri dishes (60 mm diameter, Becton Dickinson Labware, Franklin Lakes, NJ) and incubated overnight in 3 ml of media per dish. The media was then replaced with fresh media containing (±)-*anti*-BPDE (BPDE). Stock BPDE solution (3mM) was diluted in DMSO to the appropriate concentrations so that 1 µl of BPDE in DMSO was added per 3 ml of media (Final DMSO concentration was kept constant). The final BPDE concentration in the cell media varied 1000-fold, from 1 nM to 1µM. The cells were then incubated for 4 hours, after which the media was discarded and the cells rinsed twice with ice-cold phosphate-buffered saline (PBS). The cells were lysed by addition of 1 ml DNAzol reagent (Sigma) and then transferred to a 10-ml tube. Each sample was gently mixed with 500 µl of 100% ethanol to precipitate the DNA, which was then spooled onto a pipette tip and transferred to an Eppendorf tube contained 500 µl of 70% ethanol. The DNA was centrifuged and the pellet was washed twice with 95% ethanol before being dissolved in 600 µl of 8mM NaOH. The samples were stored at -20°C until needed.

#### 2.2.4 Capillary Electrophoresis Instrumentation and Methods

Capillary electrophoresis experiments were carried out using a laboratory-built capillary electrophoresis – laser induced fluorescence (CE-LIF) system as previously described (Le et al., 1995). A schematic of this instrument is provided in Figure 2-1. Electrophoresis was powered by a high voltage power supply (CZE1000R, Spellman High Voltage Elec-



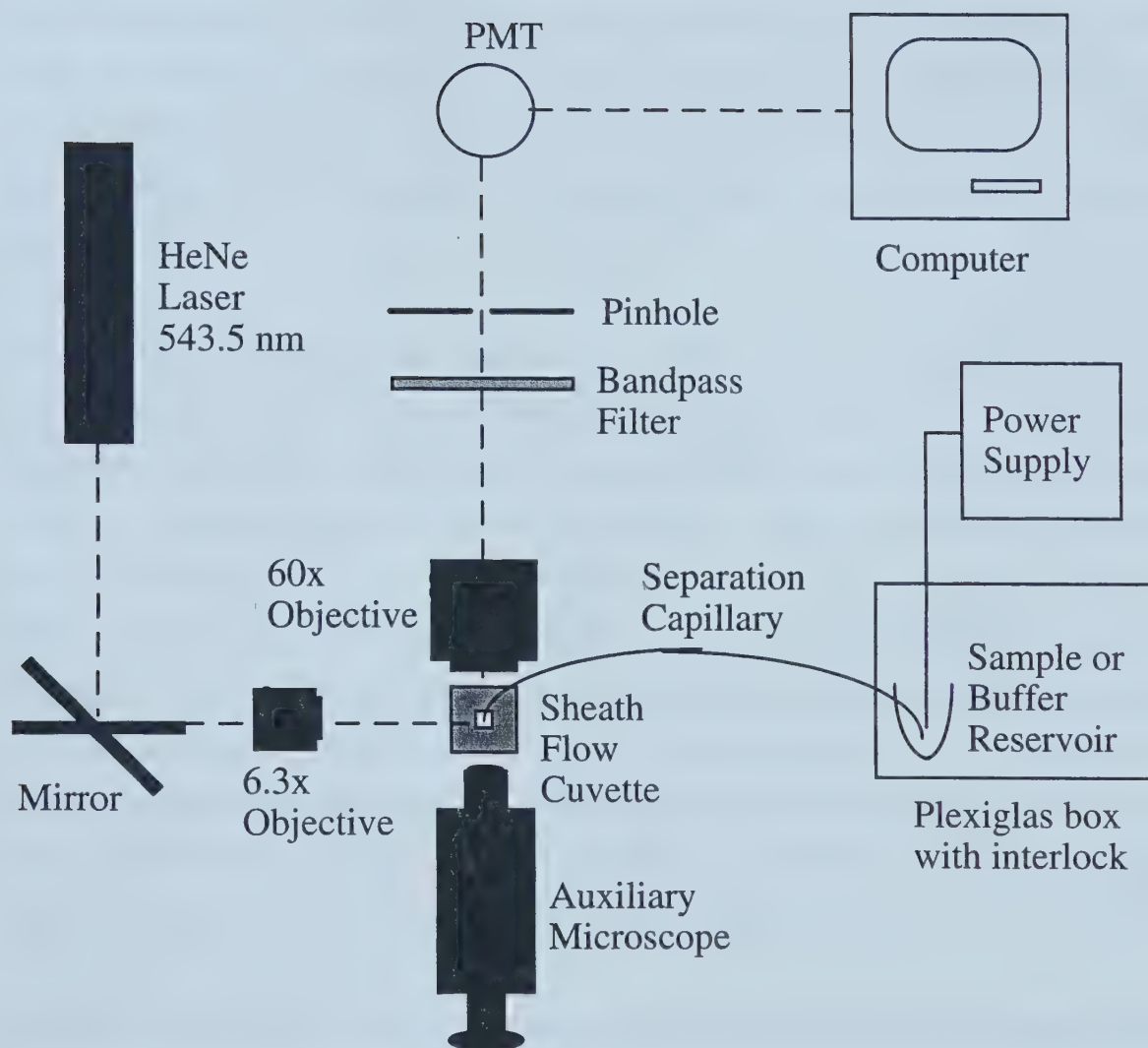


Figure 2-1. Schematic of a CE-LIF instrument.



tronics, Plainview, NY). Separation conditions including sample injection time and voltage, separation voltage and run time were controlled by a LABVIEW (National Instruments, Austin, TX) program run on a Macintosh computer. Capillaries used for these experiments were uncoated fused silica with a total length of 42 cm and an effective separation length of 37 cm. Two different sizes of capillaries were used, either 20  $\mu\text{m}$  inner diameter (i.d.) / 145  $\mu\text{m}$  outer diameter (o.d.) or 50  $\mu\text{m}$  i.d. / 150  $\mu\text{m}$  o.d. (Polymicro Technologies, Phoenix, AZ). The injection end of the capillary was placed in sample solution or running buffer, along with the high voltage lead from the power supply. The other end of the capillary was inserted through a grounded holder and into a waste vial.

The laser-induced fluorescence detector was built on an optical table using both commercial equipment and custom-made accessories. The laser source was a 1.0 mW green helium-neon laser (Melles Griot, Irvine, CA) with an excitation wavelength of 543.5 nm. The laser was focused onto the capillary through a microscope objective (6.3x), and fluorescence was collected through a second, high numerical aperture objective (60x, 0.7 NA, Universe Kogaku, Oyster Bay, NY) positioned at 90° from the direction of the laser. The fluorescence signal passed through a pinhole with an adjustable diameter to minimize background light, and also through a bandpass filter (580DF40) to eliminate scattered laser light. The signal was detected by a photomultiplier tube (R1477, Hamamatsu Photonics, Japan), and recorded by a Macintosh computer running LABVIEW software and equipped with a PCI data acquisition board.

The system was equipped with an auxiliary microscope to assist in the alignment of the optics. The microscope was used to visualize the position of the laser beam with respect to both the sample flow through the capillary and the collection optics, represented by a light-emitting diode (LED) positioned behind the pinhole in the collection assembly. Alignment was achieved by initially fixing the position of the collection assembly, then adjusting the capillary and laser-focusing objective using X-Y-Z translation stages. The angle of the fluorescence-collecting objective and the position (single direction) of the collection assembly were also adjustable for optimization of alignment.





Samples were electrokinetically injected into the capillary by typically applying an injection voltage of 10000 V for 5 seconds. The separation was carried out at room temperature with a separation voltage of 20000 V unless otherwise noted. A variety of running buffers were used in the preliminary experiments in an attempt to optimize the separation of the different species. These buffers included 1X Tris-glycine (25 mM Tris, 250 mM glycine, pH 8.3), 1X TBE (89 mM Tris, 89 mM borate, 2 mM EDTA, pH 8.3), Tris-borate (10 mM Tris, 20 mM borate, pH 10.5 and 12), and phosphate (20 mM, pH 9-12, 30 and 50 mM, pH 10). The capillary was usually washed every 3-5 injections with 0.1 M NaOH (applied by syringe for 1 min) followed by electrophoresis of the running buffer for 7 minutes. The initial voltage was kept low to prevent excessive joule heating in the capillary. As the running buffer replaced the NaOH in the capillary, current decreased allowing the running voltage to be gradually increased to 20000 V for the final 5 minutes of the reconditioning period. All capillary electrophoresis data was analyzed using Igor Pro software (version 3.1, WaveMetrics Inc., Lake Oswego, OR).

## 2.3 Results

### 2.3.1 Measurement of Protein Concentration

A method for determining protein concentration was necessary for monitoring purified antibody fractions as well as for accurate measurement of stock solutions. The inherent absorbance of protein molecules at 210 nm (peptide bond) and 280 nm (tryptophan and tyrosine amino acids) allows spectroscopic measurements to be made at these wavelengths. This method was tested with protein standards to determine its accuracy and reproducibility. A standard curve prepared from a series of bovine serum albumin samples demonstrated very good linearity over a wide concentration range using absorbance at 280 nm (Figure 2-2). Although 210 nm is a much more sensitive wavelength for protein determination, there are many substances that absorb strongly in this region, interfering with the sample measurement (Ausubel, 1992). This interference was very significant for the Tris-glycine elution buffer used for the antibody purification



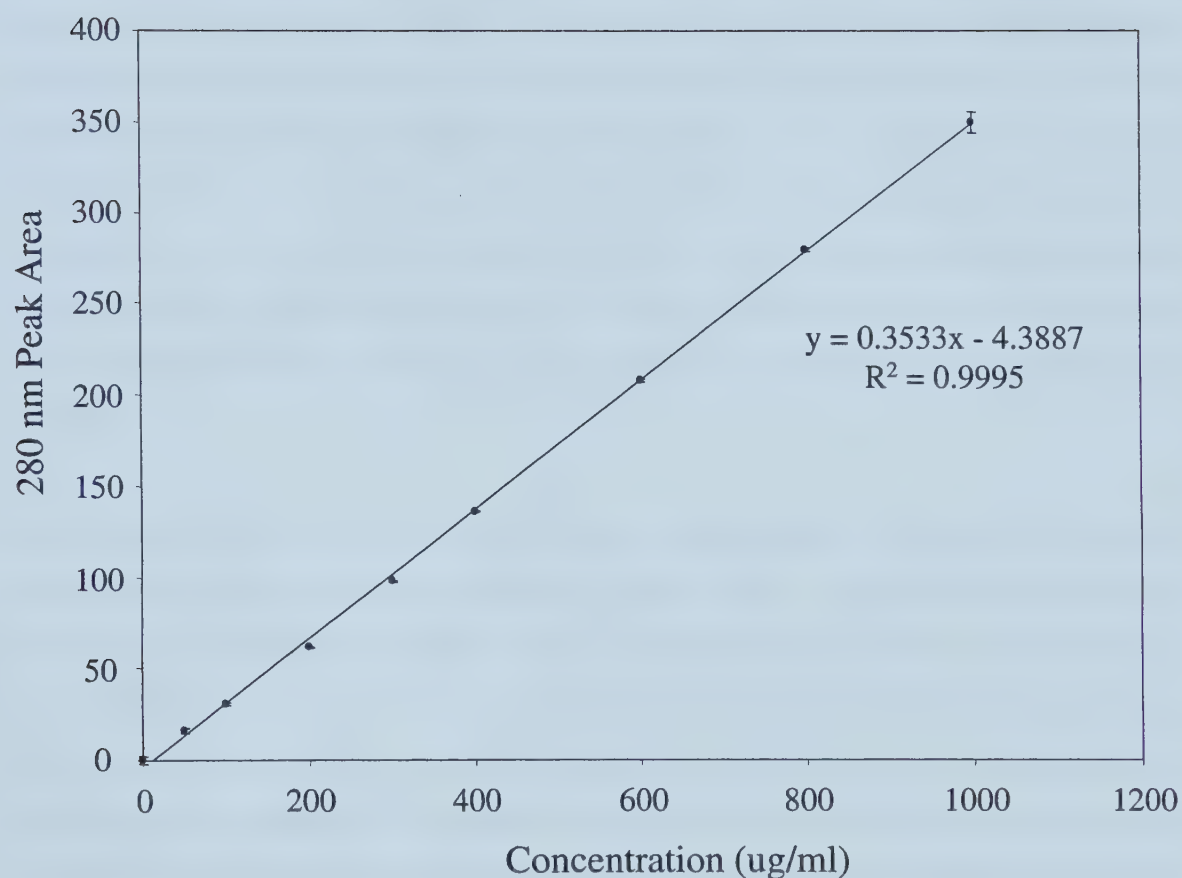


**Figure 2-2. Standard curve for protein determination at 280 nm.** Bovine serum albumin (BSA) was used to construct the standard curve. Samples were flow injected into a HPLC absorption detector set at 280 nm. Error bars indicate standard deviations based on duplicate samples at each concentration.



procedure described below. However, absorbance of the Tris-glycine at 280 nm was minimal, as was phosphate buffered saline at both wavelengths (Table 2-1). Because detection at 280 nm was sensitive enough for the samples being analyzed, this wavelength was used. The method was further tested by comparing polyclonal mouse immunoglobulin G (IgG) standards of known concentration to the BSA standard curve in Figure 2-2. The results indicated that the antibody molecules absorbed almost twice as strongly as BSA at 280 nm (Table 2-2). Variability of absorbance between different types of protein is based on the amino acid sequence and is a consideration for any of the commonly used protein assay methods (Ausubel, 1992). One possibility for addressing this problem was to use a mouse IgG standard curve to more accurately determine the concentration of the purified antibodies. However, a class of antibodies such as mouse IgG may exhibit considerable variation in the amino acid sequence in the active site of each individual antibody. Therefore, a method with less protein-protein variability was desirable.

The protein detection method chosen to replace measurement at 280 nm was the BCA (bicinchoninic acid) protein assay (Pierce). This method is based on the reaction of peptide bonds in the protein sample with  $\text{Cu}^{2+}$  to produce  $\text{Cu}^{1+}$ , which then reacts with BCA resulting in a purple product to be read at 562 nm. Unlike 280 nm measurements, the BCA assay does not rely on specific amino acids for detection and is less susceptible to protein-protein variation. The product literature states an absorbance ratio for mouse IgG / BSA of 1.18 based on protein variation in the reaction. As described above for the 280 nm method, a BCA standard curve was constructed using BSA protein standards and mouse IgG samples were compared to the curve. For 250 and 500  $\mu\text{g/ml}$  mouse IgG samples the equivalent BSA protein concentrations derived from the curve were 304 and 596  $\mu\text{g/ml}$ , respectively. This corresponded to protein variation ratios of 1.21 and 1.19, which was in agreement with the literature value. Once it was decided that this assay would most accurately determine the concentrations of the antibody samples, a standard curve was constructed using mouse IgG standards diluted in PBS buffer (Figure 2-3). The assay showed good linearity ( $R^2=0.9938$ ) and day-to-day reproducibility since the reagent mix was prepared fresh before each set of samples was analyzed. The only disadvantage





**Table 2-1.** Absorbance of buffers at 210 nm and 280 nm.

Buffer blank	210 nm peak area	280 nm peak area
Tris-glycine elution buffer	1870, 1910	9.17, 8.75
phosphate-buffered saline	17.6, 14.6	2.80, 2.69

Peak areas shown are for duplicate injections.



**Table 2-2.** Comparison of mouse IgG and BSA absorbance at 280 nm.

<b>Mouse IgG Concentration (<math>\mu\text{g/ml}</math>)</b>	<b>280 nm peak area (blank corrected)</b>	<b>Equivalent BSA Concentration (<math>\mu\text{g/ml}</math>)</b>
250	170	480
500	340	950

Equivalent BSA concentrations were calculated using the standard curve in Figure 2-2.



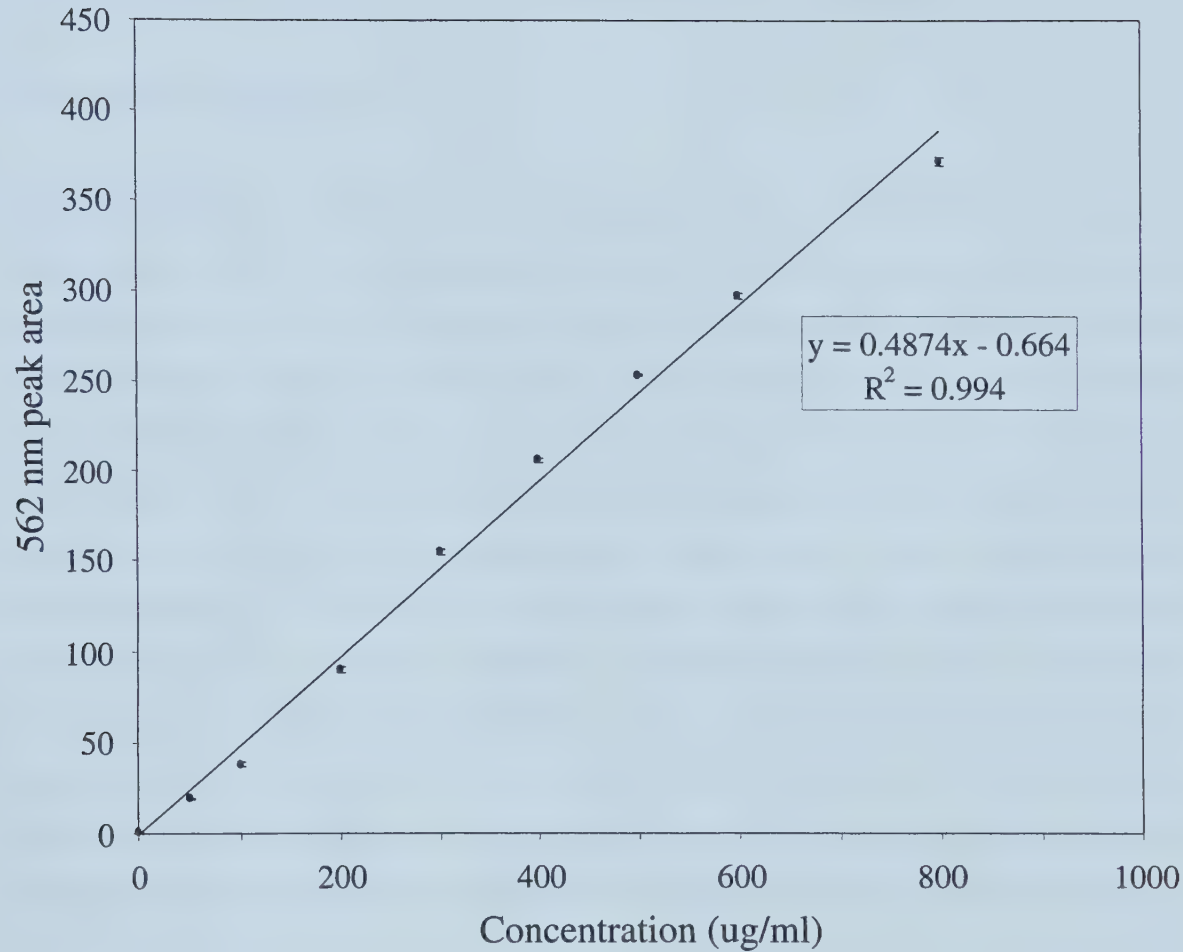


**Figure 2-3. Standard curve for protein determination using BCA method.** Polyclonal mouse IgG standards diluted in phosphate-buffered saline were used to construct the standard curve. Samples were mixed with BCA reagent, incubated at room temperature for 2 hours and absorbance was measured at 562 nm using flow-injection and a HPLC detector. Error bars indicate standard deviations based on duplicate samples at each concentration.





of the BCA assay when compared to absorbance at 280 nm was the incubation time for the reaction, either 30 minutes at 37°C or 2 hours at room temperature. For this reason, routine monitoring of antibody fractions eluted from the Protein G column was carried out using absorbance at 280 nm. The BCA assay was then used for determination of antibody concentration after the purification procedure was completed.

### 2.3.2 Antibody Purification

The antibodies to be used in the DNA damage assay were obtained from a variety of sources and were of varying degrees of purity. The monoclonal anti-BPDE DNA antibodies 5D11 and 8E11 were affinity purified by the supplier, and did not require further treatment. However, the fluorescent secondary antibody (Cy3- and TMR-labeled) preparations contained a 10-fold excess of bovine serum albumin (BSA) in the storage buffer (Figure 2-4). In addition, these antibody solutions contained a number of smaller fluorescent molecules and fragments that contributed several peaks to the electropherogram of samples run under normal capillary electrophoresis conditions. Consequently, these secondary antibodies required purification prior to subsequent experiments. The primary anti-BPDE DNA antibody clone E5 was initially received in pure form, but a second batch was shipped in the supernatant collected from the monoclonal cell line. The culture medium also contained a high concentration of serum proteins and other small molecules, and therefore purification of E5 was also necessary.

Purification of E5 and the fluorescent antibodies was achieved in two steps. The first step used immunoaffinity chromatography based on the recognition of the Fc regions of IgG antibodies by the Protein G molecule. Application of the antibody solutions to the Protein G columns resulted in binding of antibody to the column. Other proteins, fluorescent species and contaminating molecules were washed through the column. After washing, the bound antibody was eluted with an acid solution that was neutralized in the collection vial. This resulted in the antibody being dissolved in a neutral, high-salt buffer. Fractions were collected during the wash and elution steps to measure protein concentration and to determine the identity of eluted species. In each case, the elution profile was comparable



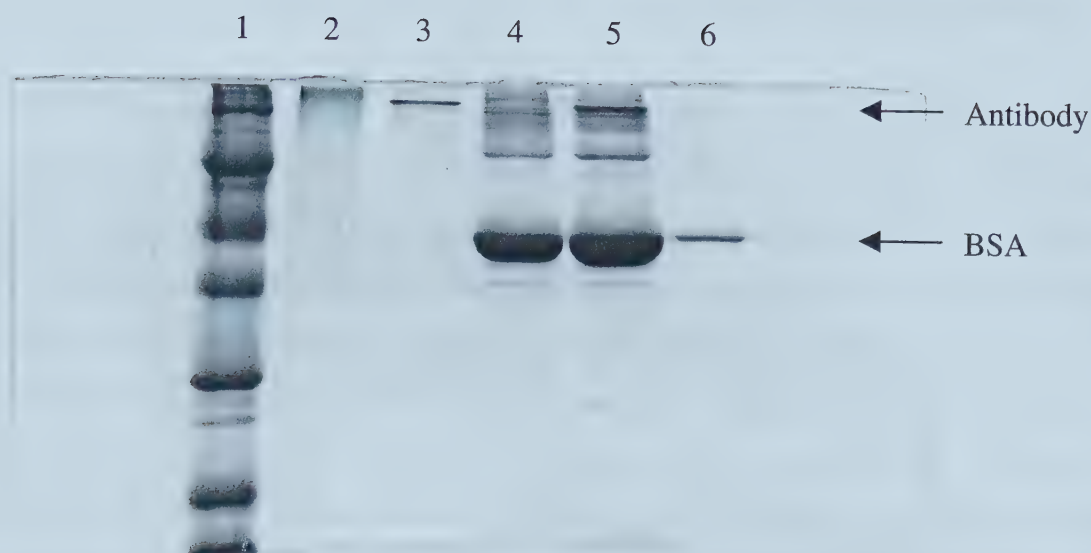


**Figure 2-4. Polyacrylamide gel electrophoresis of antibody preparations.** Samples were separated using a 10% SDS-PAGE gel and visualized by overnight staining with Coomassie Blue solution. Lanes 1-6 correspond to the following: lane 1, protein molecular weight markers; lane 2, E5 primary antibody (200  $\mu\text{g/ml}$ ); lane 3, polyclonal mouse IgG (100  $\mu\text{g/ml}$ ); lane 4, Cy3-labeled anti-mouse IgG (100  $\mu\text{g/ml}$ , containing 1 mg/ml BSA); lane 5, TMR-labeled anti-mouse IgG (100 $\mu\text{g/ml}$ , containing 1 mg/ml BSA); lane 6, BSA (50  $\mu\text{g/ml}$ ).



to the result expected for the Protein G column (Figure 2-5A). The majority of the antibody was eluted from the column in the second 1-ml fraction. To determine if there was antibody that was passing through the column without binding, the wash fractions from each application were pooled and reapplied to the column. It was found that there was not a significant breakthrough compared to the antibody levels from the first elution (Figure 2-5B). Non-IgG proteins such as BSA were found at high concentrations in the wash fractions of E5 (Figure 2-6) and the fluorescent antibodies (data not shown).

A second purification step was necessary for antibodies to be used in capillary electrophoresis experiments. The high-salt buffer (Tris-HCl / glycine) in the antibody fractions from the Protein G column may have influenced both injection of samples into the capillary and the subsequent electrophoresis run. Furthermore, it was desirable to concentrate the antibody fractions to provide a stock antibody solution for more efficient storage and use in further experiments. Techniques such as dialysis and gel filtration are commonly used to remove low molecular weight salts from solutions. However, they typically result in dilution of the desired species thereby requiring an additional concentration step. It was decided that ultrafiltration would provide the most efficient purification of antibody in a single step.

Initially, aliquots of the antibody samples were applied to ultrafiltration units with a molecular weight cut-off of 10,000 Da and a capacity of 400  $\mu$ l (Millipore Ultrafree-MC). The units were centrifuged to concentrate the solutes followed by re-dilution with de-ionized water. This buffer exchange procedure was repeated 3-4 times and effectively removed the salts from the antibody solution. However, the small capacity of the filtration units combined with a prohibitively low flow rate across the membrane resulted in very long centrifugation times for the volume of antibody to be purified (3-4 ml per application to the Protein G column). Centrifugation times of 30 minutes or longer per run were common, which was inconvenient as well as potentially damaging to the antibody. Furthermore, recovery of protein from these units was not complete; binding of the protein to the membrane was evident. Consequently, more efficient filtration units were investigated. A larger filtration unit with a volume of 4 ml was selected (Millipore





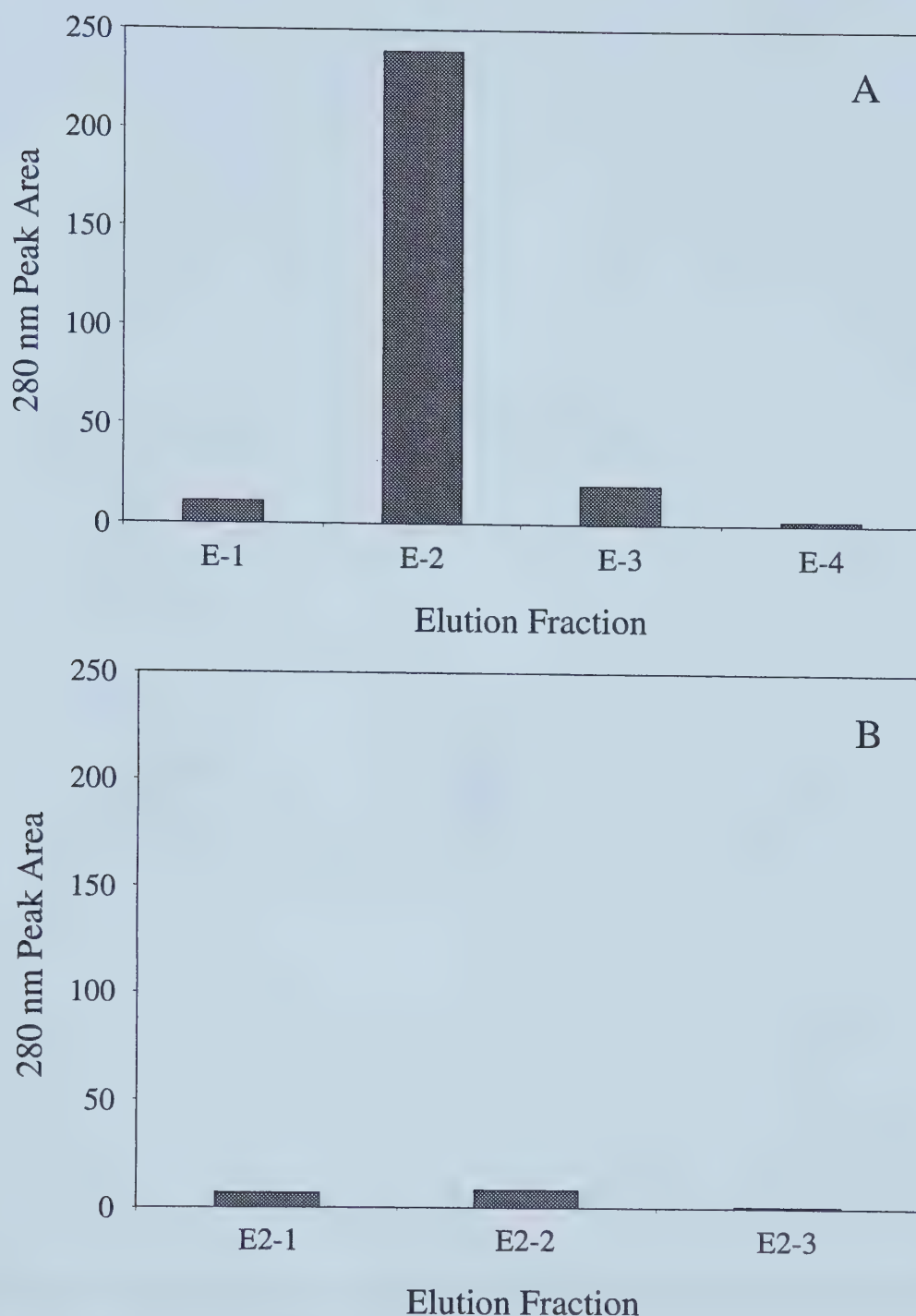


**Figure 2-5. Profile of antibody elution from a Protein G column.** E5 antibody was applied to a Protein G column and 1-ml fractions were collected and measured for protein content. **2-5A:** In the initial application of E5, the majority of the antibody was eluted in the second 1-ml fraction. **2-5B:** Re-application of wash fractions from the first elution did not result in recovery of significant amounts of E5 antibody.



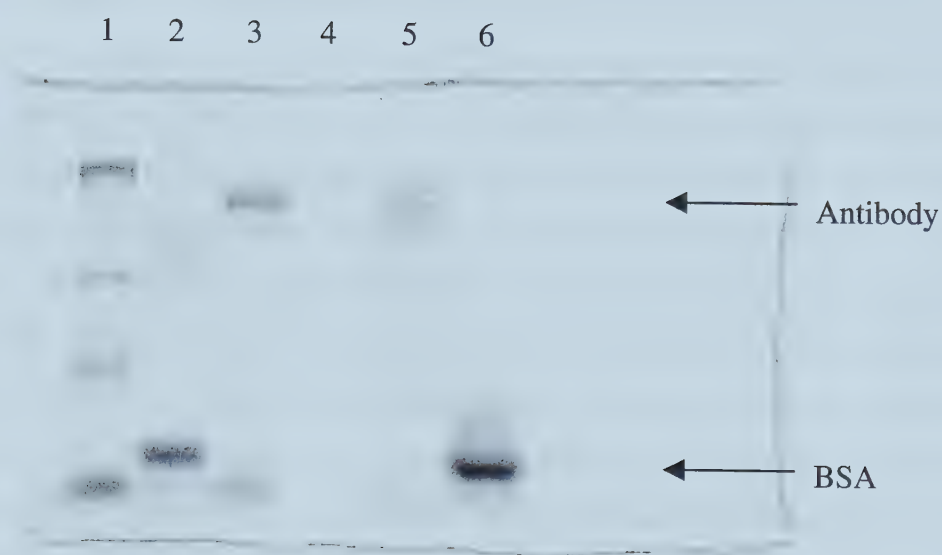


**Figure 2-6. Polyacrylamide gel electrophoresis of elution fractions from a Protein G column.** Samples were separated using a 6% SDS-PAGE gel and visualized by overnight staining with Coomassie Blue solution. Lanes 1-6 correspond to the following: lane 1, protein molecular weight markers; lane 2, BSA; lane 3, polyclonal mouse IgG; lane 4, first elution fraction from Protein G purification of E5 antibody; lane 5, second elution fraction from Protein G purification of E5; lane 6, wash fractions from E5 purification.



Ultrafree-4 centrifugal filter). This unit contained a high-flux Biomax membrane with a 10,000 Da molecular weight cutoff that allowed very rapid filtration under moderate force (3500 rpm or approximately 3100g). A typical run for 4 ml of antibody solution lasted 10 min, with the entire buffer exchange procedure being completed within about 40 min. The design of the filter unit also allowed for easier recovery of antibody from the membrane surface. To assess the efficiency of buffer exchange, the treated samples were subjected to absorbance measurements at 210 nm and 280 nm. As described in the previous section, the Tris-glycine elution buffer contributes strong interference at 210 nm. After 3 exchanges against PBS, which does not absorb significantly at 210 nm, Tris-glycine interference was eliminated when compared to the measurements at 280 nm. This was in agreement with the product literature which indicated that three exchange runs should remove 99% of the original solutes. The new filter units provided much more efficient desalting of the antibodies, which in turn reduced the possibility of a loss of antibody activity during the procedure. For the preparation of E5 antibody from cell supernatant, the final yield was approximately 2.7 mg of protein that was stored as stock solutions with a concentration between 820 and 930 µg/ml depending on the batch being purified. The concentration of antibody in supernatant from monoclonal cell lines is typically about 20 µg/ml (Harlow and Lane, 1988). Therefore, the estimated yield from the 116 ml of supernatant that was purified would be  $20 \mu\text{g/ml} \times 116 \text{ ml} = 2320 \mu\text{g} = 2.3 \text{ mg}$  E5 antibody. The actual yield exceeded this value, probably because the concentration of antibody in the supernatant was higher than the estimated level. It appears that the purification procedure did not result in significant loss of antibody. The final result of the two-step procedure was pure antibody solutions in a buffer that was consistent for use in affinity reactions as well as capillary electrophoresis.

### 2.3.3 Interaction between primary and fluorescent secondary antibodies

#### 2.3.3.1 Preliminary experiments with anti-BPDE-DNA antibody E5

Preliminary experiments were carried out to determine the affinity between the fluorescent secondary antibodies and the primary BPDE-DNA antibodies to be used in





the assay. This was necessary to confirm the formation of an antibody complex and to characterize the behavior of the complex relative to the free secondary antibody during capillary electrophoresis. Most of the initial experiments involved the E5 primary antibody, since it was the first antibody available. Typical capillary electrophoresis runs of samples containing Cy3- and TMR-labeled secondary antibodies with or without E5 are shown in Figure 2-7. Cy3 antibody (Cy3-Ab) demonstrated a very clean profile and a symmetrical peak shape. However, the Cy3-Ab / E5 complex was not seen in the corresponding electropherogram (Figure 2-7A). Higher concentrations of E5 were added in an attempt to increase the amount of complex formed, but no change was observed. It was unclear whether the antibody complex was co-migrating with the free Cy3-Ab or was disassociated during the run. Control samples of polyclonal mouse IgG mixed with Cy3-Ab were also tested, but with the same results. By comparison, TMR-labeled secondary antibody (TMR-Ab) also showed good behavior in the capillary, but a complex peak was observed for the sample containing E5. Although baseline separation was not achieved between the complex and free antibody peaks, this result was stable and reproducible. Based on these findings, TMR-Ab was chosen for use in subsequent experiments.

Some of the parameters involved in the capillary electrophoresis system were modified in an attempt to improve the separation between free TMR-labeled secondary antibody and the TMR-Ab / E5 complex. These factors included the separation voltage used during electrophoresis as well as the composition, molarity, and pH of the running buffer. The effect of varying the separation voltage is shown in Figure 2-8. Standard electrophoresis runs were carried out at 20 kV. Higher (25 kV) or lower (15 kV) voltages resulted in different migration times for both peaks, but did not significantly alter the resolution between the peaks. At 15 kV, there was also a noticeable broadening of the peaks compared to 20 kV runs. These effects were observed with Tris-borate running buffer as shown in Figure 2-8 and with 20 mM phosphate buffer in later experiments. It was decided that a running voltage of 20 kV would be used for further studies.



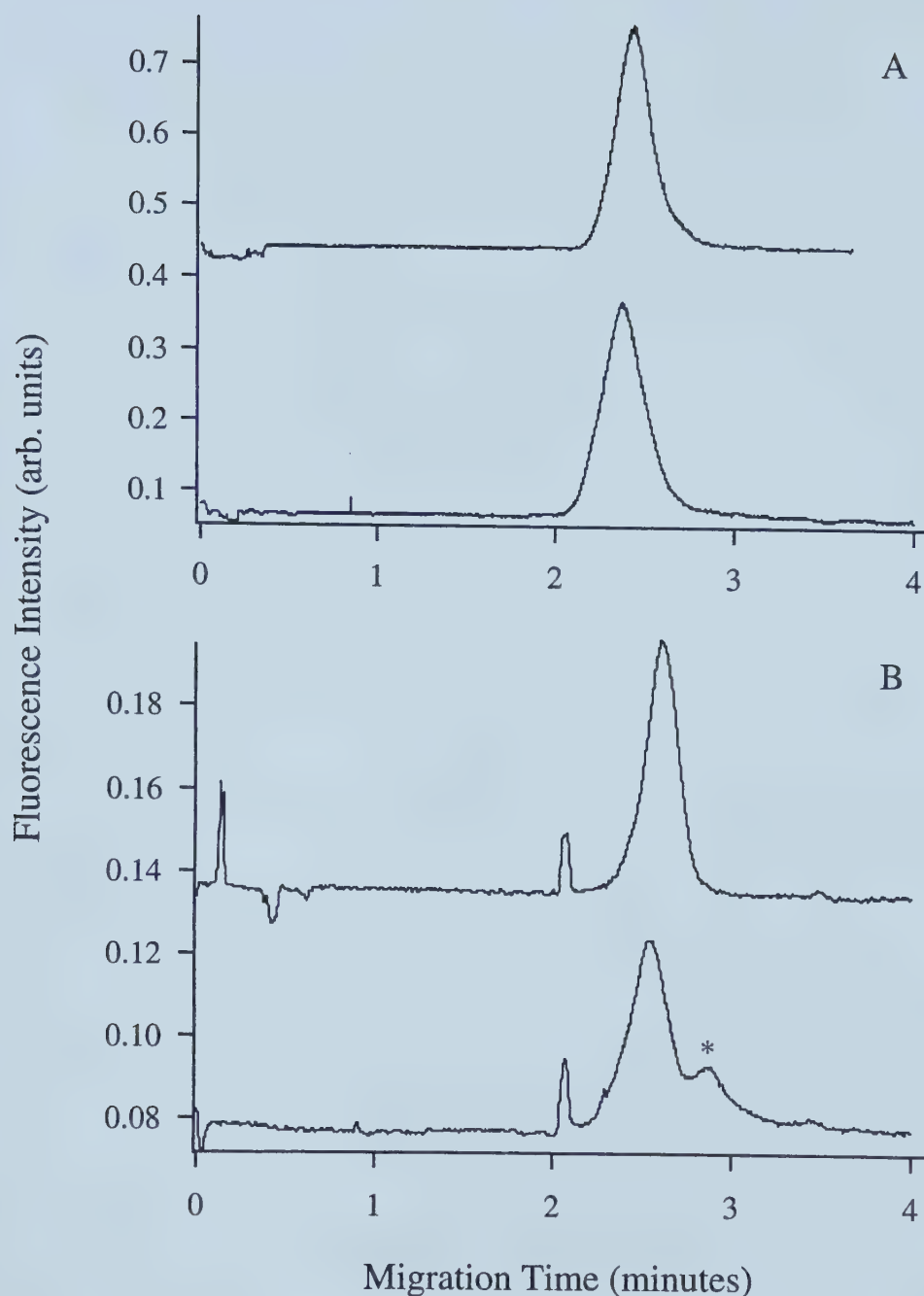


**Figure 2-7. Interaction between E5 antibody and fluorescent secondary antibodies.** **2-7A:** Electropherograms from samples containing Cy3-labeled secondary antibody only (top) and Cy3-labeled secondary antibody with E5 (bottom). **2-7B:** Electropherograms from samples containing TMR-labeled secondary antibody only (top) and TMR-labeled secondary antibody with E5 (bottom). The peak corresponding to the complex of both antibodies is identified by (\*).



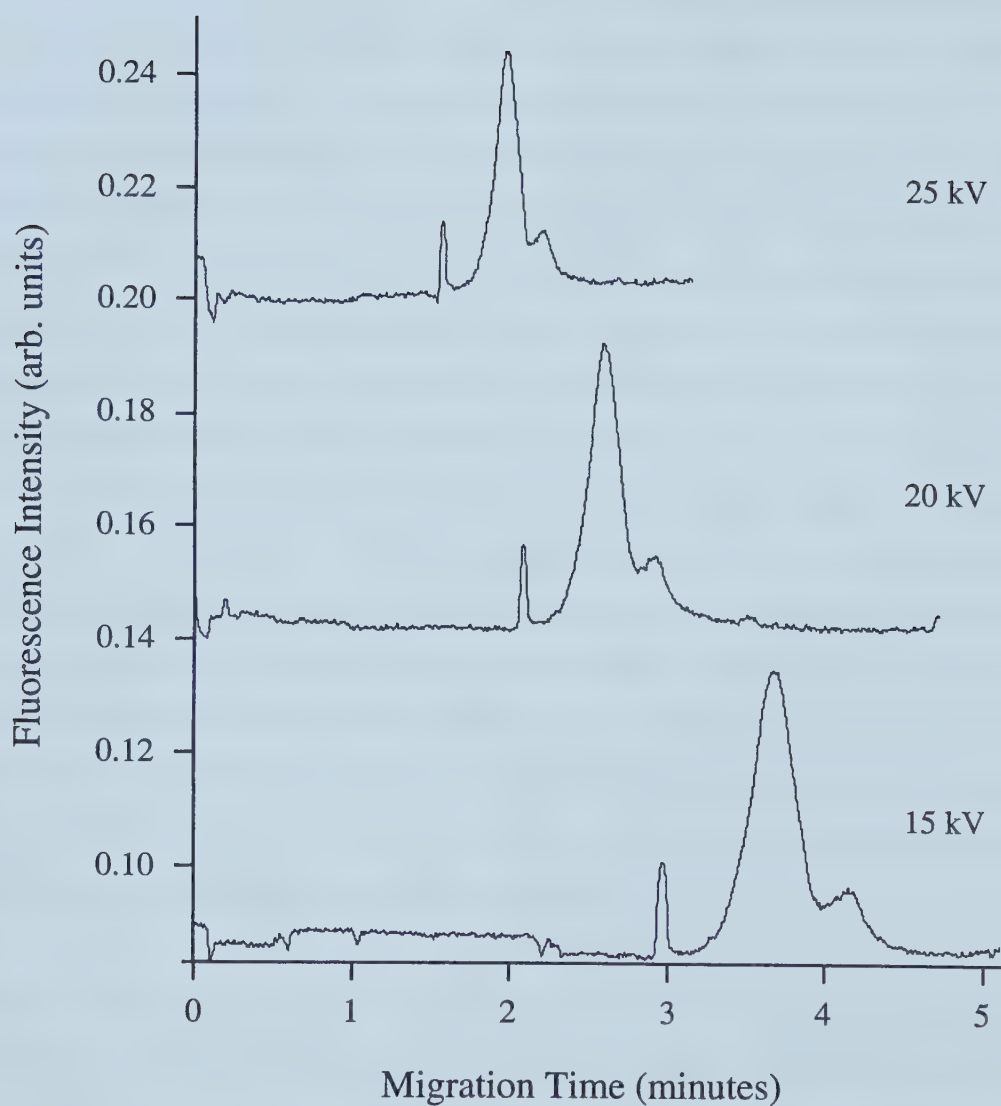


**Figure 2-8. Effect of separation voltage during capillary electrophoresis.** A sample containing TMR-antibody and E5 was subjected to a range of separation voltages (15-25 kV) using a Tris-borate running buffer.





The characteristics of the electrophoresis running buffer are important for the separation of components in a sample mixture as well as for the stability of molecular complexes. Samples containing TMR-labeled anti-mouse IgG secondary antibody and E5 primary antibody were initially tested using a Tris-borate buffer with a pH of 12. Different running buffers were then used to try to improve the stability of the antibody-antibody complex and its separation from free TMR-Ab. Typical results from runs using 20 mM sodium phosphate buffer, pH 10.2 are presented in Figure 2-9. In addition to E5 primary antibody, polyclonal mouse IgG and polyclonal human IgG were tested. Since TMR-Ab specifically recognizes mouse IgG, these samples were positive and negative controls, respectively. The phosphate running buffer seemed to improve the separation between the two peaks for the E5 antibody samples when compared to the Tris-borate buffer, but baseline separation was still not achieved. The electropherograms from the control samples indicated that the TMR-antibody was reacting as expected. Polyclonal mouse IgG at the same concentration as E5 resulted in a larger complex peak, while human IgG did not appear to react with the TMR-secondary antibody. The lack of a second peak for the human IgG sample suggested that it did correspond to an antibody-antibody complex in the other samples, and that it was not an artifact of the capillary electrophoresis system. It was not clear from this experiment why the E5 antibody produced a much smaller complex peak than equivalent amounts of polyclonal mouse IgG. One possibility was that the E5 antibody was impure or had degraded to some degree, decreasing the amount that would react with the secondary antibody.

To further investigate the interaction, a series of samples were prepared with increasing concentrations of E5 antibody added to a constant amount of TMR-antibody. A slight increase in the complex peak area was observed, but even at very high E5 levels (90  $\mu\text{g/ml}$ ) the majority of the TMR-antibody did not appear to be bound to E5 (Figure 2-10). A similar trend was also seen using increasing concentrations of polyclonal mouse IgG (positive control), but the complex peak for the 90  $\mu\text{g/ml}$  sample was considerably larger than the free TMR-antibody peak (data not shown). Despite these results, the specificity of the TMR-antibody was again evident as there was only one peak in the electropherogram for the sample containing 90  $\mu\text{g/ml}$  human IgG (negative control).



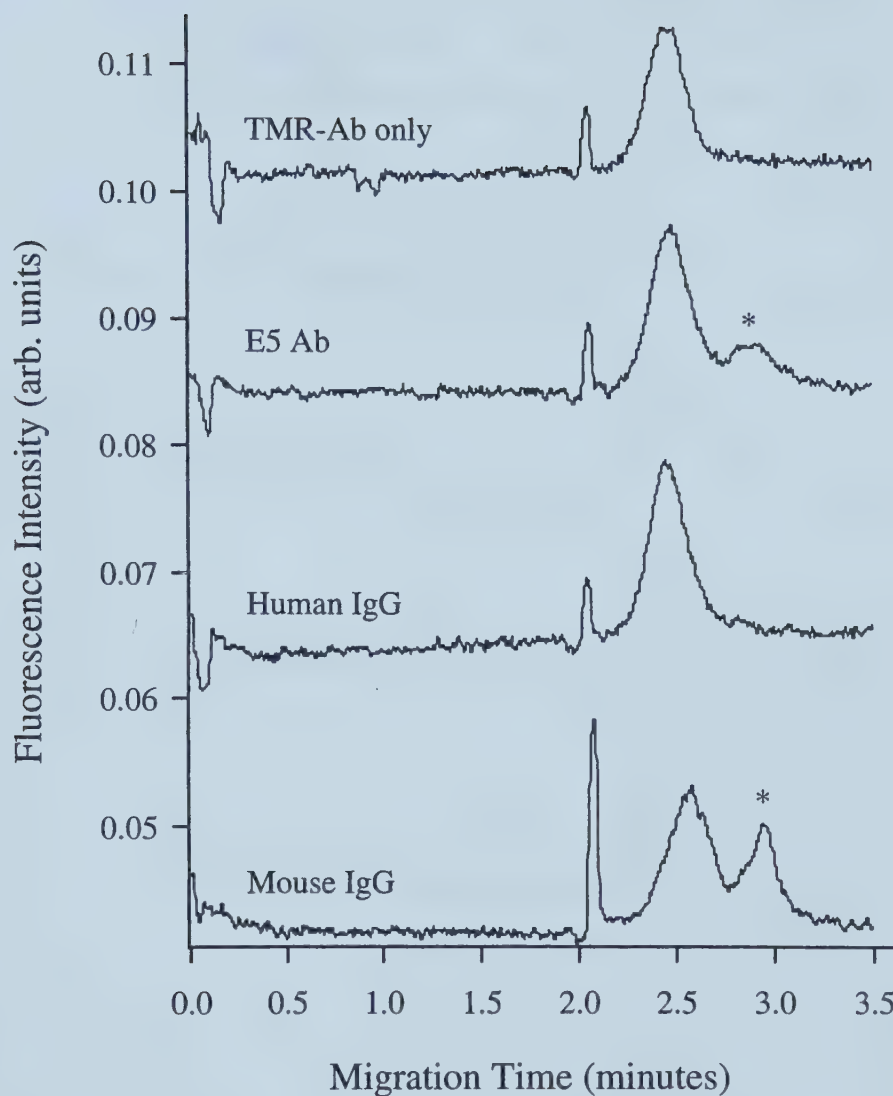


**Figure 2-9. Specificity of TMR-labeled secondary antibody.** TMR-labeled secondary antibody was mixed with E5, polyclonal mouse IgG (positive control), and polyclonal human IgG (negative control). A complex peak (\*) was observed for E5 and mouse IgG samples, but not for human IgG.



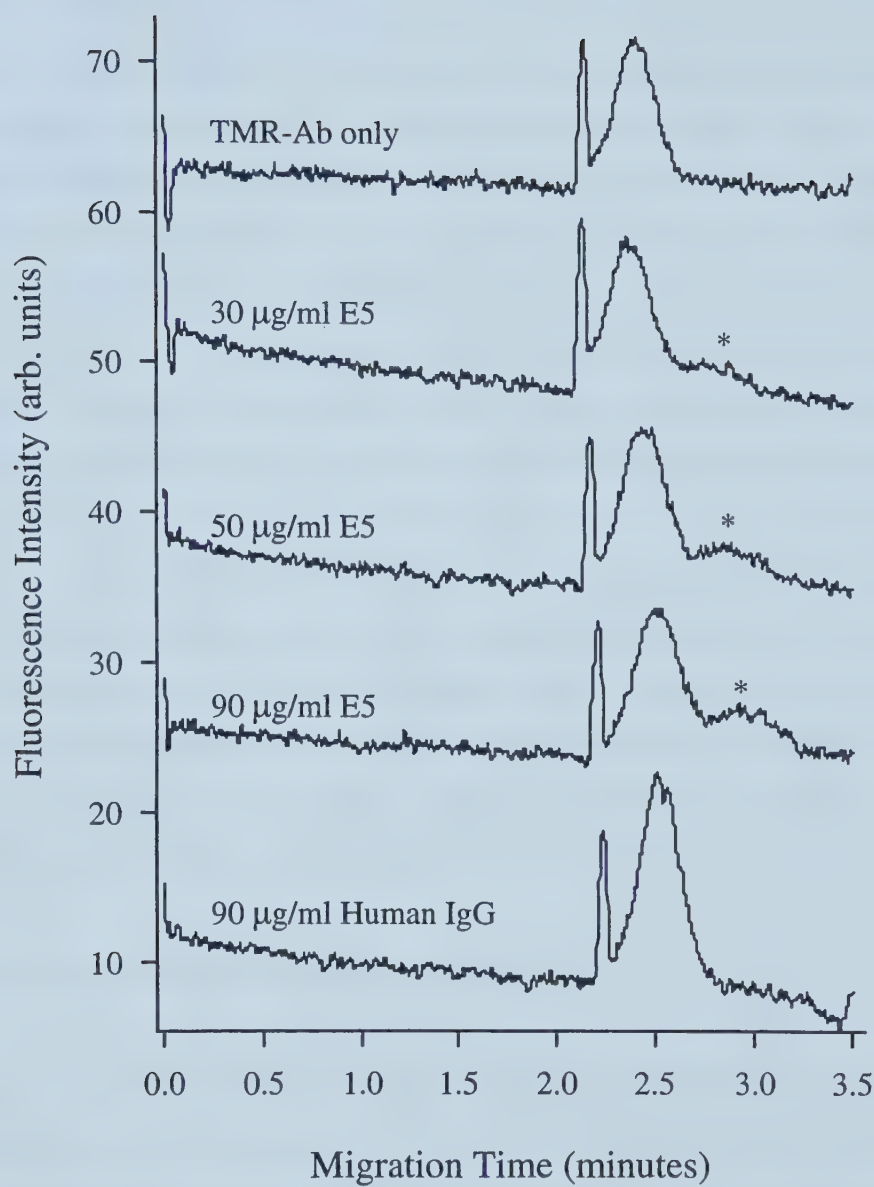


**Figure 2-10. Effect of E5 concentration on complex formation.** Samples were prepared using different concentrations of E5 antibody with a constant amount of TMR-labeled secondary antibody. Complex formation (\*) increased slightly at higher concentrations of E5. No complex formation occurred with human IgG at the highest level tested.





Some additional experiments were performed to assess the effect of running buffer composition on the formation of the antibody complex and its separation in the capillary. The effect of pH on these characteristics is presented in Figure 2-11. The phosphate buffer used was identical to that described above, but the pH varied between 9 and 12. The antibody complex appeared to be stable across this pH range in the phosphate buffer, as the ratio between the two peaks remained constant between runs. This was important because some antibodies become unstable at extreme values of pH, with maximal activity usually seen around neutral pH (7.0). The separation of free and bound TMR-antibody did not change significantly at the pH levels tested, and only at pH 12 was there a noticeable difference in the migration of the two peaks. In addition to the phosphate buffer, other common electrophoretic buffers were also tested in the capillary electrophoresis system. Samples analyzed using TBE (Tris-borate-EDTA) buffer, pH 8.3, and Tris-glycine buffer, pH 8.4, gave similar results to the experiments described above. The complex between TMR-antibody and E5 was separable from free TMR-antibody, but the relative intensity of the complex peak was small (data not shown). TBE was found to be a suitable running buffer for the DNA damage assay (Xing et al., 2001). Tris-glycine was also chosen for subsequent experiments because of its low current generation in the capillary, which reduces Joule heating, and its high electroosmotic flow (EOF). This higher EOF resulted in faster migration times than with TBE buffer.

#### 2.3.3.2 Comparison of anti-BPDE DNA antibodies

In addition to the E5 monoclonal antibody against BPDE-DNA, two commercially available antibodies (BD Pharmingen) were tested for use in the capillary electrophoresis assay. Whereas the effectiveness of E5 was uncertain in the preliminary experiments, the 5D11 and 8E11 clones were certified by the supplier and had been used extensively in the literature (Santella, 1999). The behavior of these antibodies in the capillary was compared to E5 by incubating all three with TMR-labeled anti-mouse IgG, then subjecting them to electrophoresis. Typical results from these samples using Tris-glycine running buffer are shown in Figure 2-12. The migration times of the free TMR-antibody and complex peaks were considerably faster than runs using the Tris-borate or phosphate



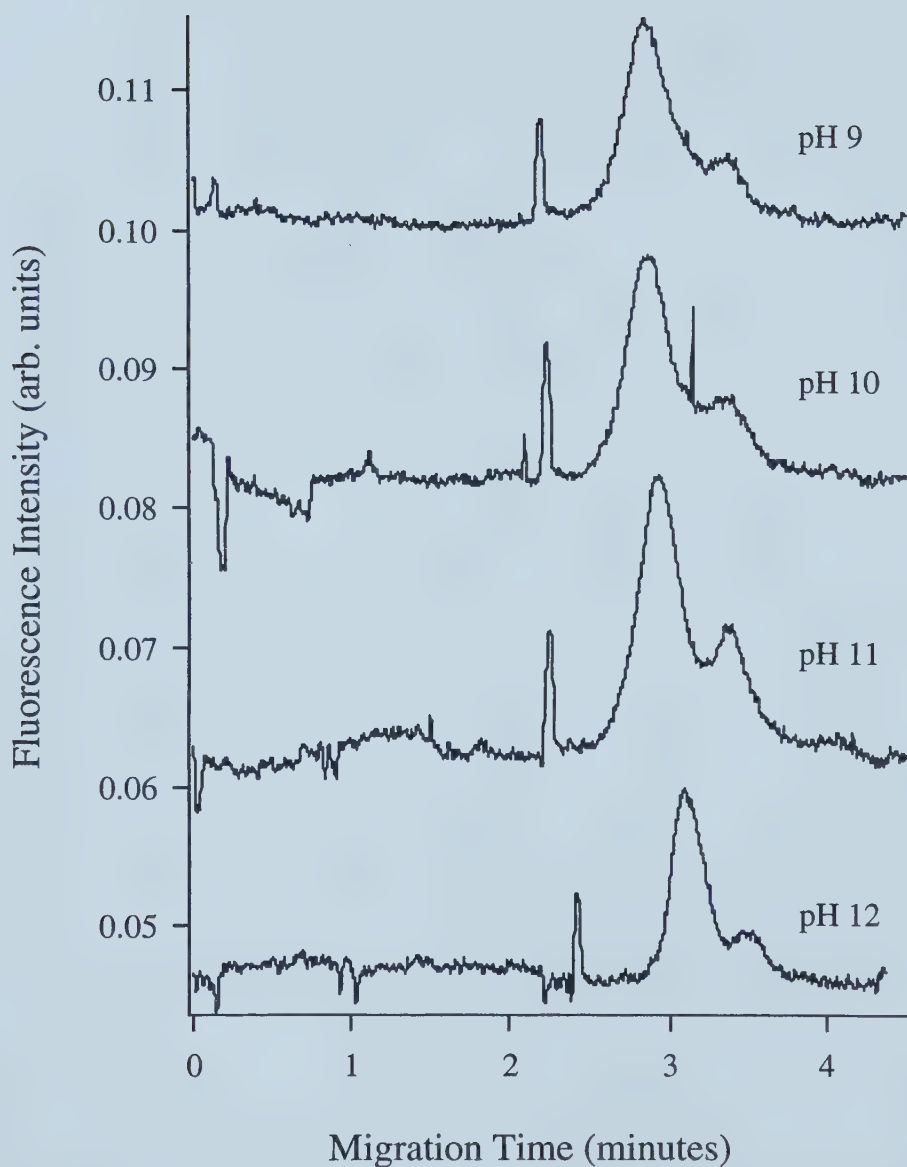


**Figure 2-11. Effect of pH on separation of antibody peaks.** A sample containing a mixture of TMR-labeled secondary antibody and E5 was subjected to capillary electrophoresis using 20 mM phosphate running buffers at different pH values (9-12).



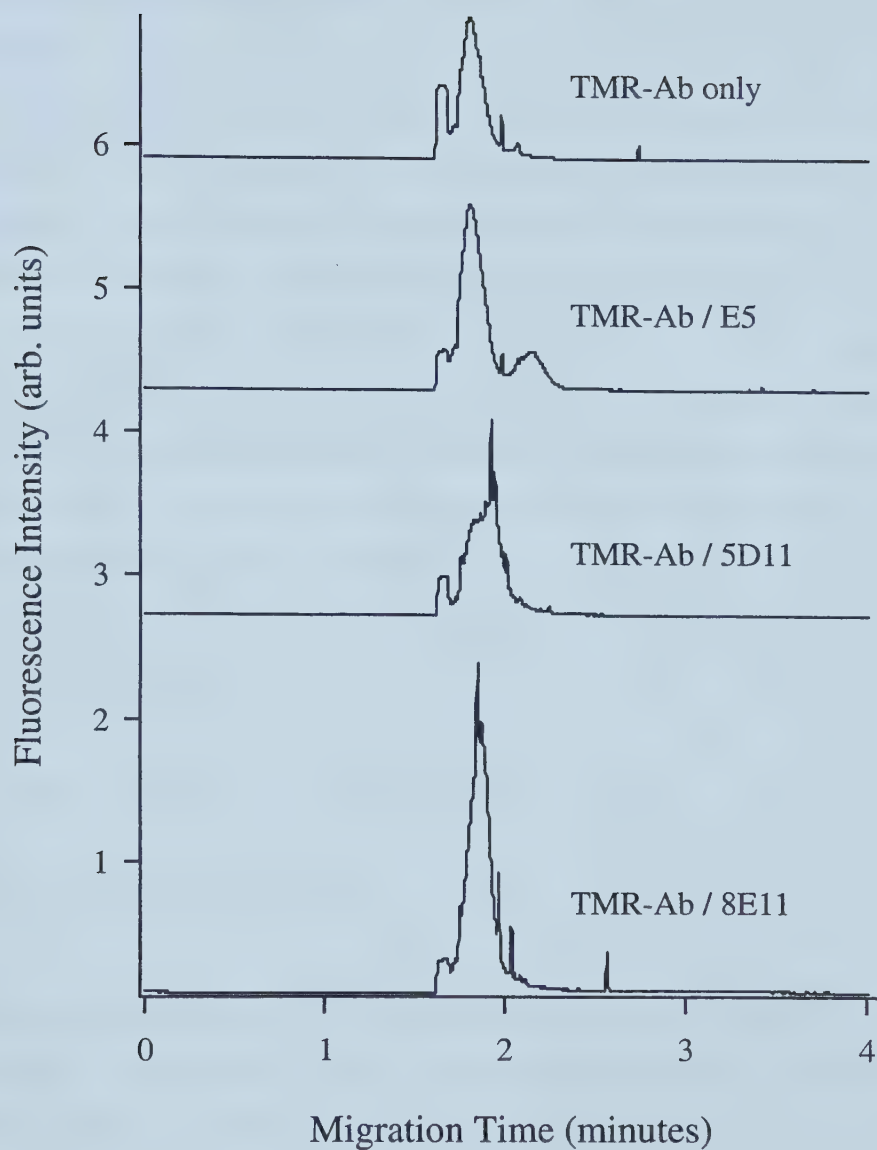


**Figure 2-12. Comparison of BPDE-DNA antibodies.** BPDE-DNA antibodies E5, 5D11, and 8E11 were incubated with TMR-labeled secondary antibody. Samples were analyzed by capillary electrophoresis using Tris-glycine running buffer (pH 8.4).





buffers described in the previous section. However, this decreased analysis time did not compromise resolution as the complex peak for the E5 sample was well separated. Complexes for the antibodies 5D11 and 8E11 were not separated from the free TMR-antibody peak under these conditions. In both cases, there was some evidence of binding with the fluorescent secondary antibody. For 5D11, there appeared to be a second peak when compared to the electropherogram for the sample containing only the TMR-antibody. This peak was unresolved from the free antibody peak. There was only one peak present for the 8E11 sample, but the fluorescent signal of the peak was enhanced when compared to an equivalent concentration of TMR-antibody only. A probable explanation for these results is that the complex peaks for both 5D11 and 8E11 were co-migrating with the free TMR-antibody. This behavior would suggest that the electrophoretic mobility and therefore the net charge of these antibodies are very similar to the fluorescent secondary antibody. In contrast, E5 would have a significantly different charge and mobility that would allow the separation of the complex peak. Despite these results, all three antibodies were tested in the DNA damage assay. DNA contains a high number of negative charges, therefore the antibody/antibody/DNA complex should be separable from the antibody peaks.

#### 2.3.4 Analysis of BPDE-modified DNA samples

##### 2.3.4.1 Experiments using E5 antibody

After preliminary characterization, the primary and secondary antibodies were tested as part of the DNA damage assay using a variety of DNA samples that had been modified with BPDE. Initial experiments were carried out using antibody E5 and TMR-labeled anti-mouse IgG with mouse skin DNA that had been treated with a large dose of BPDE. The resulting electropherograms did not show an extra peak corresponding to the complex of both antibodies with DNA as expected (Figure 2-13). Rather, there appeared to be a slight broadening of the peak corresponding to the TMR-antibody / E5 complex. It was unclear whether this result indicated that a broad DNA peak was co-migrating with the antibody complex peak or that the E5 antibody was not binding to the BPDE-DNA.



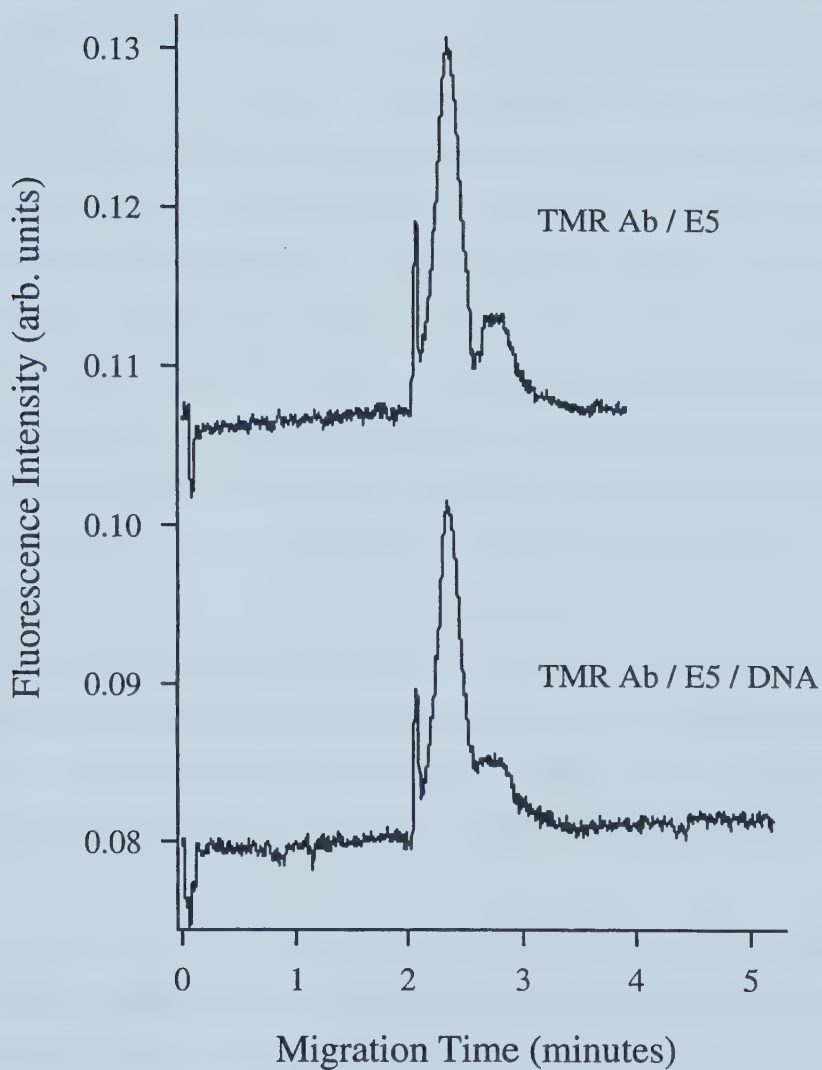


**Figure 2-13. Analysis of BPDE-damaged mouse skin DNA.** Native (non-denatured) BPDE-DNA (10  $\mu\text{g}/\text{ml}$ ) was incubated with E5 and TMR-labeled secondary antibody and analyzed by capillary electrophoresis. No DNA peak was observed, but there was a slight change in the antibody complex peak.



To verify the activity of the E5 antibody, a blotting procedure was performed. The BPDE-treated mouse skin DNA and control calf thymus DNA were immobilized on a membrane and incubated with E5 antibody. The binding efficiency was first assessed by adding an enzyme-conjugated secondary antibody that resulted in a colored precipitate being formed where E5 was present on the membrane (Figure 2-14A). Although there was a background level of color for the negative control DNA, the intensity was much stronger for the BPDE-DNA sample. This suggested that E5 was indeed binding specifically to the BPDE-DNA on the membrane. The procedure was then repeated using the fluorescent secondary antibody, which was visualized with a confocal laser microscope. Although the entire spots on the membrane were not analyzed, a visual inspection under the microscope revealed significant differences in fluorescent intensity between the BPDE and control DNA samples. Photographs representing the most intense areas of the two spots are shown in Figure 2-14B. The fluorescent points correspond to spots on the membrane where the secondary antibody is attached, either through specific or non-specific binding. The calf thymus control DNA showed very little signal, and was considered the background level of fluorescence attributable to non-specific binding. The BPDE-DNA sample showed considerably more fluorescence, indicating that the primary and secondary antibodies were forming a complex with the membrane-bound DNA. Although these results were only qualitative in nature, it was concluded that the immunoaffinity component of the DNA damage assay was working properly.

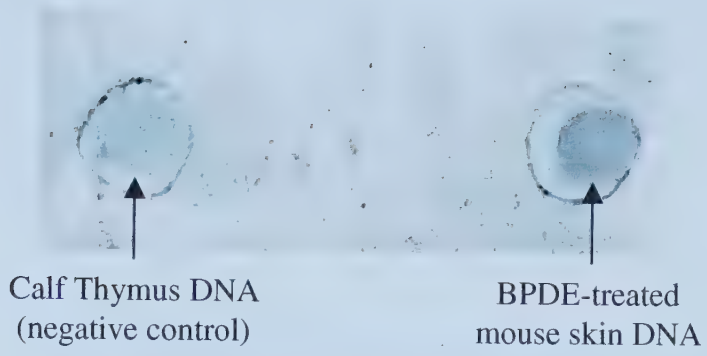
To further investigate the interaction between BPDE-DNA and the E5 antibody, new DNA samples were prepared. These samples were obtained by treating the human lung cell line A549 with varying concentrations of BPDE in solution, then extracting and purifying the cellular DNA. The range of concentrations used was much lower when compared to the mouse skin DNA. A549 and mouse skin DNA samples were then subjected to capillary electrophoresis using TBE and Tris-glycine running buffers with moderate pH (8.3-8.4). A similar result was seen for the mouse skin DNA samples as described previously. With higher levels of mouse skin DNA (50  $\mu\text{g/ml}$ ), the peak corresponding to the antibody complex was eliminated and a broad peak with a longer migration time was observed (Figure 2-15). This peak was thought to represent the com-







**Figure 2-14. Binding of E5 and TMR-labeled secondary antibody to mouse skin DNA.** Blotting experiments were performed to verify binding of antibodies to BPDE-damaged DNA. **2-14A:** Membrane-bound DNA was incubated with E5 and an enzyme-conjugated secondary antibody. DNA samples were blotted within the circles marked on the membrane. A colored precipitate was formed where the antibodies were attached to the membrane. There was significantly higher binding of E5 to the BPDE-DNA spot compared to the negative control. **2-14B:** The experiment was repeated using TMR-labeled secondary antibody, which was visualized with confocal laser microscopy. There was a stronger fluorescent signal for the BPDE-DNA sample compared to the negative control, indicating that the E5 and TMR antibodies were binding to the BPDE-DNA.

**A****B**

Calf Thymus DNA (negative control)



BPDE-treated mouse skin DNA



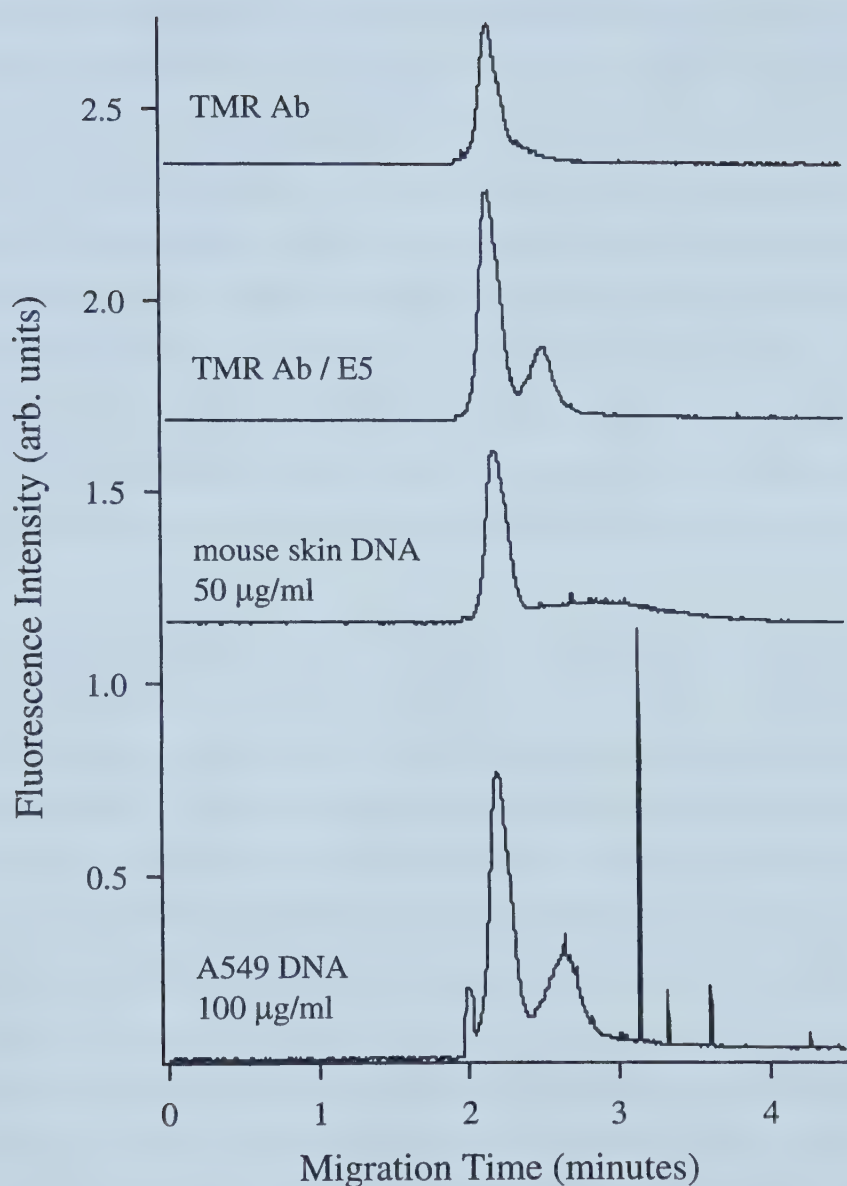


**Figure 2-15. Analysis of different BPDE-DNA samples using E5 antibody.** BPDE-damaged mouse skin DNA and A549 cellular DNA were heat-denatured then incubated with E5 and TMR-labeled secondary antibody and analyzed by capillary electrophoresis. The mouse skin DNA caused a broadening of the antibody complex peak. A549 DNA samples resulted in multiple spikes being observed in the electropherograms.





plex of both antibodies with the DNA. An explanation of the characteristics of this peak will be presented in the next section. Samples containing A549 DNA treated with the highest dose of BPDE (1 $\mu$ M) did not demonstrate a clear complex peak after capillary electrophoresis. Moderate (25  $\mu$ g/ml) and high (100  $\mu$ g/ml, shown in Figure 2-15) concentrations of A549 DNA were tested, but in both cases there were only sporadic peaks present in the electropherogram. These sharp fluorescent spikes were also visualized in the capillary using a microscope. They appeared to be intense, particle-like collections of fluorescence, as opposed to gradual bands of fluorescence typically seen for the antibody peaks. Replicate injections of these samples were then performed to assess the reproducibility of the spikes. It was observed that the spikes, although present in all replicate runs, varied considerably in their migration time, number, and intensity (Figure 2-16). Furthermore, these spikes were also seen in electropherograms from samples containing control A549 DNA (from cells that had not been treated with BPDE).

Several attempts were made to improve the performance of the DNA damage assay. The treatment conditions used for the samples described above were identical to those published previously (Xing et al., 2001). The protocol was modified by adding Tris borate buffer, pH 7.5 to the DNA sample before incubation with E5 antibody. The purpose of this addition was to neutralize the DNA solution and improve the affinity of E5 for the DNA. This change did not significantly affect the quality of the sample runs. Furthermore, the capillary treatment protocols and running buffers used previously (Xing et al., 2001) were employed to determine if the Tris-glycine buffer was unsuitable for the separation. The main difference between the Tris-glycine and TBE running buffers was the migration time of the antibody peaks; the TMR-antibody / E5 complex peak typically had a migration time of approximately 2.54 and 4.62 min, respectively (data not shown). However, the results for the A549 DNA samples were similar with non-reproducible spikes being present in the electropherograms of runs using TBE buffer. To rule out the possibility of the A549 samples being the problem, a second series of BPDE-treated A549 DNA samples were tested. These samples also yielded the same results. Finally, the length of the A549 DNA was considered as a possible reason for the separation problems. Samples were prepared using BPDE-damaged A549 DNA that was digested with EcoRI



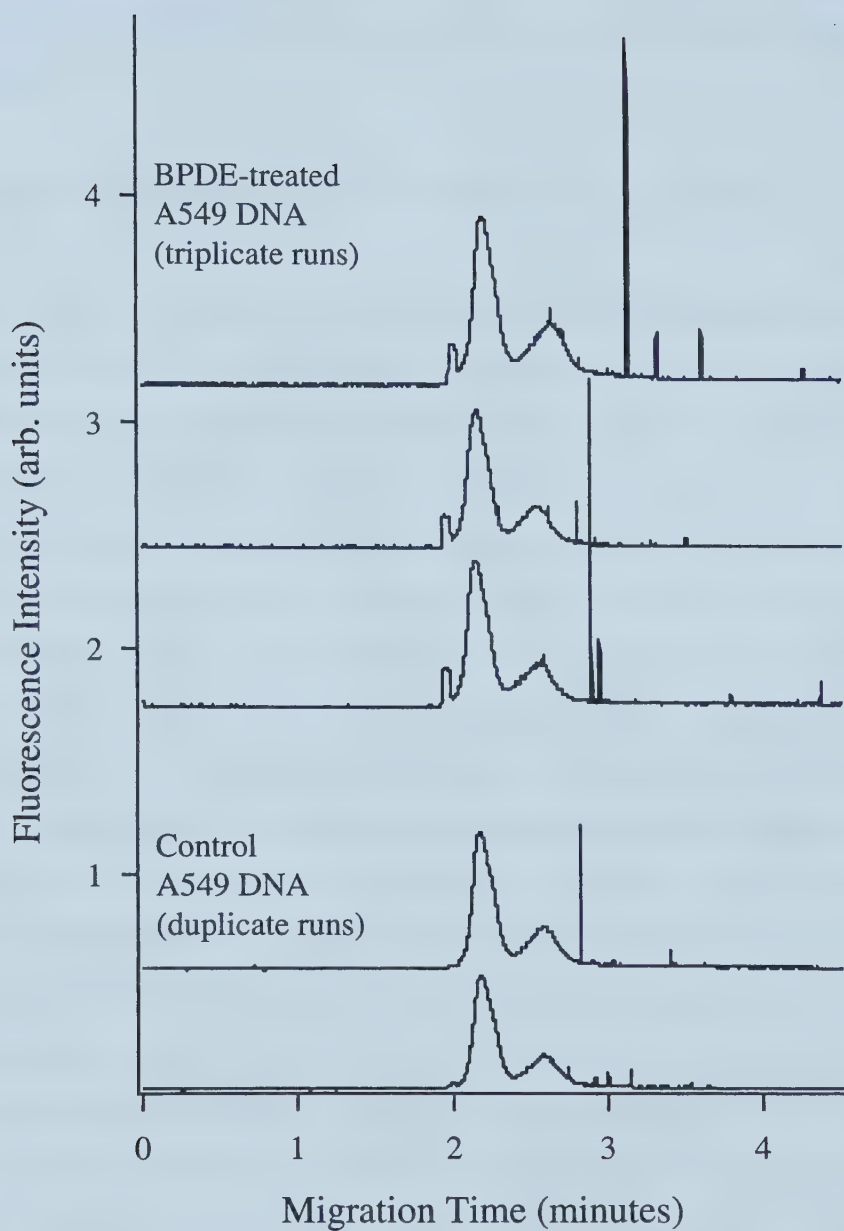


**Figure 2-16. Comparison of BPDE-treated and control A549 DNA samples.** Treated and control A549 samples were heat-denatured and then incubated with E5 and TMR-labeled secondary antibody and analyzed by capillary electrophoresis using Tris-glycine running buffer (pH 8.4). In both cases, non-reproducible spikes were observed.



restriction enzyme before incubation with E5 antibody. Again, capillary electrophoresis using TBE running buffer resulted in non-reproducible fluorescent spikes for the EcoRI digested DNA (Figure 2-17). From these results it was concluded that E5 may not be suitable for use in the DNA damage assay system, and that other primary antibodies should be tested.

#### 2.3.4.2 Interaction between BPDE-DNA and antibodies 8E11 and 5D11

A series of samples was prepared using the treated (1  $\mu$ M BPDE) and control A549 DNA combined with E5, 8E11, and 5D11 primary antibodies. They were analyzed using the Tris-glycine running buffer (pH 8.4) and a 50  $\mu$ m i.d. capillary. Because Tris-glycine generates a very low current, overheating of this larger capillary was not a concern. It was chosen to increase the sensitivity of the system relative to the 20  $\mu$ m i.d. capillary used in the previous experiments. From this series of samples, both E5 and 8E11 generated the same results as described above. Electropherograms from treated and control A549 DNA samples contained sporadic spikes for both antibodies (Figure 2-18). In contrast, antibody 5D11 demonstrated extensive binding to the A549 DNA, with the appearance of a new peak for both the treated and control samples. While there was also considerable spiking in the 5D11 electropherograms, the DNA / antibody complex peak was stable and reproducible in replicate runs. There was still no significant difference observed between the BPDE-damaged DNA and the undamaged DNA. To address this, DNA concentrations ranging from 1-100  $\mu$ g/ml were tested. Changing the concentration for both DNA samples resulted in a shifting of the migration time of the complex peak (Figure 2-19). This relationship between DNA concentration and migration time was remarkably consistent between treated and control A549 DNA, and was highly reproducible between runs. Figure 2-20 summarizes the combined data set of the two DNA types. Samples containing 1  $\mu$ g/ml DNA were not significantly different from mixtures containing only TMR-antibody and 5D11. The migration time of the free antibody peak was also consistent between runs ( $t = 1.88 \pm 0.03$  min,  $n = 19$ ), demonstrating the accuracy of the migration time measurements. A further observation





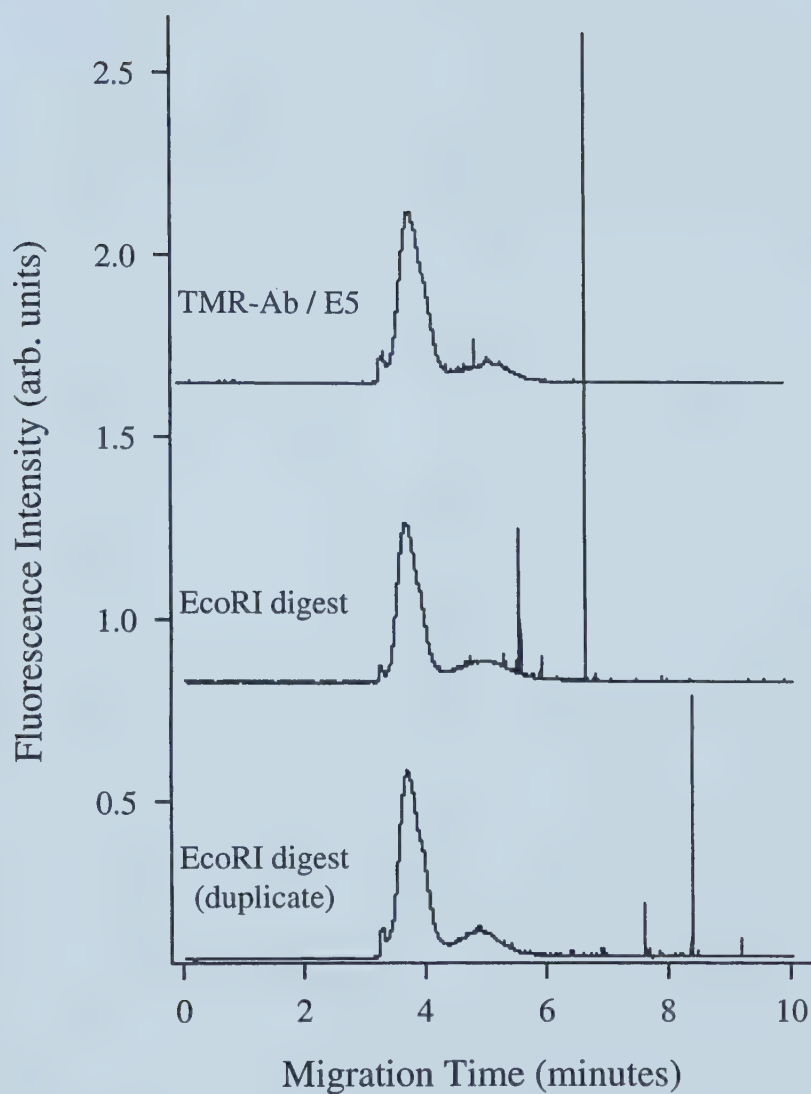


**Figure 2-17. Analysis of BPDE-treated A549 DNA digested by EcoRI.** BPDE-treated A549 DNA was digested with EcoRI restriction enzyme, heat-denatured, and incubated with E5 and TMR-labeled secondary antibody. Analysis was performed using TBE running buffer (pH 8.3). Digestion of DNA did not eliminate the spikes observed for undigested DNA samples.



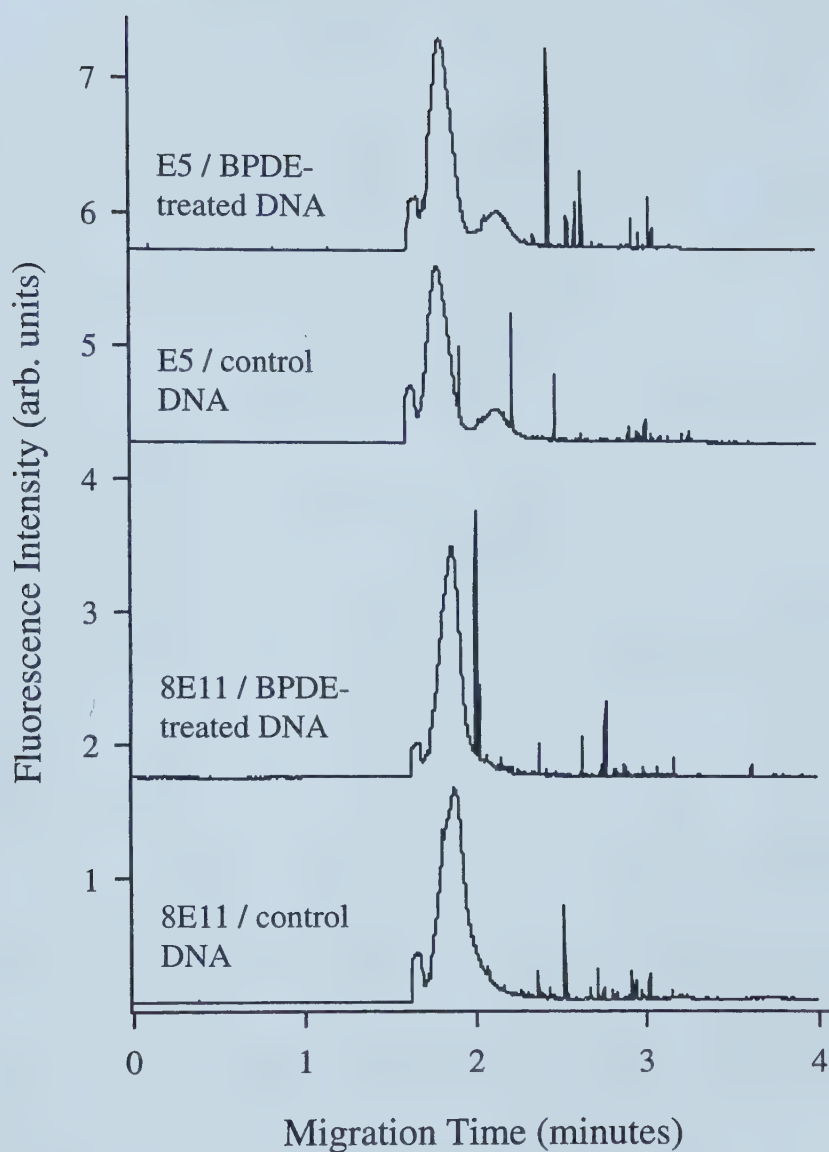


**Figure 2-18. Comparison of E5 and 8E11 antibodies with A549 DNA.** E5 and 8E11 primary antibodies were incubated with heat-denatured BPDE-treated and control A549 DNA samples and TMR-labeled secondary antibody. Samples were analyzed using Tris-glycine running buffer (pH 8.4). Non-reproducible spikes were present in the electropherograms from all samples.



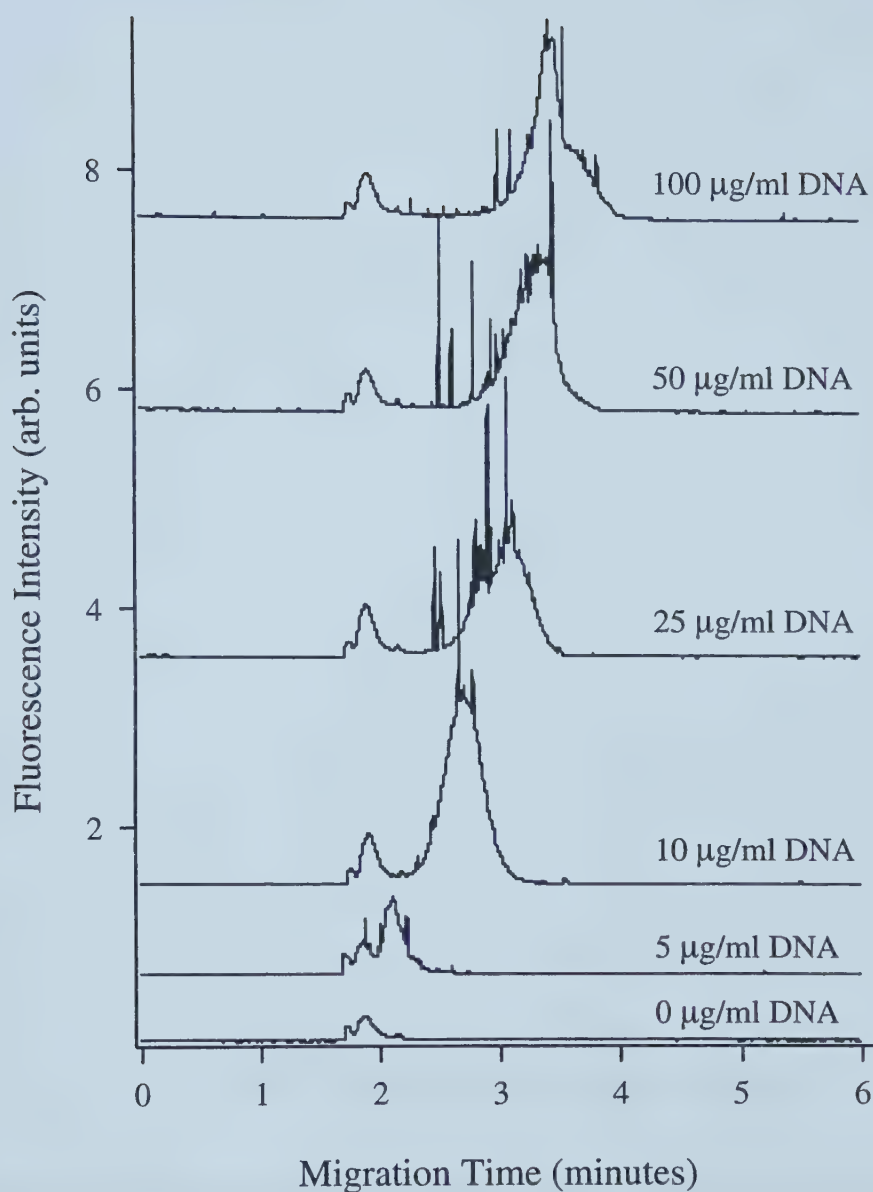


**Figure 2-19. Interaction between 5D11 antibody and A549 DNA.** Control A549 DNA samples were heat-denatured and incubated with 5D11 primary antibody and TMR-labeled secondary antibody. Samples were analyzed using Tris-glycine running buffer (pH 8.4). The migration time of the DNA complex peak was related to the DNA concentration in the sample. BPDE-treated A549 samples generated similar results.





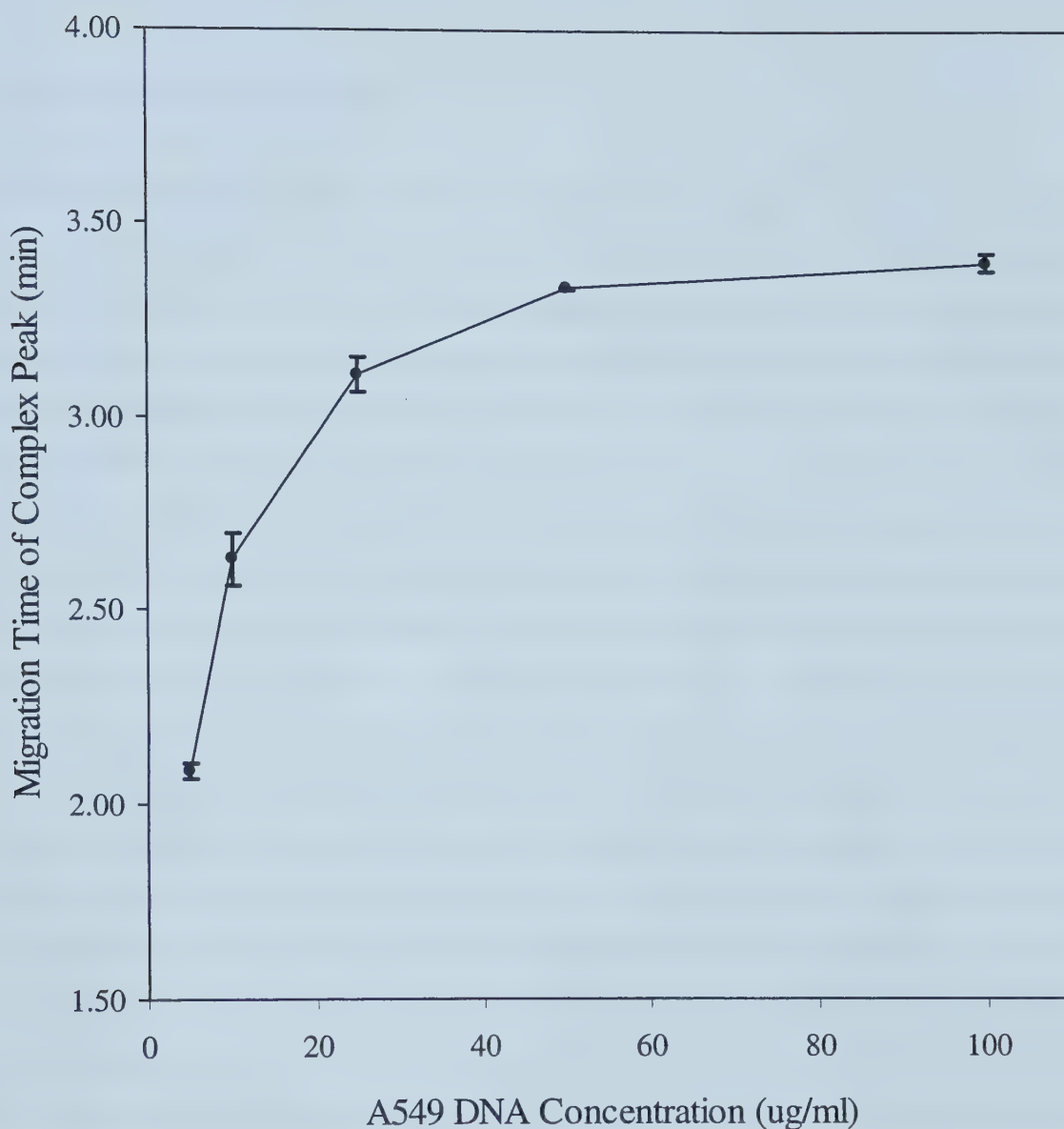


**Figure 2-20. Relationship between A549 DNA concentration and migration time of complex peak.** A range of concentrations of BPDE-treated and control A549 DNA were heat-denatured and incubated with 5D11 and TMR-labeled secondary antibody. Samples were analyzed using Tris-glycine running buffer (pH 8.4). The graph contains combined data from both types of DNA. Standard deviations of migration times are indicated by the bars for each data point. The migration time of the free antibody peak was consistent between runs ( $t = 1.88 \pm 0.03$  min,  $n = 19$ ).



from this experiment was the apparent enhancement of the fluorescent signal with DNA concentrations above 5  $\mu\text{g/ml}$ .

## 2.4 Discussion and conclusions

The results from the capillary electrophoresis studies described above were difficult to interpret. Experiments were conducted to assess the behavior of the primary and fluorescent secondary antibodies during capillary electrophoresis. The results indicated that the capillary electrophoresis system was operating as expected, and the laser-induced fluorescence detector was able to measure low levels of secondary antibody. For antibody E5 and TMR-labeled anti-mouse IgG, a complex peak was observed but was not resolved from the free TMR-antibody peak. This may be explained by the very slight difference in electrophoretic mobility of the two components of the mixture. Electrophoretic mobility in free-zone capillary electrophoresis depends on both the size and net charge of a molecule, or more specifically its charge-to-mass ratio. Antibodies are very large molecules ( $\sim 150,000$  Da) that contain a variable number of positively- and negatively-charged amino acid side chains at neutral pH values. Generally speaking, the net charge for most antibodies is very small compared to their molecular weight. The size of an antibody would therefore be the most important factor in its mobility. However, assuming that the primary and secondary antibodies have a small net charge and similar charge-to-mass ratios, the mobility of the antibody complex and free secondary antibody would not be significantly different. This was the case for the monoclonal antibodies 5D11 and 8E11, for which the complex peak could not be resolved. E5 antibody appeared to have a slightly higher negative charge than TMR-labeled secondary antibody in the pH range used ( $>8.3$ ). This resulted in a lower electrophoretic mobility and a longer migration time for the complex peak. Further analysis of the primary and secondary antibody characteristics would be useful in understanding the observed differences in mobility.

Samples containing TMR-anti-mouse IgG and E5 primary antibody incubated with BPDE-damaged DNA provided mixed results. DNA molecules have a high number of negative charges due to the phosphate component of the backbone structure. Therefore,



DNA was expected to migrate very slowly through the capillary and exhibit a significantly longer migration time than antibody molecules. Mouse skin DNA that contained a high level of BPDE adducts generated a broad peak corresponding to the DNA-antibody complex. This result suggested that there was a population of DNA molecules of varying size that was binding to the primary and secondary antibodies; this was confirmed using agarose gel electrophoresis (Xing et al., 2001). These smaller DNA fragments were likely a product of both the high level of damage induced by BPDE and the rigorous extraction procedure used. Consequently, their effective contribution to the overall mobility of the antibody-DNA complex was less than would be observed for full length genomic DNA. The high levels of BPDE adducts present in this DNA sample also meant that there would be numerous sites for the antibodies to bind to the DNA molecules. The end result was that the mobility of the DNA/primary/secondary antibody complex was very similar to the primary/secondary antibody complex. Nevertheless, these experiments seemed to indicate that E5 antibody was attached to the damaged DNA during capillary electrophoresis.

While the assay was generally successful for the mouse skin DNA samples, the opposite was the case for the BPDE-treated A549 cellular DNA. As described above, these samples resulted in the appearance of sporadic, non-reproducible spikes in the electropherogram. While these fluorescent particles migrated through the capillary after the antibody peaks (as expected for DNA), clear evidence of a complex being formed between the antibodies and A549 DNA was lacking. Furthermore, there appeared to be no difference between treated and control DNA samples. There are several potential explanations for these results. First, it is possible that the treatment of A549 cells with BPDE did not generate detectable levels of BPDE adducts in the DNA. BPDE is a very reactive compound and is relatively unstable in solution, where it decomposes into tetrol byproducts. Decomposition may occur more rapidly than uptake of BPDE into cells, migration of BPDE into the nucleus and subsequent alteration of the DNA. This may have been the case for the second series of A549 samples that were obtained for the purpose of a DNA repair study and were used to supplement the data summarized above. However, the first series of DNA samples that was used for most of the work presented in





this chapter was previously tested and found to contain BPDE adducts by Dr. James Xing, postdoctoral fellow within our research group (Xing et al., 2001).

A second explanation is that the DNA adduct levels in these original samples decreased with time between the two series of experiments. The DNA extraction and purification procedure used for these A549 DNA samples resulted in the DNA being redissolved in a sodium hydroxide solution. It is possible that the BPDE adducts in the DNA were labile under the alkaline conditions, even though the samples were stored at  $-20^{\circ}\text{C}$ . This would explain why a stable DNA complex peak was observed in the initial study, but not in the experiments presented above. After these unsuccessful results, some of the A549 samples were re-analyzed by Dr. Xing using the same protocol as previously published (Xing et al., 2001). Similar conclusions were reached, specifically the absence of a DNA complex peak and the appearance of non-reproducible spikes in the electropherogram. Blotting experiments similar to those described for mouse skin DNA were not performed with A549 DNA samples, but may have been able to support one or both of these theories.

A third possibility is that the primary and secondary antibodies were forming a complex with BPDE adducts present in the A549 DNA, but the migration of the complex through the capillary was inconsistent. The antibody/DNA complex may have formed aggregates or precipitates during the incubation step or under electrophoretic conditions in the capillary. It is possible these aggregates would not have migrated as a sharp "band" typically observed in capillary electrophoresis. Instead, they may have consisted of a collection of particles similar to those observed visually in the capillary and that resulted in spikes in the electropherogram.

Other commercially available antibodies capable of recognizing BPDE-damaged DNA were used in comparison to E5. The monoclonal antibody 8E11 (Santella et al., 1984) exhibited similar behavior to E5. This result ruled out the possibility that E5 antibody was inactive, since 8E11 has been used successfully in numerous studies and is tested for activity by the supplier. An entirely different result was obtained for samples containing A549 DNA and 5D11 monoclonal antibody. 5D11 appeared to form a non-specific



complex with both BPDE-damaged and control A549 DNA. However, instead of a stable migration time, the complex peak migrated differently depending on the concentration of the DNA in the premixed sample. The approach that is typically used in affinity capillary electrophoresis (ACE) depends on the strength of association between the antibody (or other receptor) and the antigen (or other ligand) (Heegaard et al., 1998). Monoclonal antibodies typically have a very strong affinity for their specific antigen and a stable complex is maintained in the capillary. This complex peak usually exhibits a consistent migration time. For weaker interactions, the ligand is usually added to the running buffer, and a transient complex is formed. The migration time of the complex peak changes in response to the concentration of the ligand in the buffer. This variation of time can then be used to derive the binding constant of the receptor-ligand complex (Heegaard et al., 1998). Although A549 DNA was not added to the running buffer in these experiments, the results resemble this type of experiment. 5D11 antibody has been found to cross-react to some extent with normal DNA (Santella et al., 1984). The binding constant for this non-specific interaction would probably be considerably weaker than for BPDE adducts. Dissociated 5D11 antibody would tend to migrate faster than DNA in the capillary and re-association may not occur. However, fast "on" binding kinetics combined with the viscosity of the DNA/antibody mixture in the injection plug may have inhibited separation during electrophoresis. This would explain why higher amounts of A549 DNA caused the complex peak to shift, but not the free TMR-antibody peak. The curve shown in Figure 20 appears to approach a plateau at about 3.5 min; this may approximate the migration time of DNA under these conditions. Nevertheless, it was concluded that antibody 5D11 would probably not be suitable for use in the DNA damage assay because of the significant cross-reactivity.

As described above, the reason for the inconsistent results in the detection of BPDE-DNA adducts was unclear. There are presently no commercially available BPDE-DNA standards that could be used as a positive control. For this reason, the focus of the research project was changed to address this deficiency. It was decided that the design and synthesis of a fluorescent DNA standard containing known amounts of BPDE adducts was necessary. The results of this synthesis are presented in Chapter 3. By using



this DNA standard, Dr. Hailin Wang and Ms. Paula Murphy have since been able to optimize the assay conditions and determine BPDE adducts in cellular DNA samples.



## 2.5 References

- Ausubel, F.M. (ed.). Current Protocols in Molecular Biology (volume 1-4, with updates). Greene Pub. Associates and Wiley Interscience, New York (1992-2001).
- Baan, R.A., van den Berg, P.T.M., Watson, W.P., and Smith, R.J. *In situ* detection of DNA adducts formed in cultured cells by benzo[*a*]pyrene dilepoxide (BPDE), with monoclonal antibodies specific for the BP-deoxyguanosine adduct. *Toxicol Environ Chem* 16:325-339 (1988).
- Beach, A.C. and Gupta, R.C. Human biomonitoring and the  $^{32}\text{P}$ -postlabeling assay. *Carcinogenesis* 13:1053-1074 (1992).
- Booth, E.D., Aston, J.P., van den Berg, P.T.M., Baan, R.A., Riddick, D.A., Wade, L.T., Wright, A.S., and Watson, W.P. Class-specific immunoadsorption purification for polycyclic aromatic hydrocarbon-DNA adducts. *Carcinogenesis* 15:2099-2106 (1994).
- Choi, D.J., Marino-Alessandri, D.J., Geactinov, N.E., and Scicchitano, D.A. Site-specific benzo[*a*]pyrene diol epoxide-DNA adducts inhibit transcription elongation by bacteriophage T7 RNA polymerase. *Biochemistry* 33:780-787 (1994).
- Denissenko, M.F., Pao, A., Tang, M., and Pfeifer, G.P. Preferential formation of benzo[*a*]pyrene adducts at lung cancer mutational hotspots in *p53*. *Science* 274:430-432 (1996).
- Eisenbrand, G. and Tang, W. Food-borne heterocyclic amines. Chemistry, formation, occurrence and biological activities: a literature review. *Toxicology* 84:1-82 (1993).
- Friedberg, E.C., Walker, G.C., and Siede, W. DNA Repair and Mutagenesis. ASM Press, Washington, DC (1995).
- Hanelt, S., Helbig, R., Hartmann, A., Lang, M., Seidel, A., and Speit, G. A comparative investigation of DNA adducts, DNA strand breaks and gene mutations induced by benzo[*a*]pyrene and ( $\pm$ )-*anti*-benzo[*a*]pyrene-7,8-diol 9,10-oxide in cultured human cells. *Mutat Res* 390:179-188 (1997).
- Harlow, E. and Lane, D. Antibodies: A Laboratory Manual. Cold Spring Harbor Laboratory Press, Cold Spring Harbor, NY (1988).
- Hecht, S.S. Biochemistry, biology, and carcinogenicity of tobacco-specific *N*-nitrosamines. *Chem Res Toxicol* 11:560-603 (1998).





- Heegaard, N.H.H., Nilsson, S., and Guzman, N.A. Affinity capillary electrophoresis: important application areas and some recent developments. *J Chromatogr B* 715:29-54 (1998).
- Hess, M.T., Gunz, D., Luneva, N., Geactinov, N.E., and Naegeli, H. Base pair conformation-dependent excision of benzo[*a*]pyrene diol epoxide-guanine adducts by human nucleotide excision repair enzymes. *Mol Cell Biol* 17:7069-7076 (1997).
- Le, X.C., Xing, J.Z., Lee, J., Leadon, S.A., and Weinfeld, M. Inducible repair of thymine glycol detected by an ultrasensitive assay for DNA damage. *Science* 280:1066-1069 (1998).
- Le, X., Scaman, C., Zhang, Y., Zhang, J., Dovichi, N.J., Hindsgaul, O., and Palcic, M.M. Analysis by capillary electrophoresis: laser-induced fluorescence detection of oligosaccharides produced from enzyme reactions. *J Chromatogr A* 716:215-220 (1995).
- Melikian, A.A., Sun, P., Prokopczyk, B., El-Bayoumy, K., Hoffmann, D., Wang, X., and Waggoner, S. Identification of benzo[*a*]pyrene metabolites in cervical mucus and DNA adducts in cervical tissues in humans by gas chromatography-mass spectrometry. *Cancer Letters* 146:127-134 (1999).
- Pavanello, S., Favretto, D., Brugnone, F., Mastrangelo, G., Dal Pra, G., and Clonfero, E. HPLC/fluorescence determination of *anti*-BPDE-DNA adducts in mononuclear white blood cells from PAH-exposed humans. *Carcinogenesis* 20:431-435 (1999).
- Pfeifer, G.P., Denissenko, M.F., and Tang, M. PCR-based approaches to adduct analysis. *Toxicol Letters* 102-103:447-451 (1998).
- Poirier, M.C., Santella, R., Weinstein, I.B., Grunberger, D., and Yuspa, S.H. Quantitation of benzo[*a*]pyrene-deoxyguanosine adducts by radioimmunoassay. *Cancer Res* 40:412-416 (1980).
- Santella, R.M. Immunological methods for detection of carcinogen-DNA damage in humans. *Cancer Epidemiology Biomarkers & Prevention* 8:733-739 (1999).
- Santella, R.M., Lin, C.D., Cleveland, W.L., and Weinstein, I.B. Monoclonal antibodies to DNA modified by a benzo[*a*]pyrene diol epoxide. *Carcinogenesis* 5:373-377 (1984).
- Shinozaki, R., Inoue, S., and Choi, K.S. Flow cytometric measurement of benzo[*a*]pyrene-diol-epoxide-DNA adducts in normal human peripheral lymphocytes and cultured human lung cancer cells. *Cytometry* 31:300-306 (1998).



- Shuker, D.E.G. and Farmer, O.B. Relevance of urinary DNA adducts as markers of carcinogen exposure. *Chem Res Toxicol* 5:450-460 (1992).
- Szeliga, J. and Dipple, A. DNA adduct formation by polycyclic aromatic hydrocarbon dihydrodiol epoxides. *Chem Res Toxicol* 11:1-11 (1998).
- Thrall, B.D., Mann, D.B., Smerdon, M.J., and Springer, D.L. DNA polymerase, RNA polymerase and exonuclease activities on a DNA sequence modified by benzo[a]pyrene diolepoxide. *Carcinogenesis* 13:1529-1534 (1992).
- van Agen, B., Maas, L.M., Zwingmann, I.H., van Schooten, F.J., and Kleinjans, J.C.S. B[a]P-DNA adduct formation and induction of human epithelial lung cell transformation. *Environ Mol Mutagen* 30:287-292 (1997).
- Wang, J.S. and Groopman, J.D. DNA damage by mycotoxins (Review). *Mutat Res* 424:167-181 (1999).
- Weinfeld, M. and Soderlind, K.M.  $^{32}\text{P}$ -postlabeling detection of radiation-induced DNA damage: identification and estimation of thymine glycols and phosphoglycolate termini. *Biochemistry* 30:1091-1097 (1991).
- Wu, X., Gu, J., Amos, C.I., Jiang, H., Hong, W.K., and Spitz, M.R. A parallel study of *in vitro* sensitivity to benzo[a]pyrene diol epoxide and bleomycin in lung carcinoma cases and controls. *Cancer* 83:1118-1127 (1998).
- Xing, J.Z., Carnelley, T., Lee, J., Watson, W.P., Booth, E., Weinfeld, M., and Le, X.C. Assay for DNA damage using immunochemical recognition and capillary electrophoresis. In: *Methods in Molecular Biology 162: Capillary Electrophoresis of Nucleic Acids*, Vol. 1: Introduction to the Capillary Electrophoresis of Nucleic Acids (Mitchelson K.R., and Cheng, J. Eds.) pp 419-428. Humana Press Inc., New Jersey (2001).
- Zeisig, M. and Moller, L.  $^{32}\text{P}$ -HPLC suitable for characterization of DNA adducts formed *in vitro* by polycyclic aromatic hydrocarbons and derivatives. *Carcinogenesis* 16:1-9 (1995).



## **Chapter 3: Synthesis and characterization of a fluorescent BPDE-DNA damage standard**

### **3.1 Introduction**

As described in Chapter 2, attempts to analyze BPDE-DNA adducts in cellular DNA samples lead to inconclusive results. We realized that a standard DNA molecule containing BPDE adducts was needed to better characterize antibody binding and to optimize the assay parameters. Such a standard would be very useful in the development of DNA damage assays, but there are none currently available to serve this purpose.

An additional consideration in the development of the assay is calibration of the fluorescent signal of the DNA-antibody complex. The initial application of the assay was calibrated by comparing the fluorescent intensity of the DNA-antibody peak for samples with damaged DNA to a calibration curve constructed from samples containing known amounts of bromodeoxyuridine (BrdU) and an anti-BrdU antibody (Le et al., 1998). Ideally, this indirect calibration would be replaced by a direct calibration using a DNA standard and the antibodies for the DNA damage type being investigated.

To help address these issues, a synthetic, fluorescent-labeled DNA damage standard was designed using BPDE adducts as the model damage type. This chapter describes the procedure for synthesis of the standard, as well as some examples of its utility relative to the capillary electrophoresis DNA damage assay.

### **3.2 Materials and Methods**

#### **3.2.1 Reagents**

Unmodified oligonucleotides were synthesized by the Department of Biochemistry DNA synthesis laboratory, University of Alberta, or by Integrated DNA Technologies (Coralville, IA). All oligonucleotides were purified by sequencing polyacrylamide gel







electrophoresis prior to use. Purity of the oligonucleotides was confirmed by  $^{32}\text{P}$ -radiolabeling and gel electrophoresis. Tetramethylrhodamine (TMR) - labeled oligonucleotide was synthesized by University Core DNA Services, (University of Calgary, AB).  $(\pm)$ -r-7,t-8-dihydroxy-t-9,10-epoxy-7,8,9,10-tetrahydrobenzo[*a*]pyrene (anti)  $[(\pm)$ -anti-BPDE] was supplied by the National Cancer Institute Chemical Carcinogen Reference Standard Repository (Midwest Research Institute, Kansas City, MO). Premixed polyacrylamide / bisacrylamide (19:1) solution was purchased from BioRad Laboratories. Enzymes were supplied by Amersham Pharmacia Biotech. Antibodies 5D11 and 8E11 were purchased from BD Pharmingen. Cell supernatant containing antibody E5 (Baan et al., 1988) was kindly provided by Dr. William Watson, Shell International Chemicals BV, Shell Research and Technology Center, Amsterdam, Netherlands, and was prepared as described by Booth et al. (1994). Polyclonal mouse IgG antibody was purchased from Calbiochem (La Jolla, CA). Solvents and other chemicals including buffer reagents were supplied by Sigma Chemical Co., Fisher Scientific, or VWR Canlab.


### 3.2.2 Design of Standard


In order to imitate DNA damage as it occurs naturally in cellular DNA, a 90-base pair double-stranded oligonucleotide complex was designed. The desired characteristics of this complex were that it be fluorescently-labeled, contain a known amount of damage, and be long enough to be recognized by a variety of antibodies and other DNA-binding proteins. The complex consists of 6 overlapping, complementary oligonucleotides of varying lengths which when annealed and ligated form a complete double-stranded 90-mer (Figure 3-1). The oligo sequences used in the current study were: oligo 1: 5'-CCTTAAGCTTCCTCAACCACTTACCATACTCGAGATT-3'; oligo 2: 5'-GAGTATGGTAAGTGGTTGAGGAAGCTTAAGG-3'; oligo 5: 5'-GTCATATGCCGCCTCTGACCTTCCTAGAATTCCATCC-3'; oligo 6: 5'-GGATGGAATTCTAGGAAGGTCAGAGGCGC-3'. The sequence of oligo 3 and its complementary strand (oligo 4) may be changed to create a variety of desired damage types, typically with a single damaged nucleotide in the middle of oligo 3. In the current study the sequences used were: oligo 3:

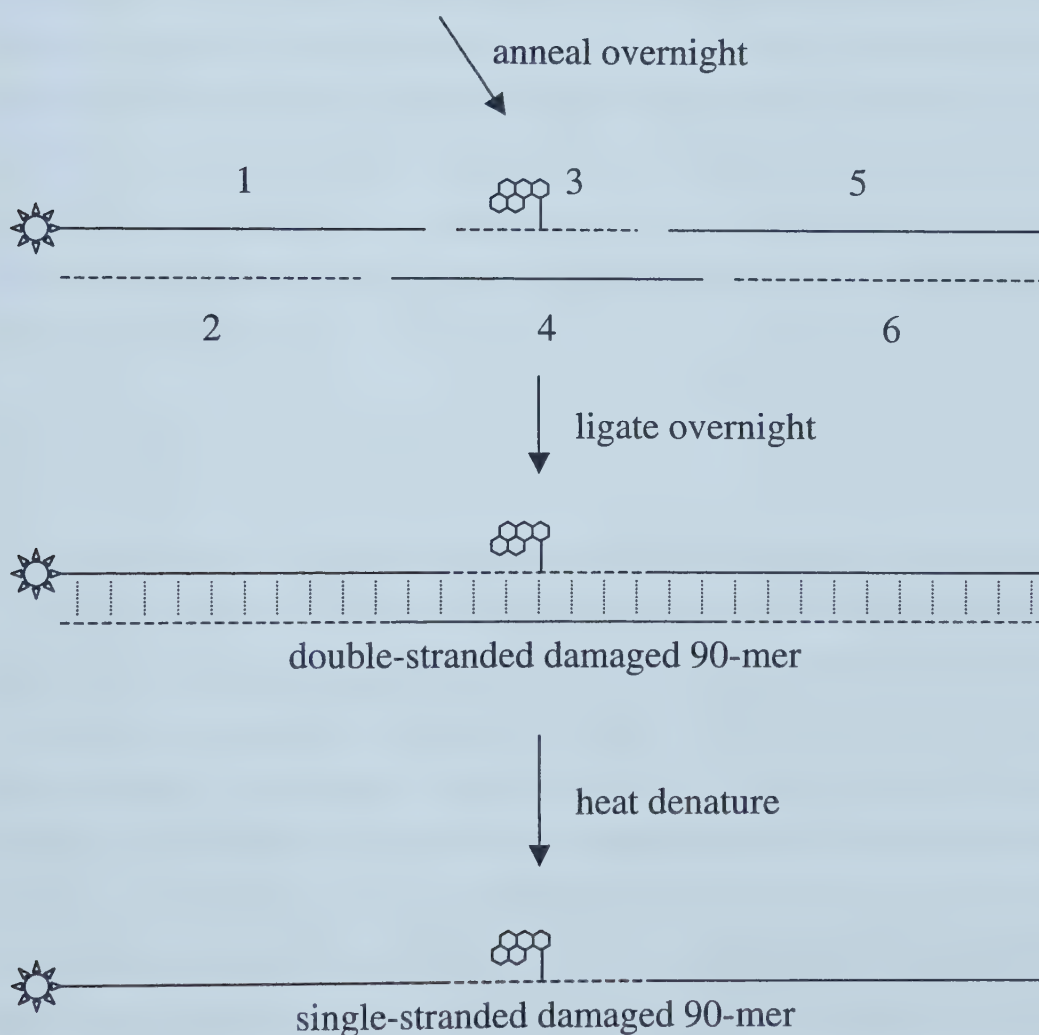




**Figure 3-1. Schematic representation of the DNA damage standard design.** A total of six overlapping, complementary oligonucleotides of varying lengths were annealed and ligated to form a 90-base pair double-stranded DNA molecule. Oligo 1 was modified at the 5'-end with the fluorescent dye tetramethylrhodamine () . Oligo 3 contained a damaged base, BPDE-N<sup>2</sup>-deoxyguanosine () , which was introduced by reacting oligo 3 with (±)-*anti*-BPDE. The dye label and damaged base were on the same strand to allow for either single- or double-stranded experiments.

  
 Oligo 1: 5'-CCTTAAGCTTCCTCAACCACTTACCATACTCGAGATT-3'  
 Oligo 2: 5'-GAGTATGGTAAGTGGTTGAGGAAGCTTAAGG-  
 Oligo 5: 5'-GTCATATGCCGCCTCTGACCTTCCTAGAATTCCATCC-3'  
 Oligo 6: 5'-GGATGGAATTCTAGGAAGGTCAGAGGCGC-3'

  
 Oligo 3: 5'-CCCATTATGCATAACC-3'  
 Oligo 4: 5'-CATATGACGGTTATGCATAATGGGAATCTC-





5'-CCCATTATGCATAACC-3'; oligo 4: 5'-CATATGACGGTTATGCATAATGGG-AATCTC-3'. The fluorescent label (oligo 1) and damaged nucleotide (oligo 3) are on the same strand to allow both double- and single-stranded studies.

### 3.2.3 Synthesis of damaged oligonucleotide

( $\pm$ )-*anti*-BPDE was used as the model carcinogen for synthesis of the damaged oligonucleotide. A 16-mer with the sequence 5'-CCCATTATGCATAACC-3' was synthesized to encourage maximum yield of the BPDE-N<sup>2</sup> deoxyguanosine (dG) adduct (Margulis et al., 1993; Funk et al., 1997). The BPDE-oligonucleotide reaction was based on the procedure described by Margulis et al., with slight modifications. The 16-mer was diluted in 20 mM phosphate buffer, pH 11 containing 1.5% triethylamine, to a concentration of 60  $\mu$ M in a volume of 400  $\mu$ l. A fresh 3mM solution of ( $\pm$ )-*anti*-BPDE in DMSO was prepared, and 40  $\mu$ l was added to the oligo solution. This corresponded to a BPDE:oligo ratio of 5:1. The reaction was carried out at room temperature for 20 hours, in the dark with gentle shaking. Appropriate controls for the HPLC purification were also prepared at this time.

### 3.2.4 Purification of BPDE-oligonucleotide

The components in the BPDE-oligonucleotide reaction mixture were separated using reversed-phase HPLC. The HPLC system consisted of a Dionex AGP1 advanced gradient pump with online-degassing module, either an analytical or preparative C18 column, and a Waters 484 tunable absorbance detector in series with a Shimadzu RF-551 fluorescence HPLC monitor. The detectors were connected to a Hewlett Packard Model 35900 multichannel interface, which converted the signals for use by a PC running ChemStation software. Initial separations were performed using a 4.6 X 250 mm, 5  $\mu$ m Inertsil ODS-2 analytical C18 column (Phenomenex). Preparative work was done on a 10.0 X 250 mm, 5 $\mu$ m Luna C18(2) preparative column (Phenomenex). The reaction products were initially assessed on the analytical column using a protocol described previously (Margulis et al., 1993; Cosman et al., 1990). This procedure employed a linear 0-90%





methanol gradient in 20 mM sodium phosphate buffer (pH 7.0) in 60 min, with a flow rate of 0.75 ml/min. To reduce separation times for large volumes of the reaction mixture, HPLC purification of the BPDE-16-mer was carried out in two steps. The first separation was under isocratic conditions, using a mobile phase of 70% methanol / 30% 20 mM sodium phosphate, pH 7.0 buffer and a flow rate of 0.75 ml/min and 3.5 ml/min for the analytical and preparative columns, respectively. Elution of products were monitored in series by the Waters absorbance detector (wavelength = 260 nm for DNA) and the Shimadzu fluorescence detector (excitation wavelength = 343 nm, emission wavelength = 400 nm for BPDE). This first separation removed unreacted BPDE as well as the tetrol hydrolysis products. DNA fractions were collected, dried using a centrifugal evaporator, and redissolved in deionized water (ddH<sub>2</sub>O). The second step separated the BPDE-oligonucleotide from unreacted oligonucleotide. Preliminary experiments for the second separation were performed under isocratic conditions as the gradient pump was not functioning properly. A range of methanol / 20 mM sodium phosphate ratios were tested to optimize the separation of the oligonucleotides. It was determined that a mixture of 27% methanol in phosphate buffer was optimal (data not shown). In later preparations, a gradient pump was used to improve the efficiency of the procedure. The separation conditions consisted of a linear 10-40% methanol / 20 mM sodium phosphate, pH 7.0 buffer gradient in 7.5 min (4%/min) followed by an additional 5 minutes at 40% methanol. BPDE-oligonucleotide fractions were collected, dried to remove methanol and redissolved again in ddH<sub>2</sub>O. The samples were subsequently desalted using Sep-Pak C18 reversed-phase columns (Waters). The sample was applied to a prepared Sep-Pak cartridge, then washed with 10 ml of the following solutions: 25 mM ammonium bicarbonate (pH 8.0); 25 mM ammonium bicarbonate / 5% acetonitrile; H<sub>2</sub>O / 5% acetonitrile; H<sub>2</sub>O / 5% acetonitrile. The BPDE-oligonucleotide was then eluted with 4 X 1 ml of H<sub>2</sub>O / 30% acetonitrile, dried and redissolved in ddH<sub>2</sub>O.

### 3.2.5 Synthesis and purification of 90-mer oligonucleotides

Prior to ligation with the other 5 oligonucleotides, it was necessary to phosphorylate the freshly purified BPDE-16-mer on the 5'-end, as this modification was omitted during the



original synthesis. Reaction mixtures included: ~200 pmol of BPDE-16-mer or control 16-mer, 4  $\mu$ l of 100  $\mu$ M ATP (400 pmol), 1.2  $\mu$ l of 10X polynucleotide kinase reaction buffer, and ddH<sub>2</sub>O to a total volume of 12  $\mu$ l. T4 polynucleotide kinase (PNK) was added (1  $\mu$ l, 6.1 units/ $\mu$ l), then samples were mixed and incubated at 37°C for 1 hour. PNK was denatured by heating the oligonucleotide samples to 70°C for 10 minutes. The 16-mers were then mixed with the TMR-labeled 37-mer and the other 4 oligonucleotides so that all would be in 2:1 excess over the 16-mers. 5X DNA ligase buffer was added to a final concentration of 1X in order to encourage annealing of the oligonucleotides. The mixture was heated in a water bath to 70°C for 10 minutes, then allowed to cool over several hours to room temperature by turning off the bath and leaving it covered. DNA ligase was added (2  $\mu$ l, 8.5 Weiss units/ $\mu$ l) and the sample was incubated overnight at 16°C.

Purification of the BPDE and control ligation products was achieved using preparative, native polyacrylamide gel electrophoresis (native PAGE). A 7.5% native gel was prepared by mixing: 15 ml of a prepared 40% acrylamide/bisacrylamide (19:1) solution (BioRad), 8 ml of 10X TBE buffer (1X = 89 mM Tris, 89 mM borate, 2 mM EDTA), 800  $\mu$ l of 10% ammonium persulfate, ddH<sub>2</sub>O to 80 ml, and 48  $\mu$ l of TEMED added last. The gel was cast and run using a 30 cm preparative PAGE system with 1.5 mm spacers. Electrophoresis was carried out at 600 V for 6 hours with a water cooling core to prevent denaturation of the ligation products. The bands were visualized by brief exposure to ultraviolet light, causing the TMR label to fluoresce. A photograph was not taken in order to prevent excessive exposure to UV which may result in the formation of UV-damaged bases or photobleaching of the fluorescent products. Full-length ligation products were cut from the gel, minced, and eluted overnight in 0.3 M sodium acetate, pH 5.2 on a rotary shaker protected from light. After elution, polyacrylamide fragments were removed from solution using filter units prepared in the lab. The solution was passed through silanized glass wool followed by GF/C glass microfibre filter paper (Whatman). The samples were then extracted and back-extracted with equal volumes of phenol/chloroform/isoamyl alcohol (25:24:1) followed by chloroform/isoamyl alcohol (24:1). Oligonucleotides were precipitated by adding 3 volumes of ice-cold 95% ethanol and MgCl<sub>2</sub> to 10 mM, then placed at -20°C overnight. The following day samples were



centrifuged for 45 minutes at 14000 rpm and 4°C, supernatant was removed, and the pellets were washed once with 95% ethanol. Samples were again centrifuged for 10 minutes, dried and redissolved in ddH<sub>2</sub>O. UV-Vis absorbance scans were performed on the resulting oligonucleotide solutions to determine concentration as well as to confirm the presence of the TMR dye and BPDE moiety.

### 3.2.6 Instrumentation for analysis of ligation products

Analysis and characterization of the BPDE and control ligation products was carried out using the laboratory-built capillary electrophoresis – laser induced fluorescence (CE-LIF) system described in detail in the Materials and Methods section of Chapter 2. Capillaries used for these experiments were uncoated fused silica, with a 50 µm i.d., 150 µm o.d., 42 cm total length, and 37 cm effective separation length (Polymicro Technologies, Phoenix, AZ).

Samples were electrokinetically injected into the capillary by applying an injection voltage of 10000 V for 5 seconds. The separation was carried out at room temperature with a separation voltage of 20000 V. The running buffer used was 1X Tris-glycine (25 mM Tris, 250 mM glycine), pH 8.3. The capillary was washed approximately every 5-10 injections with 0.1 M NaOH (applied by syringe for 1 min) followed by electrophoresis using 1X Tris-glycine, pH 8.3 for 7 minutes. The initial voltage was kept low to prevent excessive joule heating in the capillary. As the running buffer replaced the NaOH in the capillary, current decreased allowing the running voltage to be gradually increased to 20000 V for the final 5 minutes of the reconditioning period. All capillary electrophoresis data was analyzed using Igor Pro software (version 3.1, WaveMetrics Inc., Lake Oswego, OR).

### 3.2.7 Characterization of BPDE and control 90-mers

Prior to analysis, 90-mer samples were diluted to appropriate concentrations in running buffer (1X Tris-glycine, pH 8.3). The 90-mer products were analyzed either in their







native form (non-denatured) or their denatured, single-stranded form. Denaturation of the 90-mers was achieved by heating the samples at 100°C for 10 minutes in a heating block, then transferring directly to ice to prevent reannealing. After cooling, the samples were briefly centrifuged in a microcentrifuge (Z233M, Hermle) to collect condensation from the side of the tube, then gently mixed to ensure a homogenous solution. Total sample volume was typically 20 µl, which allowed for convenient injection into the capillary. For experiments involving antibodies, fresh dilutions of antibody stock solutions were prepared immediately before analysis and kept on ice. After addition of antibody to the 90-mer solution, the sample was gently vortexed to ensure complete mixing.

### 3.3 Results

#### 3.3.1 Purification of BPDE-16-mer oligonucleotide

The reaction of ( $\pm$ )-*anti*-BPDE with the 16-mer described above resulted in a mixture of products including unreacted 16-mer, BPDE-modified 16-mer, and numerous BPDE metabolites resulting from hydrolysis in solution. These reaction products were separated by reversed-phase HPLC. The initial conditions used were essentially identical to those used by Margulis et al. (1993), and the results were very similar (Figure 3-2). The top trace represents the UV absorbance signal (260 nm) and the bottom trace is the fluorescence emitted by BPDE species. The large peak in the UV signal at 23.6 min indicated unreacted 16-mer. Smaller peaks at 26.4 and 27.3 min represent the *cis*- and *trans*-modified ( $\pm$ )-*anti*-BPDE-N<sup>2</sup>-dG 16-mer adducts. These peaks were distinguished from the unreacted oligonucleotide by the accompanying peaks in the fluorescence trace. The large fluorescent signals at 50.2 and 52.3 min correspond to the *cis*- and *trans*-BPDE tetrols, which resulted from hydrolysis of unreacted BPDE in solution. The yield of BPDE-16-mer was determined by comparing the UV peak areas for the unmodified and modified 16-mers, and was determined to be approximately 14%.



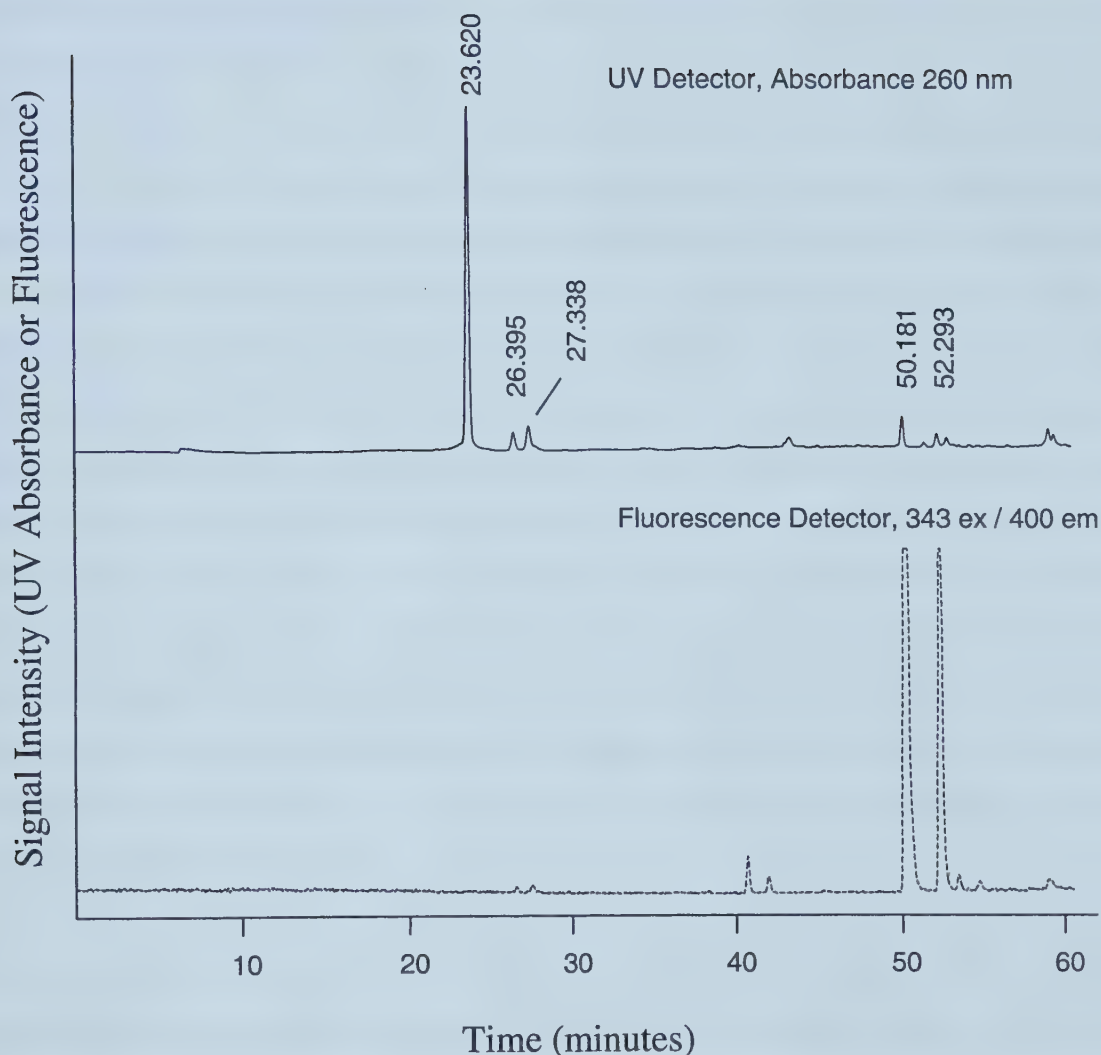


**Figure 3-2. Preliminary reversed-phase HPLC characterization of products from a reaction involving ( $\pm$ )-*anti*-BPDE and a 16-mer oligonucleotide.** Separation was achieved using a linear 0-90% methanol gradient in 20 mM sodium phosphate buffer (pH 7) in 60 min. Major species eluted from the column were: unmodified 16-mer (23.62 min); BPDE-modified 16-mers (26.40, 27.34 min); BPDE tetrol hydrolysis products (50.18, 52.29 min). DNA was detected by UV absorbance (top trace) and BPDE was detected by fluorescence (bottom trace).



To reduce the time and volume of mobile phase required to purify large amounts of the BPDE-16-mer, the purification protocol was revised using two separation steps. The first step was intended to separate the unreacted BPDE and hydrolysis products from the BPDE-16-mer and unmodified 16-mer. Because of the large difference in hydrophobicity of BPDE with the oligo species, they were easily separated over a relatively short period of time. Figure 3-3 shows a typical chromatogram from this first separation using the analytical column. The three major species eluted from the column with retention times of 2.24, 6.25, and 7.26 min. The first peak corresponds to a mixture of unmodified 16-mer and BPDE-16-mer, and was identified based on both the strong UV absorbance and the fluorescent signal from the BPDE. For the control sample containing only 16-mer (no BPDE), the retention time of the DNA peak was identical, but there was no signal in the fluorescence trace. The two later peaks correspond to the tetrol hydrolysis products. These peaks, as well as small peaks between 3 and 6 minutes, were identical in the control sample containing only reaction buffer and BPDE (no oligonucleotide). When these samples were applied to the preparative column the separation was very similar, with retention times of the peaks described above varying by only a few seconds. The main difference between the analytical and preparative columns was that the injection volume was scaled up significantly for preparative work to reduce the number of injections. This resulted in a much larger signal from the two detectors, without significant peak broadening.

The second step in the purification method was intended to separate the mixture of BPDE-16-mer and unmodified 16-mer collected in DNA fractions from the first step. This step utilized a linear gradient of methanol in sodium phosphate buffer (10-40%, 4%/min) to improve the separation. A typical run using the analytical column is shown in Figure 3-4. The difference between the damaged and unmodified oligos was clearly demonstrated based on the presence or absence of peaks in the fluorescent (bottom) trace. The peak eluted at 12.01 min in the UV trace represented the unmodified 16-mer, with no significant fluorescence detected. The broad peak that was evident before the unmodified 16-mer was an artifact of the gradient separation, and was present in blank runs. The non-baseline-resolved doublet peak with local maxima at 13.07 and 13.45 min represented a



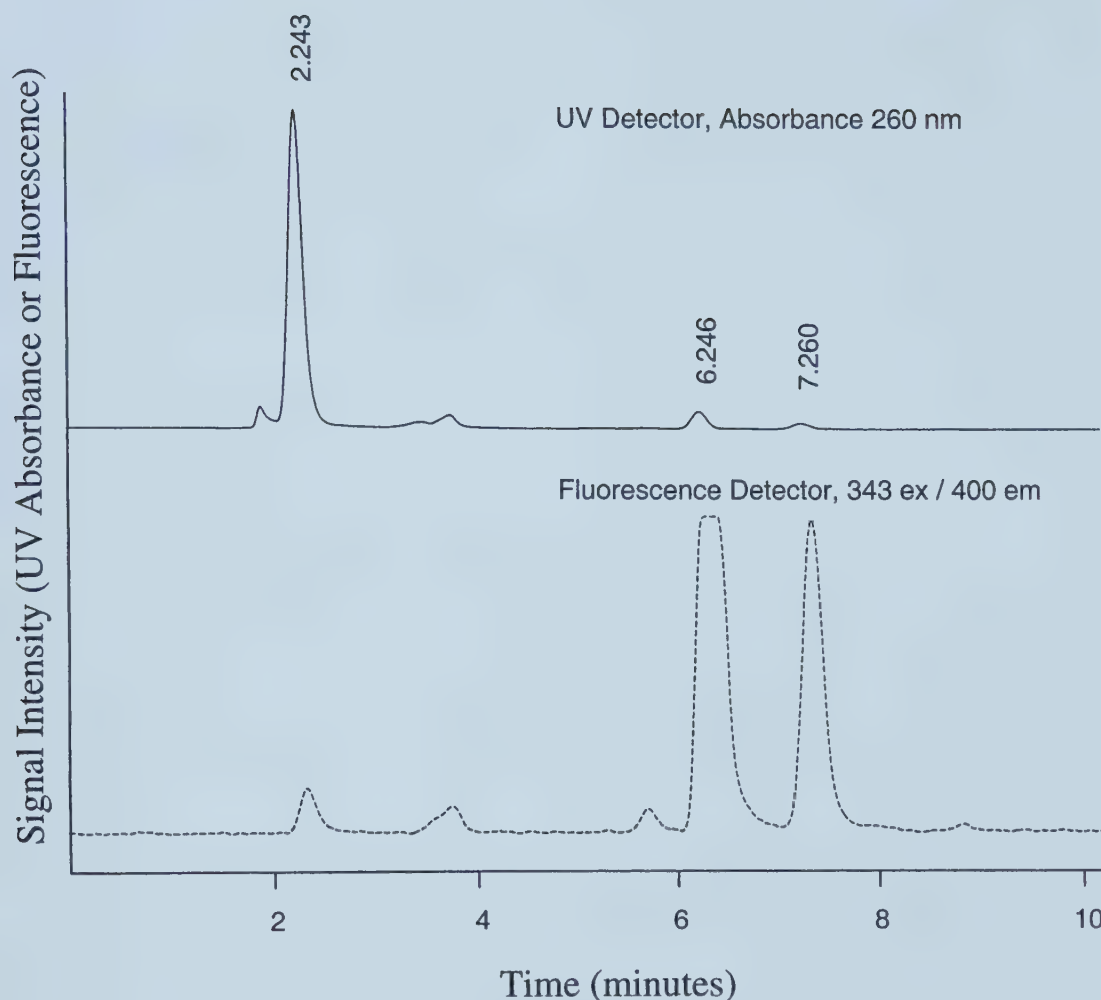


**Figure 3-3.** First step in the HPLC purification of BPDE-modified 16-mers from a reaction involving ( $\pm$ )-*anti*-BPDE and a 16-mer oligonucleotide. Removal of BPDE hydrolysis products was achieved using an isocratic mobile phase of 70% methanol / 30% 20 mM sodium phosphate buffer (pH 7). Major species eluted from the column were: a mixture of unmodified and BPDE-modified 16-mers (2.24 min); BPDE tetrol hydrolysis products (6.25 and 7.26 min). The 16-mer fraction was collected and subjected to a second purification step.





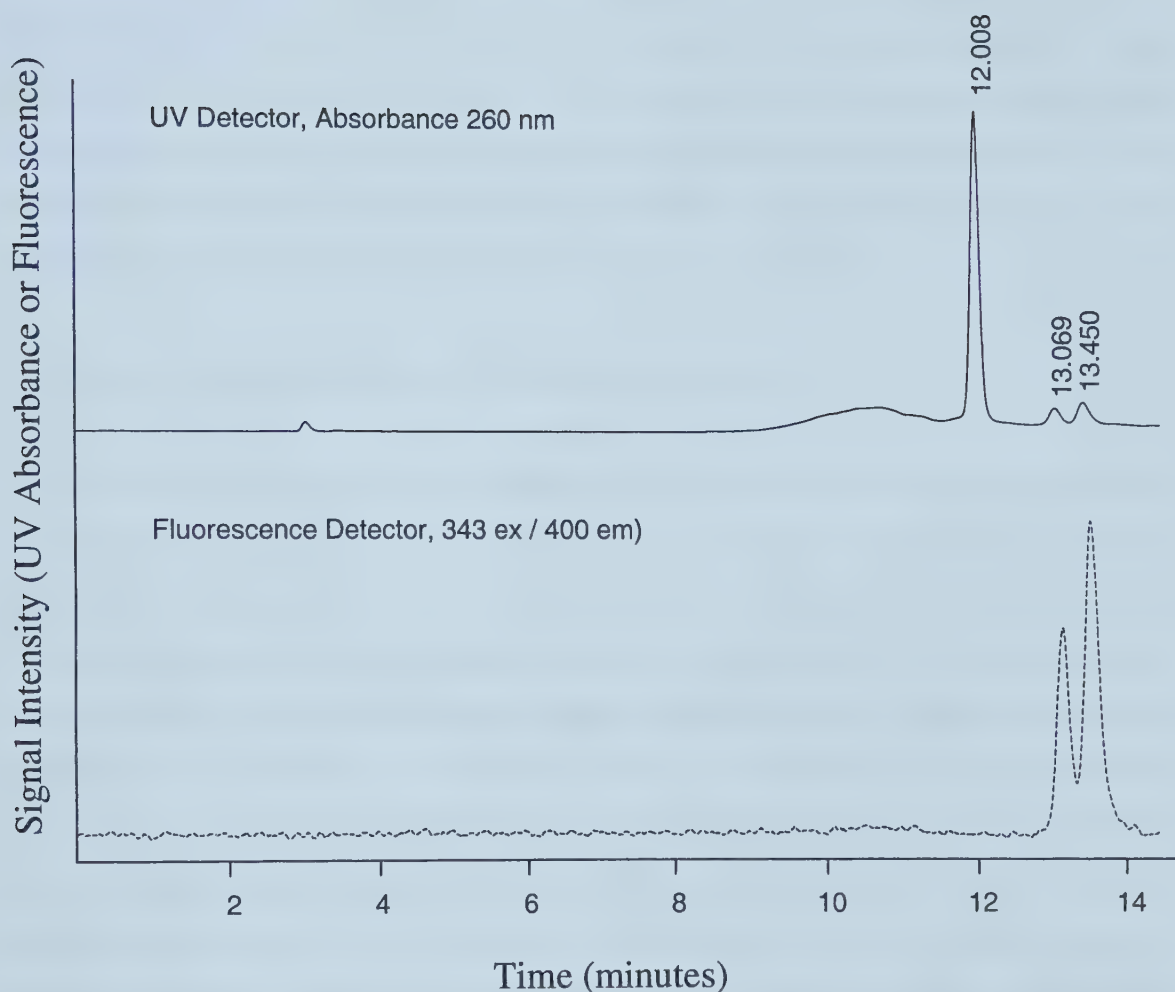


**Figure 3-4. Second step in the HPLC purification of BPDE-modified 16-mers.** The oligo species in the DNA fraction collected during the first step were separated using a linear 10-40% methanol gradient in 20 mM sodium phosphate buffer (pH 7) in 7.5 min (4%/min), followed by an additional 5 min at 40% methanol. Species eluted from the column were: unmodified 16-mer (12.01 min); BPDE-modified 16-mer stereoisomers (13.07 and 13.45 min).



mixture of different stereoisomers of the BPDE-16-mer reaction product. These different isomers have been described previously (Cosman et al., 1990). For our purpose, the isomers were pooled together to generate more starting material for the ligation procedure and to more fully represent the characteristics of DNA damaged by ( $\pm$ )-*anti*-BPDE. When the separation was scaled up using the preparative column, the results were very similar retention times and peak shapes, with a higher signal corresponding to the larger amount of sample injected. The purified BPDE-16-mer was collected in fractions from the preparative column, dried and redissolved for use in the ligation reaction. A UV-visible wavelength scan of the BPDE-16mer showed local maxima of 260 nm and 352 nm, corresponding to absorbance by DNA and BPDE, respectively.

### 3.3.2 Synthesis and purification of 90-mer ligation products

Ligation reactions involving the six different oligonucleotides were carried out using the BPDE-16-mer purified by HPLC as well as a control 16-mer with the same sequence but without the BPDE modification. An initial attempt at the ligation failed because the TMR-37-mer was incorrectly labelled at the 3'-end instead of the 5'-end by the supplier. Analysis of this product by capillary electrophoresis revealed very little reactivity with the BPDE-DNA antibodies. For the second attempt, the products of the ligation reaction were run on a preparative native-PAGE gel to identify and recover the full length, double-stranded ligation products. Both the BPDE and control lanes contained a number of different bands that were visualized by TMR fluorescence after brief exposure to ultraviolet light. A photograph of the gel was not taken, in order to prevent both photobleaching of the TMR dye as well as UV-induced damage to the 90-mer construct. In both cases there was a major band corresponding to the full-length product, several minor bands of lower molecular weight indicating partial ligation products, and excess TMR-labelled 37-mer. The 37-mer was identified by running it alone in an adjacent lane on the gel. These extra bands were expected in the reaction as the TMR-labelled 37-mer and the other four oligos were in 2:1 excess over the BPDE- or control-16-mer. The full-length BPDE and control 90-mers were recovered from the gel, filtered, purified by phenol-chloroform extraction and ethanol precipitation, and redissolved for further



analysis. In addition, the BPDE lane contained another minor band migrating above the major product. This band was also recovered for identification.

### 3.3.3 Characterization of the 90-mer ligation products

Both the BPDE-90-mer and control 90-mer were subjected to a UV-visible wavelength scan to confirm the nature of the modifications. The control 90-mer showed an absorbance maximum at 260 nm as well as a local maximum at 556 nm. This corresponded to the absorbance properties of DNA and TMR, respectively. The BPDE-90-mer also demonstrated absorbance maxima at 260 nm and 558 nm, as well as a local maximum at 347 nm that was not present in the scan from the control 90-mer. This wavelength was slightly different than the local maximum measured for the BPDE-16-mer (352 nm). However, this slight shift in the BPDE absorbance was likely due to the oligonucleotide being double-stranded instead of single-stranded. These wavelength scans support the incorporation of BPDE into the BPDE-90-mer and the absence of this modification in the control 90-mer. The minor top band from the BPDE lane on the preparative gel produced a similar wavelength scan to the main BPDE-90-mer product, however there was not a clear absorbance maximum around 350 nm. This result combined with the absence of a similar band in the control lane suggested that this product was probably not the primary, full-length ligation product containing the BPDE modification. Consequently, the purified product from the major band was used in subsequent experiments.

Further characterization of the BPDE and control 90-mers was carried out using capillary electrophoresis with laser-induced fluorescence detection. Both products were injected in either their native or denatured state, resulting in electropherograms shown in Figure 3-5. The two 90-mers were similar in their behavior in CE. In the native samples, there was a doublet peak migrating between 4.0 and 4.5 minutes. The ratio of the two peaks varied slightly between runs for a given 90-mer, but the doublet was stable and reproducible. When the 90-mers were denatured by heating at 100°C for 10 minutes before injection, the result was a single peak migrating at 4.1 min and 4.2 min for the BPDE and control,





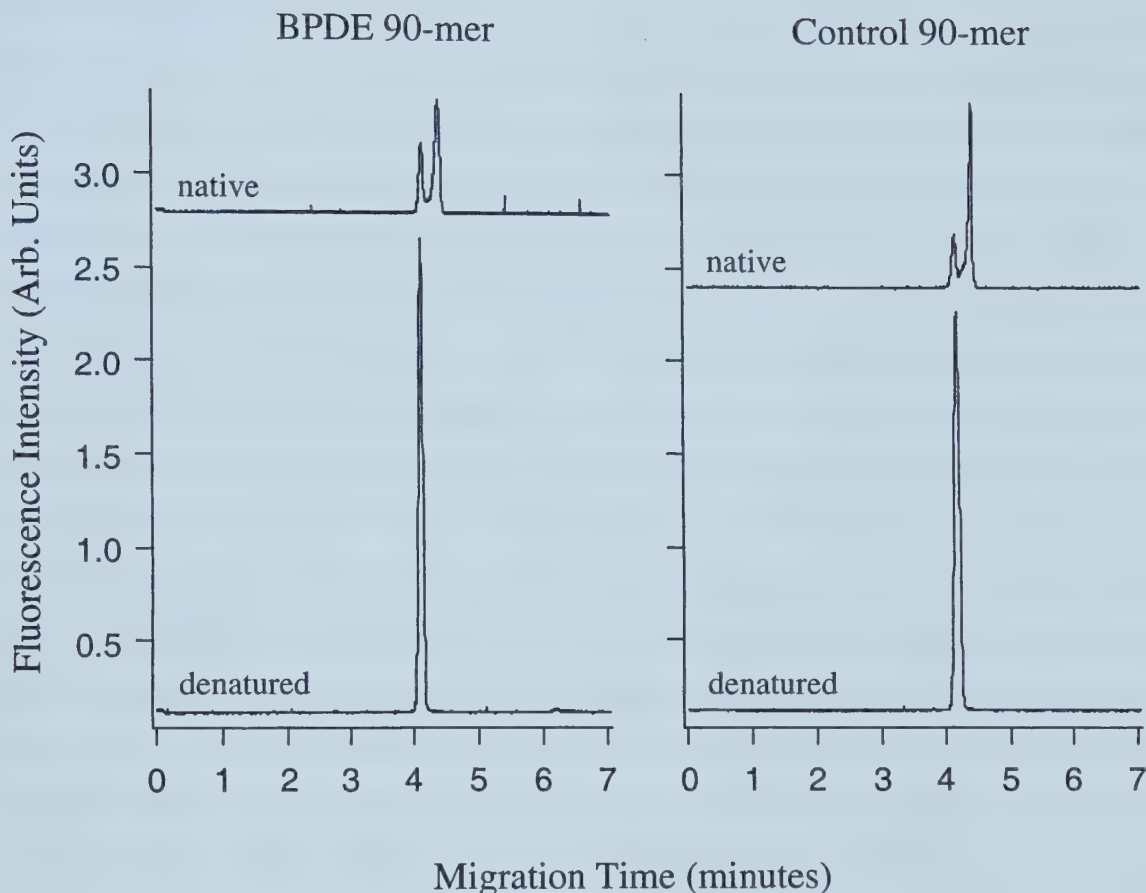


**Figure 3-5. Effect of heat denaturation on BPDE-modified and control 90-mers.** In the native state, both 90-mers exist as a mixture of single- and double-stranded DNA during capillary electrophoresis (doublet peak). After denaturation, both 90-mers are completely in the single-stranded form (single peak). Capillary electrophoresis experiments were carried out using bare fused silica capillaries (50  $\mu\text{m}$  i.d., 37 cm effective length), 1X Tris-glycine running buffer (pH 8.3), and a running voltage of 20000 V. 90-mer samples ( $5 \times 10^{-9}$  M) were electrokinetically injected into the capillary by applying an injection voltage of 10000 V for 5 sec, and were detected by laser-induced fluorescence of the tetramethylrhodamine label.



respectively. For both 90-mers the migration of the denatured peak was very similar to the first of the two peaks in the doublet observed for the native samples. This suggests that the native samples under electrophoretic conditions exist as a mixture of double-stranded and single-stranded oligo-DNA. After heat denaturation the 90-mer existed entirely in the single-stranded form, resulting in a single peak in the electropherogram. This peak possessed a clean, symmetric shape and was relatively sharp, with a full width at half maximum height of between 0.076 and 0.092 min (4.5 and 5.5 sec) for samples with a concentration of  $5 \times 10^{-9}$  M. It was observed that the single peak achieved a higher fluorescent intensity (peak height) than the doublet peak. Furthermore, the total area of the single peak was significantly higher than the total area of the doublet peak for identical injections from the same sample before and after heat denaturation. This occurred for both the BPDE and control 90-mers, and was typically an increase of 120-130% in the total fluorescent signal. This difference was likely a result of the TMR fluorescence being quenched when in the double-stranded oligonucleotide complex. Upon denaturation to the single-stranded form, the TMR dye recovered its full fluorescence yield. This effect has been demonstrated previously in melting curve experiments (Vamosi and Clegg, 1998). The overall quantum yield, fluorescence lifetime, and fluorescence intensity of TMR-labeled oligonucleotides ranging in length from 8 to 34 base pairs increased significantly during the transition from double-stranded to single-stranded form. Furthermore, it has been shown that TMR is selectively quenched by guanine bases in DNA (Seidel et al., 1996), with photo-induced electron transfer from TMR to guanine resulting in lower fluorescence lifetimes and quantum yields (Eggeling et al., 1998). This has been demonstrated by measuring fluorescence lifetimes of individual TMR-labeled oligonucleotide molecules (Eggeling et al., 1998; Edman et al., 1996). Although there are no guanines in the immediate vicinity of the TMR label at the 5'-end of oligo 1, the complementary oligonucleotide (oligo 2) has two guanine residues at its 3'-terminus. In the double-stranded form these two bases are directly adjacent to the TMR dye, and are the likely reason for the observed quenching of the fluorescent signal.



### 3.3.4 Interaction between 90-mers and BPDE-DNA antibodies

#### 3.3.4.1 Interaction of 90-mers with monoclonal antibody 8E11

The main objective of this project was to generate a BPDE-modified DNA standard for use in the capillary electrophoresis-based DNA damage assay. For this molecule to be useful, it was necessary that there be a stable, specific interaction between the standard and antibodies against BPDE-damaged DNA. Preliminary experiments using monoclonal antibody 8E11 demonstrated a difference in reactivity of the antibody with the BPDE and control 90-mers (Figure 3-6). These results were obtained by first denaturing the 90-mers ( $5 \times 10^{-9}$  M), then adding 8E11 antibody to a final concentration of 20  $\mu\text{g/ml}$  and incubating for 10 min at room temperature ( $21^\circ\text{C}$ ). The molar ratio of 8E11 to 90-mer in these samples was approximately 26:1. The same fluorescence intensity scale was used for both 90-mers for ease of comparison. For the mixture of the BPDE 90-mer and 8E11, an additional peak was present in the electropherogram with a migration time of approximately 3.0 min. This peak represented the complex between the antibody and single-stranded BPDE-DNA, and was well-resolved from the denatured 90-mer peak at 4.1 min. The formation of an antibody-DNA complex was not observed with the control 90-mer, indicating a specific interaction with the BPDE 90-mer. This provided additional evidence supporting the incorporation of BPDE-modified DNA into the oligonucleotide complex. When comparing the fluorescent signals between runs, the total area of the two peaks for the mixture of BPDE 90-mer and 8E11 was very similar to the area of the peak for the BPDE 90-mer alone. The peak areas for the control 90-mer with or without 8E11 were also similar, however the peak shape was significantly different. Upon addition of the antibody, the peak became much narrower with a corresponding increase in intensity.

Because the initial runs resulted in less than 50% of the BPDE 90-mer being bound by an excess of 8E11, optimization of the DNA-antibody interaction was attempted. The same concentrations of BPDE 90-mer ( $5 \times 10^{-9}$  M) and 8E11 (20  $\mu\text{g/ml}$ ) were tested, with differing incubation times and temperatures. The effects of incubation time and temper-



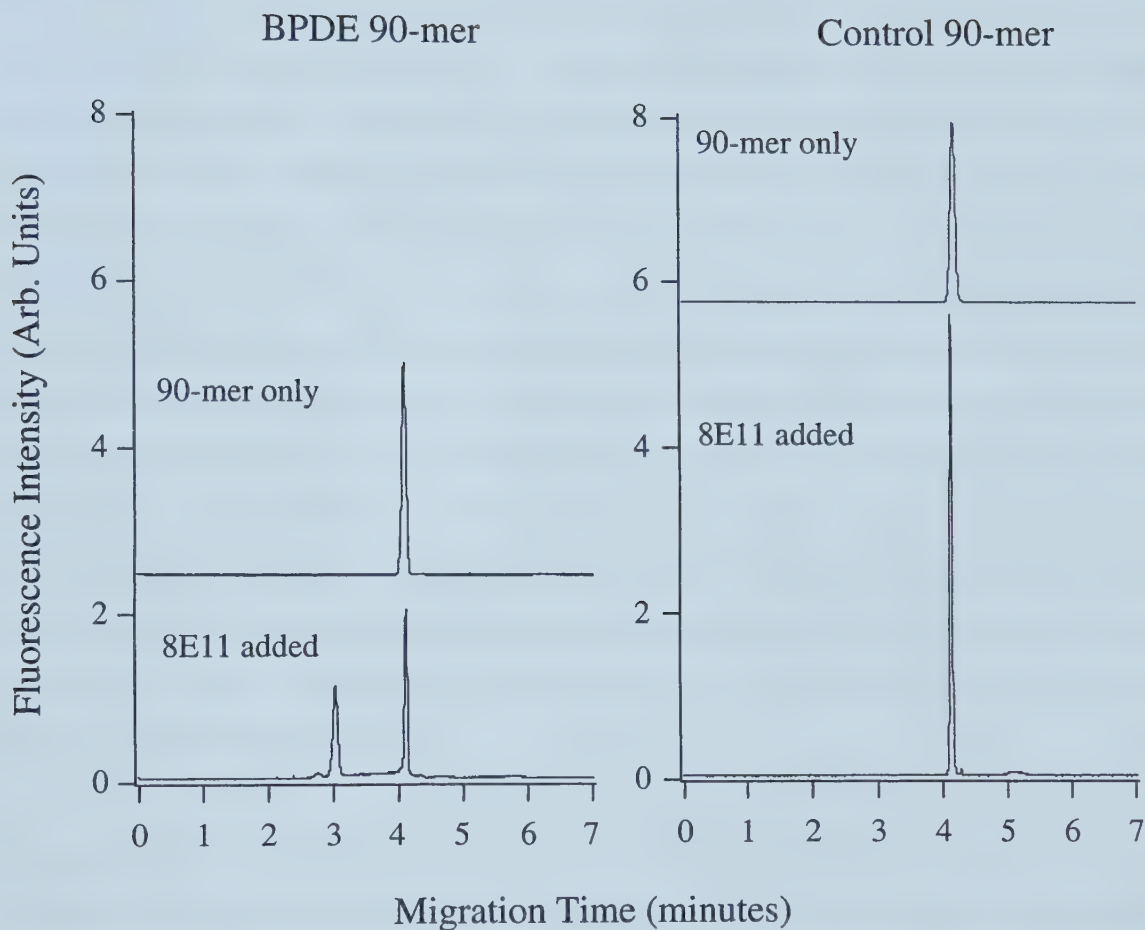


**Figure 3-6. Interaction between antibody 8E11 and BPDE 90-mer.** The addition of 20  $\mu\text{g/ml}$  8E11 to heat denatured BPDE 90-mer ( $5 \times 10^{-9}$  M) resulted in the formation of a second peak corresponding to the DNA-antibody complex ( $t = 3$  min). This complex peak was not present for the control 90-mer.





ature on complex formation are shown in Figure 3-7. The values for % complex formation were obtained by dividing the area of the DNA-antibody complex peak by the sum of the areas of both the DNA-antibody complex and free 90-mer peaks (complex area / total area of two peaks X 100). For incubations carried out at both room temperature and on ice, the interaction did not change significantly between 1 min and 20 min. After 45 min, the sample incubated on ice began to show a decrease in the complex peak. At both temperatures, overnight incubations resulted in a significant loss of the DNA-antibody complex, as well as a reversion to the doublet shape for the free 90-mer peak as demonstrated in Figure 3-8. This result suggests that 90-mer samples left overnight tended to re-anneal to the double-stranded form, causing dissociation of the DNA-antibody complex. This also implies that the affinity of 8E11 for double-stranded BPDE-DNA is less than for single-stranded BPDE-DNA. Data supporting this assumption will be presented later. In general, room temperature incubations with 8E11 resulted in more stable and reproducible complex formation than incubations on ice. This result is expected since the recommended temperature for conventional immunoassays using 8E11 is 37°C (Hsu et al., 1995; Santella et al., 1984), and most immunochemical procedures require incubation temperatures of either 37°C or room temperature (Harlow and Lane, 1988). Based on these results, further experiments with 8E11 antibody were carried out at room temperature. An incubation time of 5 min was chosen for ease of sample preparation and analysis.

The possibility of a difference in reactivity between 8E11 antibody and single- or double-stranded BPDE-modified DNA was investigated to confirm the use of appropriate sample preparation methods. Duplicate samples of heat-denatured BPDE 90-mer were compared to native samples by incubating with 20 µg/ml 8E11. The reactivity was significantly different, with complex formation being approximately 6 X higher for single-stranded 90-mer (Table 3-1). This result suggests that 8E11 more readily binds to BPDE-N<sup>2</sup>-dG adducts that are not partially concealed in the double-stranded DNA structure. It also supports the earlier observation that 90-mer samples which had re-annealed overnight contained a decreased amount of the antibody-DNA complex. Denaturation of samples by heat before incubation with antibodies was therefore retained for further experiments.



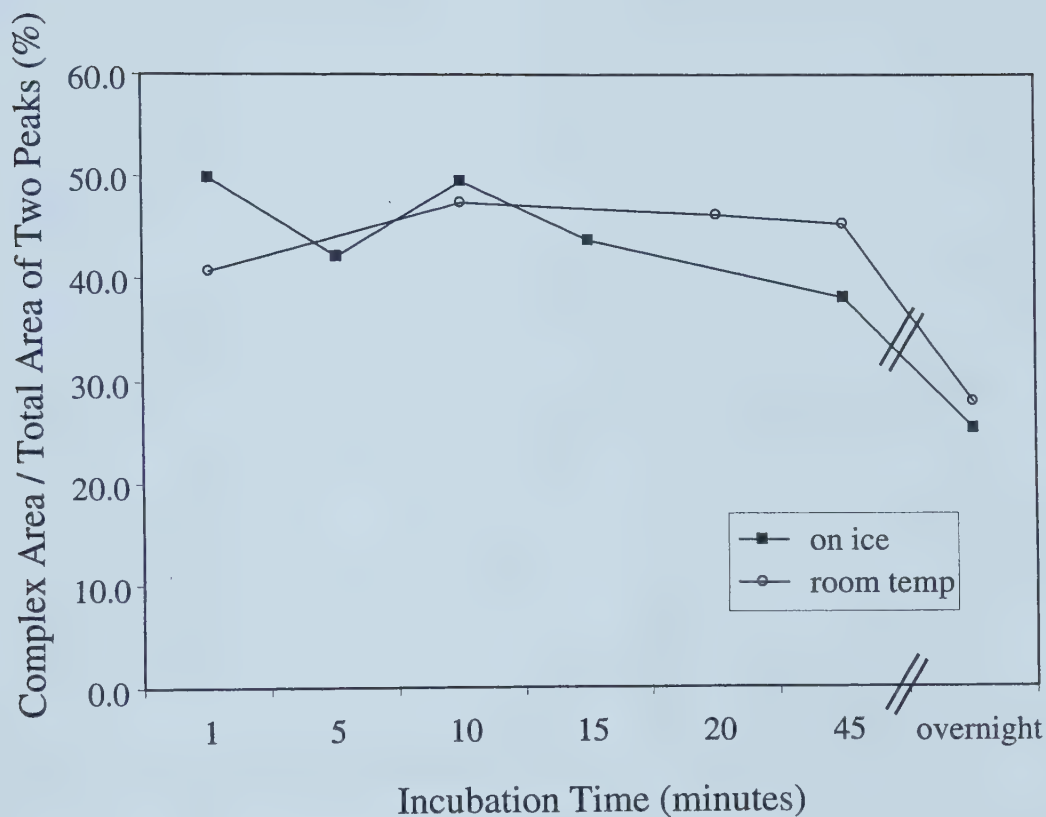


**Figure 3-7. Effect of incubation time and temperature on complex formation.** Samples containing antibody 8E11 (20  $\mu\text{g/ml}$ ) and BPDE 90-mer (5 X  $10^{-9}$  M) were incubated under different conditions before injection into the capillary. The x-axis is a non-linear time scale. Values for the y-axis were obtained by integrating the areas for the free 90-mer and complex peaks in the corresponding electropherograms, and dividing the complex area by the total area of both peaks. The result was the percentage of 90-mer that formed a complex with the antibody.



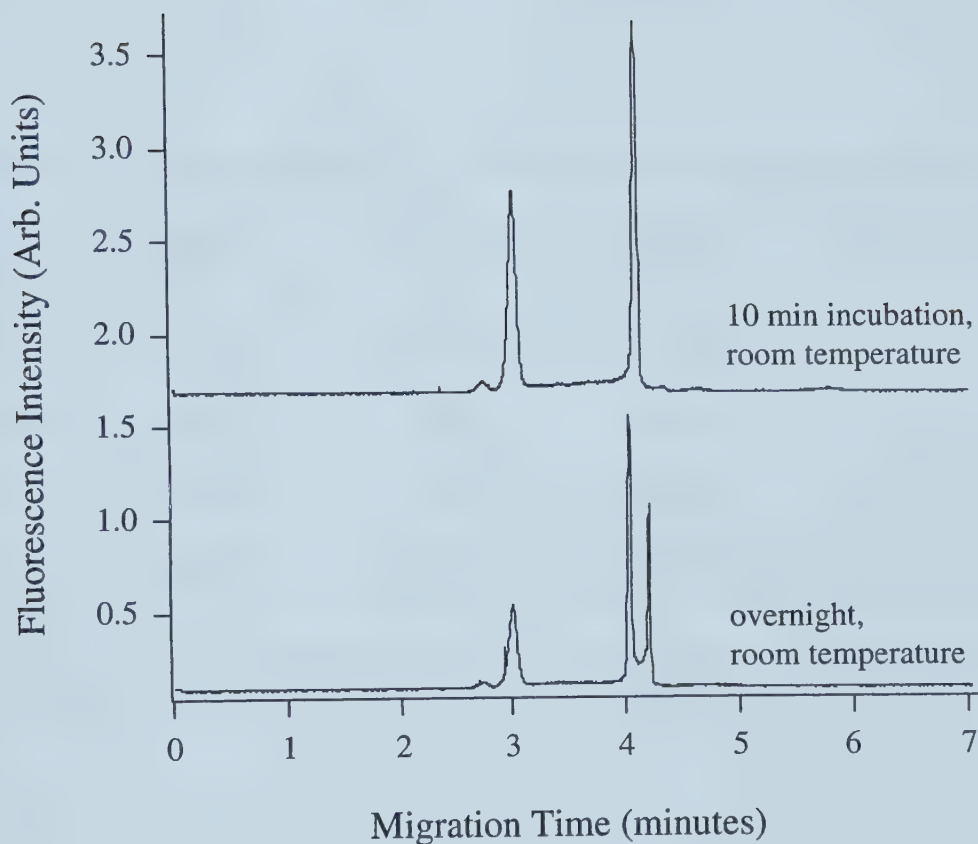


**Figure 3-8. Effect of overnight incubation for BPDE 90-mer and 8E11 antibody.** During the longer incubation time, the complex peak decreased and the free 90-mer peak reverted to a doublet shape. This indicated that the 90-mer had partially re-annealed, displacing some of the antibody in the process.





**Table 3-1.** Reactivity of antibody 8E11 with native and denatured BPDE 90-mer.

<b>90-mer form</b>	<b>Complex area*</b>	<b>Free 90-mer area*</b>	<b>Sum of areas*</b>	<b>Complex / total area*</b>
denatured	0.0993	0.0996	0.1989	50
denatured	0.0966	0.0860	0.1826	53
native	0.0084	0.0882	0.0966	8.7
native	0.0083	0.0851	0.0934	8.9

\* Peak area values were obtained from integrations performed using Igor Pro version 3.15 data analysis software and are expressed in arbitrary units



To better demonstrate the interaction of 8E11 antibody with the BPDE 90-mer standard, different amounts of 8E11 were added to denatured 90-mer samples with a constant concentration of  $5 \times 10^{-9}$  M. A DNA-antibody complex peak was observed with 8E11 concentrations as low as 0.1  $\mu\text{g/ml}$  (Figure 3-9, inset). At this concentration the molar ratio of 8E11 to BPDE 90-mer was 1:7.5, based on a molecular weight of 150,000 Da for antibodies. The area of the complex peak increased at higher concentrations of 8E11, up to 10  $\mu\text{g/ml}$  (Figure 3-9). At this point complex formation appeared to reach saturation, since further attempts to use higher concentrations of antibody did not increase the proportion of 90-mer bound to 8E11. This concentration of 8E11 (10  $\mu\text{g/ml}$ ) corresponded to a molar ratio of 8E11 to 90-mer of approximately 13:1. The maximum amount of bound 90-mer observed in all experiments with 8E11 was approximately 53% of the total area of both peaks in the electropherogram. Possible reasons for the inability to achieve 100% of the BPDE 90-mer in the complex form will be discussed later.

To follow up the experiment of varying amounts of 8E11 in the incubation mixture, the reverse experiment was performed. The concentration of 8E11 antibody was kept constant at 1  $\mu\text{g/ml}$ , an intermediate level used in the previous experiment. The concentration of BPDE 90-mer was then changed to simulate different amounts of damaged DNA in the sample. The injection parameters were kept constant (5 sec / 10 kV injection). Because the 90-mer was the species being monitored by laser-induced fluorescence, the total fluorescent signal varied between samples depending on concentration. However, the method used previously to quantify the amount of complex formed (peak area of complex / total area of both peaks) was suitable in this situation. Limited data representing this relationship is shown in Figure 3-10. With the amount of antibody remaining constant, a higher 90-mer concentration should result in a smaller percentage of the total signal being present in the complex peak. This trend was observed with the exception of the lowest amount of BPDE 90-mer (0.5 nM). In general, the relationship was consistent for samples within the same order of magnitude at the nanomolar level.



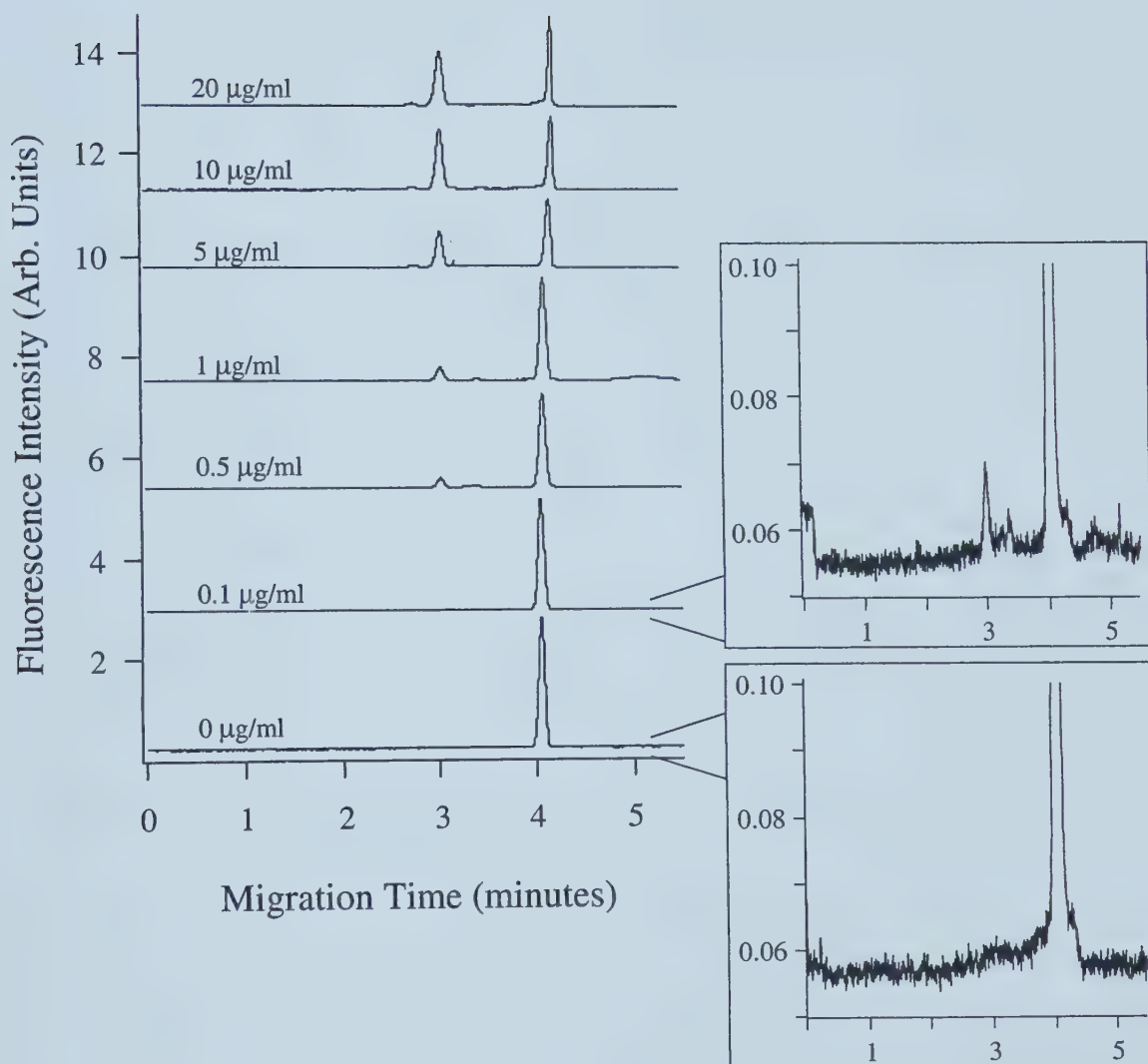


**Figure 3-9. Incubation of BPDE 90-mer ( $5 \times 10^{-9}$  M) with varying concentrations of antibody 8E11.** As the antibody concentration in the sample increased, the area of the complex peak increased until reaching a maximum at 10 µg/ml. Inset, right: expanded scale of 0.1 µg/ml and 0 µg/ml (control) 8E11 samples.



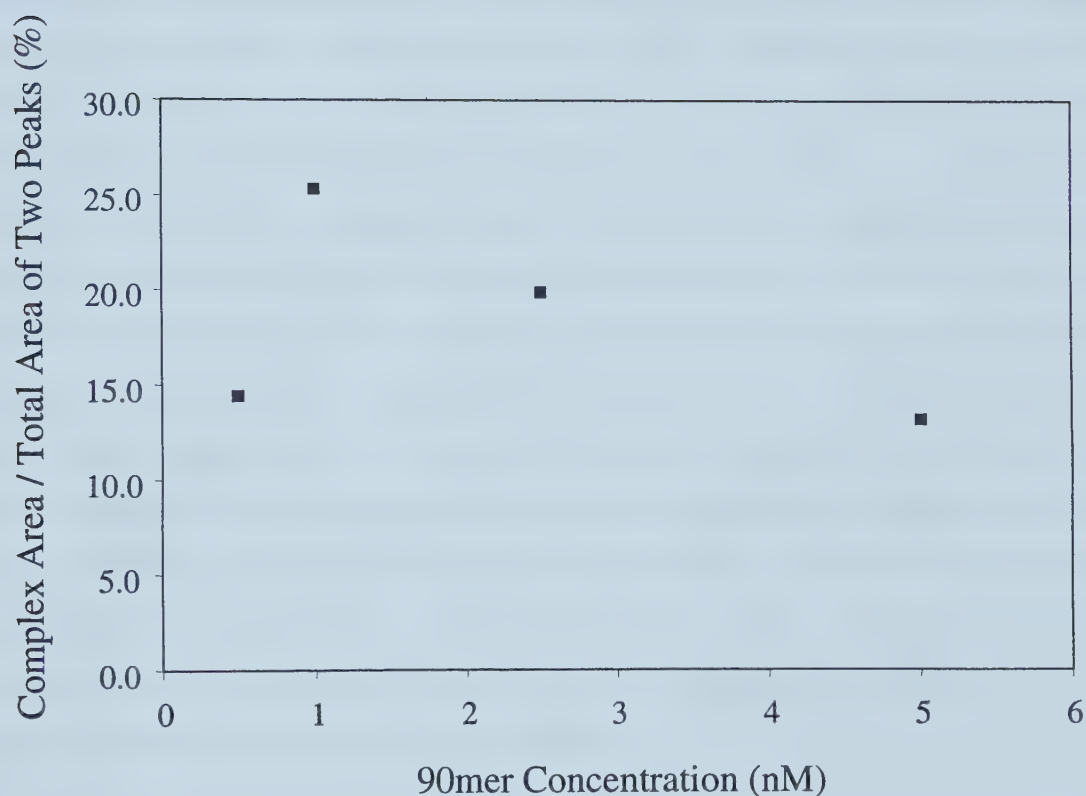


**Figure 3-10. Incubation of 8E11 (1  $\mu\text{g}/\text{ml}$ ) with varying concentrations of BPDE 90-mer.** Because the fluorescent intensity of the complex and free 90-mer peaks changed depending on the 90-mer concentration, % complex formation was used. 90-mer concentrations between 1 and 5 nM showed the expected trend for the limited data available. With a limiting amount of antibody, increasing levels of 90-mer resulted in a lower fraction being present in the complex peak.





### 3.3.4.2 Comparison of anti-BPDE-DNA antibodies

Monoclonal antibodies 8E11, 5D11 and E5 are all specific for BPDE-modified DNA. A comparison between these antibodies was conducted to determine differences in their reactivity to the BPDE 90-mer standard as well as their behavior in the capillary electrophoresis system. Conditions used for sample preparation were identical to earlier experiments: heat denaturation of the 90-mer at 100°C for 10 min, cooling on ice, then incubation with antibody at room temperature for 5 min before injection. Polyclonal mouse IgG was used as a negative control since it is essentially the same molecular structure (isotype) as the monoclonal antibodies but is not expected to react with the BPDE 90-mer. The BPDE 90-mer concentration was again fixed at  $5 \times 10^{-9}$  M and the antibodies were added in varying amounts. All three monoclonal antibodies reacted with the 90-mer standard, with 8E11 giving the highest formation of complex (Figure 3-11). As indicated previously, 8E11 appeared to plateau at about 10 µg/ml with a maximum complex formation of approximately 53%. 5D11 also leveled off around 10 µg/ml, but only reached a maximum of 39% complex formation. Antibody E5 reacted less strongly with the BPDE 90-mer than the others, and did not appear to reach a maximum level over the concentration range tested. The highest antibody concentration (20 µg/ml) corresponds to a molar excess of approximately 26:1 over the 90-mer. The negative control showed a very slight reactivity but was insignificant compared to the other antibodies, even at concentrations up to 40 µg/ml.

The efficiency of complex formation was not the only difference observed between the BPDE-DNA antibodies 8E11 and 5D11. The peak corresponding to the BPDE 90-mer complex with 5D11 migrated slightly faster than with 8E11 during capillary electrophoresis (Figure 3-12). The migration time of the free 90-mer peak during this experiment was constant at 4.20 min. The complex peak migrated at 2.93 min for 5D11 and 3.06 min for 8E11, a difference of 0.13 min or 7.5 sec. This indicates that free 5D11 antibody migrates faster than 8E11 in the capillary, likely due to a higher positive charge under electrophoresis conditions. The second difference with 5D11 was its reactivity with the control 90-mer. This cross-reaction with undamaged DNA was small, about 2.1% by



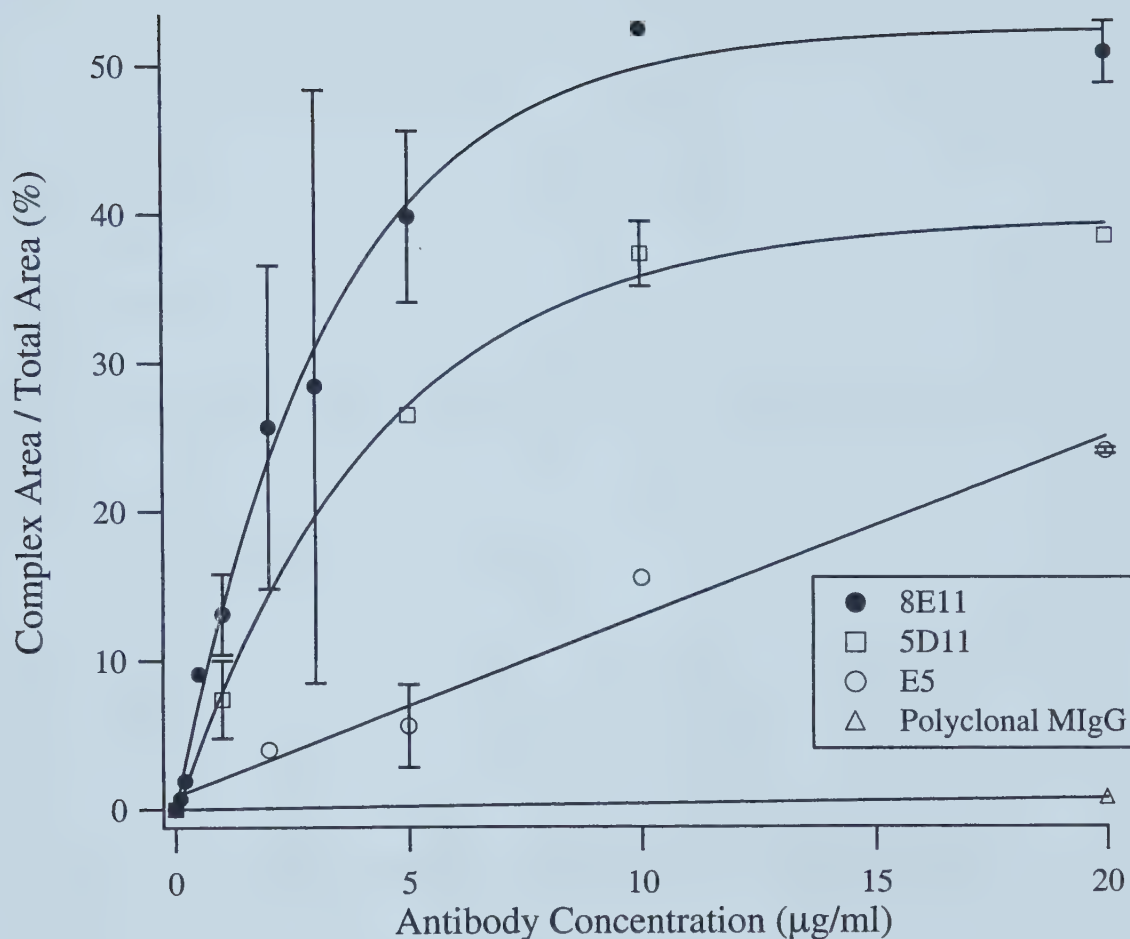


**Figure 3-11. Comparison between BPDE-DNA antibodies using the BPDE 90-mer standard.**  $5 \times 10^{-9}$  M 90-mer was incubated with antibody for 5 minutes at room temperature and subjected to capillary electrophoresis. Polyclonal mouse IgG (MIgG) was the negative control. Error bars indicate the standard deviation of complex formation for antibody concentrations with replicate samples. Values for complex formation were calculated as described in Figure 3-7.



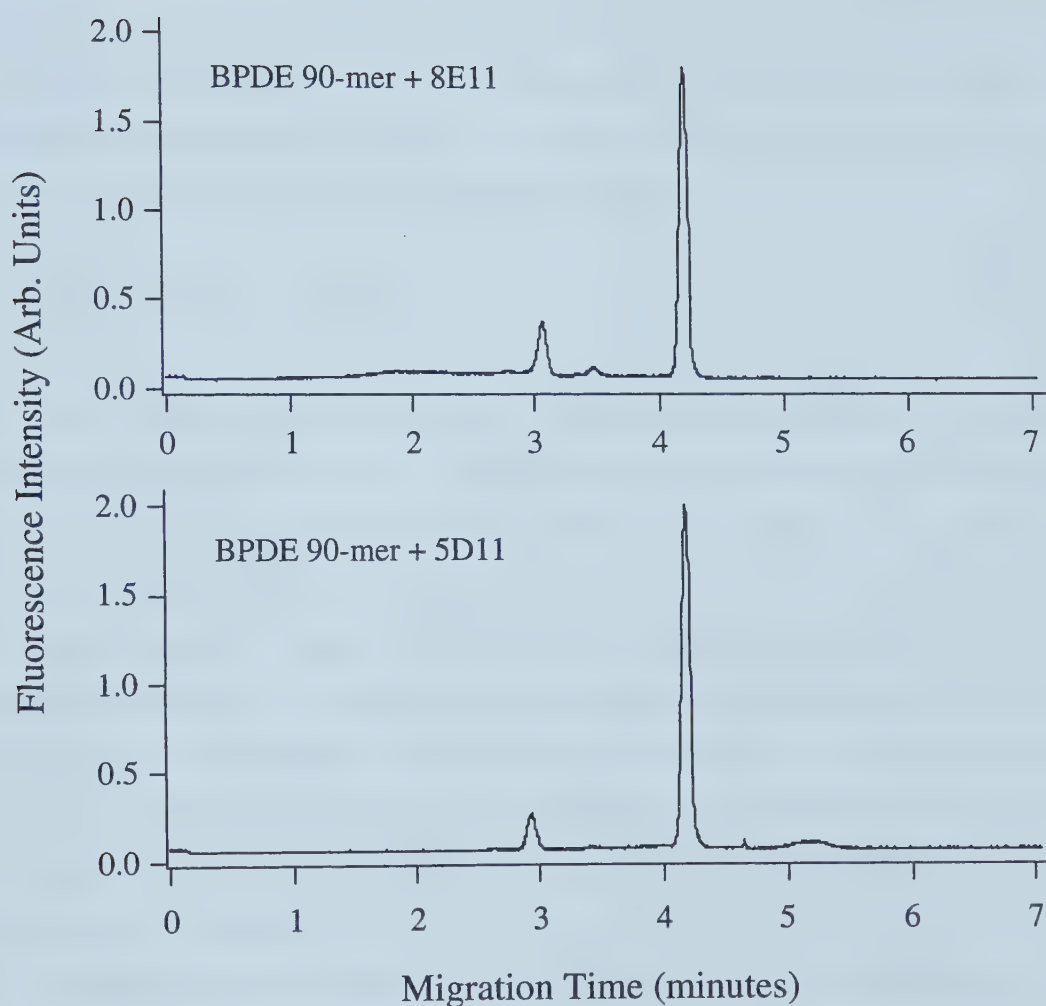


**Figure 3-12. Comparison of BPDE-DNA antibody electrophoretic mobility.** Antibodies 8E11 and 5D11 were incubated with  $5 \times 10^{-9}$  M BPDE 90-mer. Antibody mobility was observed indirectly by the migration of the 90-mer-antibody complex. Antibody 5D11 migrated slightly faster than 8E11, indicating it possessed a higher net-positive charge under the electrophoretic conditions employed.





comparison of complex formation (% of total peak areas) for BPDE and control 90-mers incubated with 20 µg/ml 5D11. However, no cross-reactivity was observed for either 8E11 or E5, indicating that 5D11 was unique among these antibodies in being able to bind to undamaged DNA in the capillary electrophoresis assay. This non-specific interaction between 5D11 and undamaged DNA is in agreement with previous studies (Santella et al., 1984) that have demonstrated cross-reactivity, and is a result of its being raised against a full-length BPDE-DNA antigen. Both 8E11 and E5 were raised against BPDE-guanosine monomers conjugated to carrier proteins (Santella et al., 1984; Baan et al., 1988) and therefore do not recognize undamaged DNA.

### 3.4 Discussion and Conclusions

The goal of this project was to design a standard DNA molecule for characterizing antibody binding and for use in the capillary electrophoresis (CE)-based DNA damage assay. It was necessary that this standard contain a known amount of a specific damage type, and that it be fluorescently-labeled for detection by the laser-induced fluorescence (LIF) system utilized. Using available molecular biology techniques we succeeded in generating a 90-base pair double-stranded oligonucleotide containing a BPDE-N<sup>2</sup> deoxyguanosine (dG) adduct in the middle of one strand, with a tetramethylrhodamine dye attached to the 5'-end of the same strand. This characteristic allowed for studies using either single- or double-stranded DNA to be performed using the CE-LIF system. The control and BPDE-modified 90-mers were very similar during electrophoresis, indicating that modification of this construct does not significantly affect its behavior in the capillary. Injection of 90-mers in their native state resulted in what appeared to be a mixture of single- and double-stranded DNA being separated in the capillary. This partial denaturation of the 90-mer may have been a result of "melting" during the run. Since the length of the DNA is relatively short and the base-pairing in the middle of the strand would be disrupted by the BPDE-N<sup>2</sup>-dG adduct, the 90-mer would denature at lower temperatures than most double-stranded DNA molecules. However, the Tris-glycine running buffer used in these experiments yields a very low current, and significant Joule heating in the capillary is not expected. The second peak in native samples may also have



been due to TMR-labeled 37-mer resulting from incomplete ligation as described below. Whatever the reason, if denaturation were to occur during the CE run it is unlikely that the DNA would reanneal in the capillary due to the absence of a stabilizing physical matrix. On-column denaturation was not a concern for most of these experiments as the samples were denatured prior to injection. This pre-treatment was necessary for optimum activity of the anti-BPDE-DNA antibodies (Hsu et al., 1995; Santella et al., 1984), since the antibodies were raised against either single-stranded, full-length BPDE-DNA or the BPDE-N<sup>2</sup>-dG mononucleotide conjugated to a carrier protein.

Denatured 90-mer samples demonstrated a very clean, symmetric, reproducible peak shape in the Tris-glycine buffer system. The 90-mer peak was also relatively narrow (width at half maximum approximately 5 seconds) and had a fast migration time of about 4 minutes. For samples containing both the BPDE 90-mer and BPDE-DNA antibody the resulting DNA-antibody complex was well-resolved from the free-90-mer peak, even with the fast separation times in the Tris-glycine buffer. The separation efficiency for a typical run under these conditions can be calculated using the following equation:

$$N = 5.54 (t_M / W_{1/2})^2$$

where: N is the number of theoretical plates

$t_M$  is the migration time of a species in the capillary

$W_{1/2}$  is the peak width at half maximum height for a species

For example, the theoretical plate numbers for the 90-mer / 8E11 complex and free 90-mer at an antibody concentration of 10 µg/ml from Figure 3-9 were  $9 \times 10^3$  and  $4 \times 10^4$ , respectively. Although these values are not very high, the ample resolution between the species suggests that optimization of the electrophoretic conditions may lead to significantly higher separation efficiencies. These characteristics support the use of the 90-mer as a DNA damage standard in the CE-LIF system.

One concern that was evident with the BPDE 90-mer was the inability to achieve 100% complexation with the addition of saturating amounts of antibody, in particular with the



most efficient one tested (8E11). After reviewing the protocol for synthesizing the 90-mer, a few possible reasons for this occurrence were investigated. One possibility was a result of the phosphorylation of the BPDE 16-mer after the HPLC purification and before the ligation procedure. For this reaction, ATP was added in 2:1 molar excess over the oligonucleotide and the incubation time was increased to 1 hour (30-45 minutes is recommended). The addition of phosphate to the 5'-end of the oligonucleotide was assumed to proceed essentially to completion under these conditions. However, it is possible that some of the BPDE 16-mer was not phosphorylated. It has been shown that a 1:1 molar ratio of oligonucleotide and [ $\gamma$ - $^{32}\text{P}$ ]ATP results in only 50% of the oligo being radiolabeled at the 5'-end (Sambrook et al., 1989). To achieve virtual completion of the phosphorylation reaction, a 10:1 molar excess of ATP is recommended. Even with the increased incubation time, the 2:1 ratio used in this experiment likely resulted in a measurable portion of the BPDE 16-mer that was not phosphorylated. Furthermore, it has been shown that the presence of a cytosine at the 5'-end of the oligonucleotide may significantly decrease the efficiency of the PNK reaction when compared to the other three bases (van Houten et al., 1998). The BPDE 16-mer does contain 3 cytosine residues at the 5'-end, supporting the hypothesis that phosphorylation was incomplete. Without this 5'-phosphate modification, ligation of the 16-mer to the TMR-labeled 37-mer would not succeed. Because the gel purification of the ligation products was performed under native conditions, these incomplete strands may have remained annealed to the complementary strand during electrophoresis. The result would be a mixture of complete and incomplete strands being present in the purified stock 90-mer solutions. This problem would present itself during the heat denaturation of the 90-mer to the single-stranded form (Figure 3-13). Intact strands containing both the TMR dye and the BPDE-N<sup>2</sup>-dG adduct would bind to the antibody. Incomplete strands would separate during denaturation, resulting in a fluorescent species (TMR-labeled 37-mer without BPDE adduct) that would not be recognized by the antibody 8E11. The fragment containing the adduct would bind to the antibody, but would not be detected due to the lack of the fluorescent label. This possibility was investigated by running the BPDE and control 90-mer samples on a denaturing urea-PAGE gel (Figure 3-14). Oligonucleotide DNA in this gel system migrates in single-stranded form. 90-mer samples that did not properly ligate





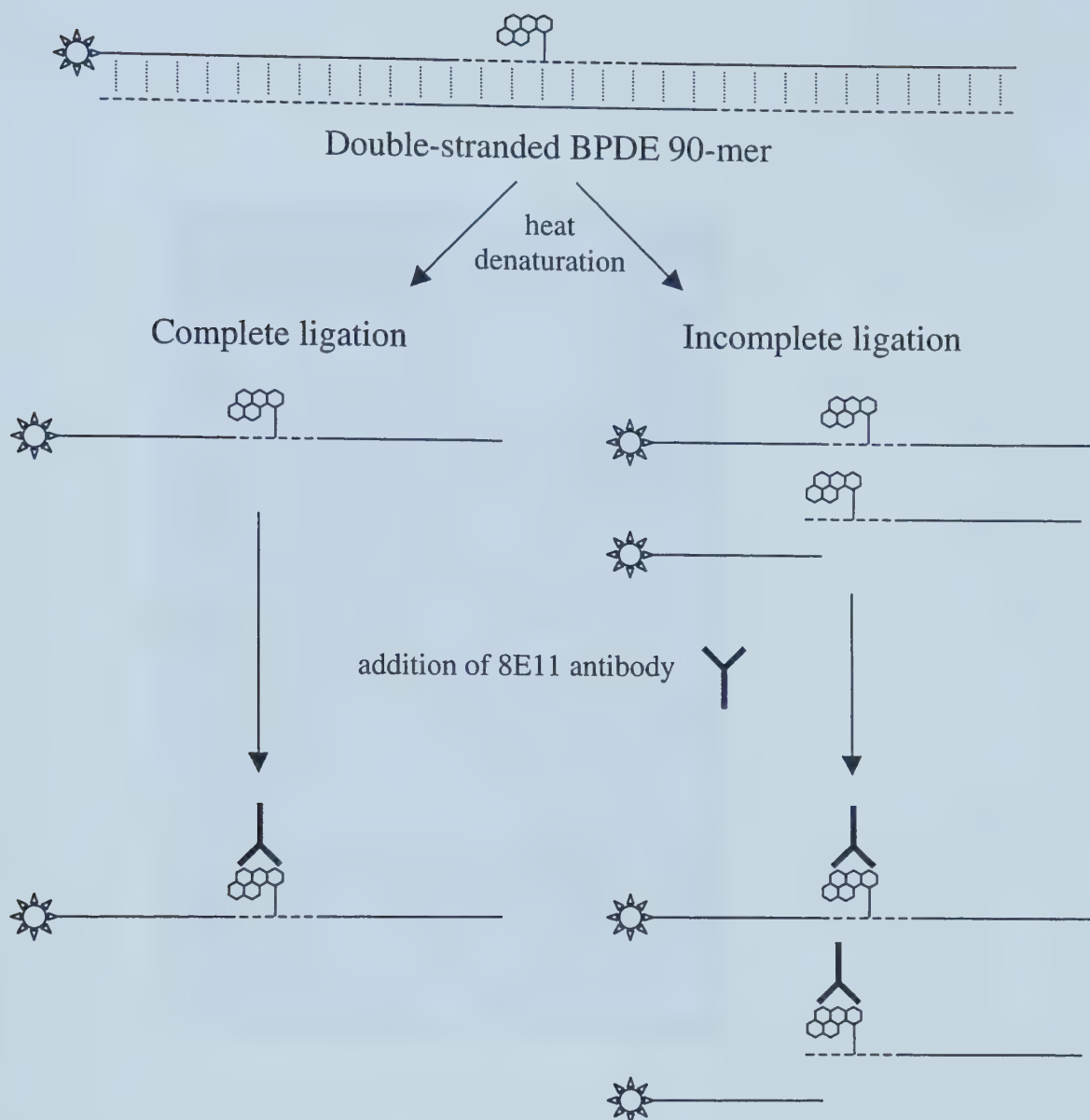


**Figure 3-13. Schematic representation of the effect of incomplete 5'-phosphorylation of the BPDE 16-mer prior to the ligation step.** If complete phosphorylation is achieved, ligation is also complete and denaturation of the gel-purified double-stranded 90-mer yields an intact single-stranded 90-mer (left). If phosphorylation is incomplete, a portion of the BPDE 16-mer will not ligate to the TMR-labeled 37-mer. Denaturation of the double-stranded 90-mer results in a mixture of intact and fragmented single-stranded 90-mers (right). Upon incubation with 8E11 antibody, only the intact 90-mer forms a complex that is detectable in the CE-LIF instrument. TMR-labeled 37-mer from the fragmented strands is also detected, but does not form a complex with the antibody.





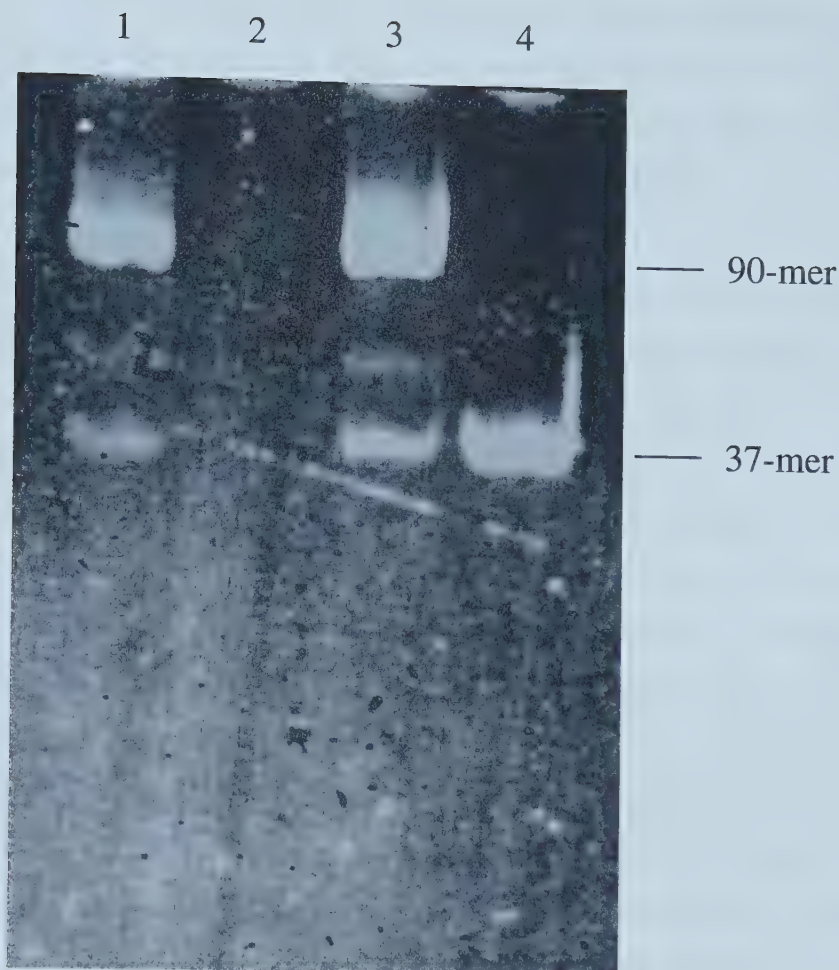


**Figure 3-14. Denaturing urea-PAGE of gel-purified BPDE and control double-stranded 90-mer samples.** Lane 1: purified BPDE 90-mer; Lane 2: blank; Lane 3: purified control 90-mer; Lane 4: TMR-labeled 37-mer. Samples were visualized by UV-induced fluorescence of the TMR dye. The presence of two bands in the BPDE and control 90-mer lanes, corresponding to the intact single-stranded 90-mer and the TMR-labeled 37-mer, indicated that ligation of both samples was incomplete.



would be expected to separate into two bands (TMR fluorescence) corresponding to the full-length 90-mer and the 37-mer. For both the BPDE and control 90-mers there was some 37-mer present, indicating incomplete ligation. However, this result offers only a partial explanation since the ratio of the two bands for the BPDE 90-mer did not fully account for the observed saturation level of approximately 53% with 8E11. This indicated that there was a second mechanism limiting the effectiveness of the binding.

The most likely explanation for this second limitation of the standard's reactivity is based on the stereochemistry of the BPDE-N<sup>2</sup>-dG adduct. In the preparation of the BPDE-modified 16-mer, (±)-*anti*-BPDE was reacted with the oligonucleotide. The covalent bond that forms between BPDE and guanosine may be either *cis*- or *trans*- relative to the hydroxyl group on the adjacent carbon atom. Therefore, there may be as many as four different configurations of the BPDE 16-mer: (+)-*trans*, (+)-*cis*, (-)-*trans*, and (-)-*cis* (Szeliga and Dipple, 1998). The stereochemistry of BPDE adduct formation is presented in Figure 3-15. Of these configurations, (+)-*trans* is the predominant form. The reaction protocol was designed to minimize the formation of *cis*- adducts (Funk et al., 1997), but a mixture of (+)-*trans* and (-)-*trans* adducts with a small amount of *cis* adducts would be expected in the BPDE 16-mer reaction products (Cosman et al., 1990). Because these stereoisomers were pooled together after purification by HPLC and before the ligation reaction, the 90-mer product would also contain these configurations. The advantage of this mixture is that it more accurately represents the spectrum of damage that would occur in human DNA samples. The disadvantage is that BPDE-DNA antibodies exhibit different affinities for these stereoisomers (Hsu et al., 1995). In competitive inhibition studies using BPDE-modified 11-mers, Hsu et al. demonstrated a lower affinity for the (-)-*trans-anti*-BPDE-N<sup>2</sup>-dG adduct than for the (+)-*trans-anti*-BPDE-N<sup>2</sup>-dG adduct. For antibodies 8E11 and 5D11 this lower affinity was 66% and 20% of the (+)-*trans* adduct, respectively. Both antibodies exhibited much lower affinities for the *cis* adducts compared to the (-)-*trans* adduct, and since the proportion of these isomers in the 90-mer would be low compared to the *trans* adducts it is not expected that they would contribute significantly to the binding observed. Since the 90-mer contained a combination of both *trans* adducts, the stereospecific difference in affinity may in part be responsible for the



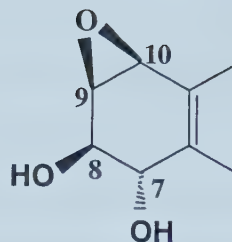
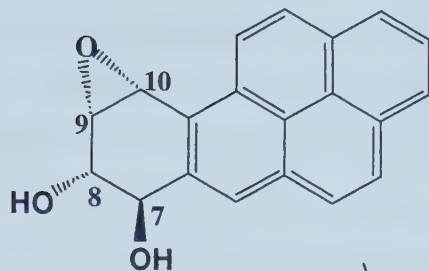


**Figure 3-15. Stereochemistry of BPDE adduct formation.** A mixture of (+)-*anti* and (-)-*anti*-BPDE was used to generate the BPDE-16-mer. The *anti*-nomenclature refers to the epoxide group being in opposite configuration relative to the OH-group on carbon 7 (top). The (+)/(-) designation is with respect to the remainder of the aromatic ring structure. The predominant adduct formed is (+)-*trans*-BPDE-N<sup>2</sup>-deoxyguanosine, but four different stereoisomers are possible: (+)-*trans*, (+)-*cis*, (-)-*trans*, and (-)-*cis* (bottom). The *cis*- and *trans*- designations describe the orientation between guanine and the OH-group formed on carbon 9.

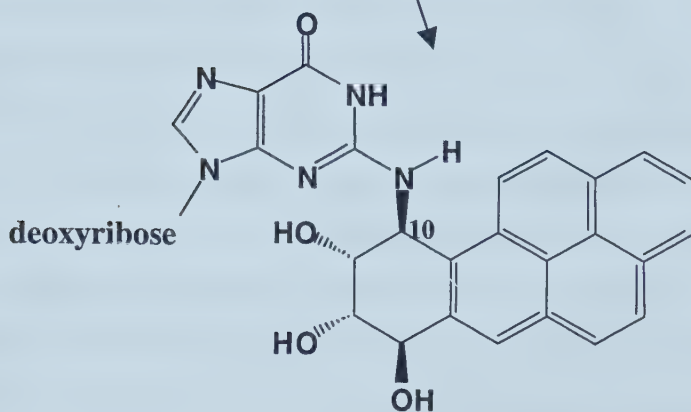


Benzo[*a*]pyrene-7,8 diol-  
9,10 epoxide (BPDE)

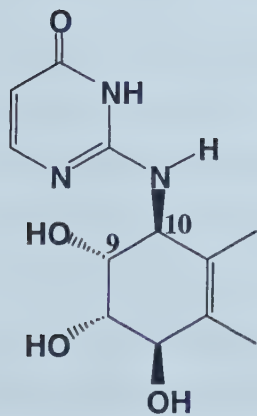
[(+)-*anti*]



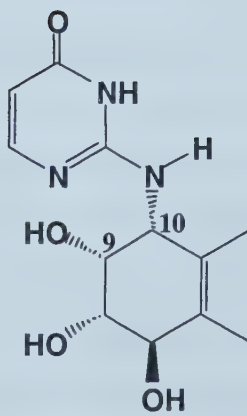
[(-)-*anti*]



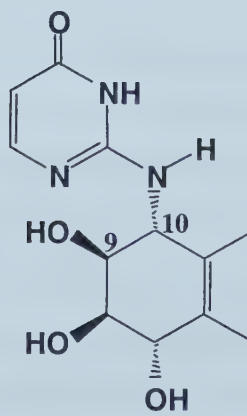
(+)-*trans*-BPDE-N<sup>2</sup>-deoxyguanosine adduct



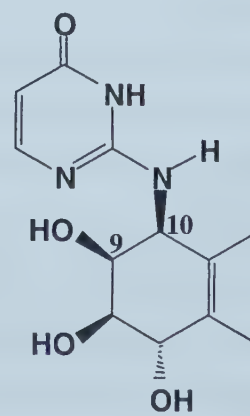
(+)-*trans*



(+)-*cis*



(-)-*trans*



(-)-*cis*



different plateaus of complex formation observed for these antibodies. An improved synthesis of the BPDE 90-mer, perhaps using only the (+)-*trans*-anti-BPDE-N<sup>2</sup>-dG adduct, would serve to address these issues.

Despite this uncertainty, experiments using the standard were able to provide information about the different antibodies specific for BPDE-DNA. In addition to the isomer-specific reactivities described above, Hsu et al. (1995) showed a difference in affinity between 8E11 and 5D11 when considering only the (+)-*trans* adduct. 8E11 was approximately 7 times more sensitive than 5D11 for the very short 11-mer oligonucleotide. For full-length heat-denatured BPDE-DNA, the two antibodies were almost identical. This difference is likely due to the antigens against which these antibodies were raised: BPDE-N<sup>2</sup>-dG mononucleotide for 8E11, full-length BPDE-DNA for 5D11. 5D11 may require a longer sequence of DNA surrounding the damaged site for binding which would not be present in the 11-mer. Given these results one might predict that for DNA of intermediate length (90 bases), 8E11 would still have a higher affinity than 5D11, but to a lesser extent. This prediction combined with the larger difference observed between (+)-*trans* and (-)-*trans* isomers for 5D11 may help to explain the results in the current study. 5D11 exhibited a lower reactivity with the standard than 8E11, but by less than 2 times at all concentrations tested (Figure 3-11). The difference in the slope of the binding curves may be attributed to the higher total affinity of 8E11 for the 90-mer, whereas the difference in plateaus may be a combination of the stereospecific affinity and the incomplete ligation described earlier. Antibody E5 was obtained from a different source than 5D11 and 8E11, and displayed an even lower reactivity with the standard. Although it appeared the maximum complex formation was not achieved for E5, it was still less than 50% as effective as 8E11 at the highest concentration tested (20 µg/ml). The poor performance by E5 in this study may be due to the age of the antibody or a loss of activity due to repeated freezing and thawing. These results indicate that monoclonal antibody 8E11 is likely the best choice for detecting BPDE-damaged DNA using the capillary electrophoresis / laser-induced fluorescence assay. In addition to affinity values, the standard also provided information on antibody migration during electrophoresis. This would be useful in



predicting how the antibodies would behave under assay conditions with normal DNA samples.

One of the most useful characteristics of the CE-LIF system is its ability to detect minute quantities of analytes. Laser-induced fluorescence was chosen as the detection system for our assay because of its excellent sensitivity. This was demonstrated by injecting BPDE 90-mer samples of decreasing concentration. 90-mer samples with concentrations as low as  $5 \times 10^{-11}$  M (based on UV absorbance measurements of stock solutions) were detectable in our instrument based on a signal-to-noise ratio of 3:1. Since a typical injection under these conditions is approximately 1 nL, this corresponds to a mass detection limit for the instrument of  $5 \times 10^{-20}$  moles or about 50 zeptomoles of BPDE adducts. Although the robustness of the detection method was not rigorously tested, duplicate samples at this concentration yielded similar results. This level of sensitivity could be improved further by using a sheath flow cuvette (Le et al., 1995; Chen and Dovichi, 1994) as opposed to the on-column detection method used in this study. Nevertheless, it is a significant improvement over established DNA damage assays. The detection limit for ELISA methods is about 1 adduct per  $10^8$  normal nucleotides (Santella, 1999). For typical samples of between 35-50  $\mu\text{g}$  DNA per well, this corresponds to a molar detection limit of approximately  $2 \times 10^{-15}$  moles of BPDE adducts.  $^{32}\text{P}$ -postlabeling is more sensitive (Beach and Gupta, 1992), being able to detect approximately  $2 \times 10^{-17}$  moles of BPDE adducts in a 5  $\mu\text{g}$  DNA sample. This is still considerably less sensitive than CE-LIF. One potential advantage of this increased sensitivity is the ability to measure low levels of damaged bases in human samples which might not be detectable using these methods. In addition, the minute amounts of DNA required for this assay would allow for easier sample collection in human studies. Currently, methods such as conventional ELISA require as much as 200  $\mu\text{g}$  of DNA. For DNA extracted from white blood cells this corresponds to a volume of approximately 40 ml of blood to be collected (Santella et al., 1995). This requirement could be reduced by using the method we have developed. Typical samples prepared for convenient injection into the capillary are 25  $\mu\text{l}$ , but volumes as small as 5  $\mu\text{l}$  or lower may be used without difficulty. Previous studies on BPDE-adduct levels in human blood samples have shown





typical values between 1-10 adducts /  $10^8$  normal nucleotides, with samples often being below the detection limit of the assay (Dickey et al., 1997; Kang et al., 1995; Santella et al., 1995). For a hypothetical DNA sample with 1 adduct /  $10^8$  nucleotides, the amount of DNA required for analysis using our technique can be estimated as follows:

D.L. for BPDE standard:  $5 \times 10^{-20}$  moles BPDE adduct

Suitable amount for quantitation:  $1.5 \times 10^{-19}$  moles BPDE adduct

Amount of DNA injected:  $1.5 \times 10^{-19} \times 10^8 = 1.5 \times 10^{-11}$  moles nucleotides

Average nucleotide = 325 g/mol

$1.5 \times 10^{-11}$  moles \* 325 g/mol =  $4.9 \times 10^{-9}$  g  $\approx$  5 ng DNA

DNA concentration: 5 ng / 1 nl injection = 5 g/l

Total DNA in sample: 5 g/l \* 5  $\mu$ l = 25  $\mu$ g

Because very little sample (nl) is injected per run, one sample could produce as many replicate injections as desired. By decreasing the sample volume or increasing the DNA concentration even further, or by improving sensitivity using a sheath flow cuvette, adduct levels below 1 /  $10^8$  nucleotides could be detected.

The 90-mer standard described in this paper has many potential uses in DNA damage research. An improved synthesis procedure using a more homogenous 16-mer (5'-phosphorylated, single BPDE-guanine isomer) would increase the quality of this standard. In addition to providing information on antibody-DNA interactions, it could be used for more accurate calibration of the CE-LIF instrument before and during analysis of DNA samples. An additional application of the standard is the optimization of parameters in the DNA damage assay, including incubation time and temperature of DNA with antibodies as well as capillary electrophoresis conditions such as running buffer composition and pH. The standard also enables the investigation of alternate assay methods, including CE-based competitive immunoassays (Lam et al., 1999; Tao and Kennedy, 1996) using the 90-mer as a fluorescent tracer species. This approach is based on competition between damaged DNA and the fluorescent tracer for the binding sites of a limited amount of antibody. With little or no damaged DNA in a sample, the tracer, in





this case the 90-mer, achieves maximum complex formation with the antibody. As the amount of damaged DNA in the sample mixture increases, the tracer is displaced from the antibody. This would result in an increase in the free 90-mer peak and a decrease in the 90-mer / 8E11 complex peak. This method has been studied in our laboratory by Dr. Woei Tan using oligonucleotide and genomic DNA competitors containing BPDE-damaged sites (Tan et al., 2001). These experiments have shown the expected relationship, indicating that this method may be a suitable alternative to the use of a fluorescent secondary antibody. The fluorescent BPDE-90mer has also been used as a fluorescent probe to study antibody binding stoichiometry (Wang et al., 2001).

Another important aspect of the standard's design is the opportunity to substitute different damage types in the molecule with relative ease. The sequences of the two center oligonucleotides may be changed depending on the desired modification. By inserting these different damaged oligos, a variety of DNA damage detection systems may be investigated using the CE-LIF assay and the corresponding damage standard.

The fluorescent BPDE-90mer standard has proven useful for characterizing antibody binding and for optimizing parameters involved in DNA damage assays. Our research group has since used this standard in a series of studies to address some of the issues described in Chapter 2. Dr. Hailin Wang and Ms. Paula Murphy have now reproduced and improved the assay for BPDE-DNA adducts described previously (Xing et al., 2001). The assay is being used to study adduct formation in human cell lines incubated with BPDE and to study effects of environmental contaminants (such as arsenic) on the repair of DNA damage.



### 3.5 References

- Abbas, A.K., Lichtman, A.H., and Pober, J.S. Cellular and Molecular Immunology, 2<sup>nd</sup> ed. W.B. Saunders Company, Philadelphia, PA (1994).
- Baan, R.A., van den Berg, P.T.M., Watson, W.P., and Smith, R.J. *In situ* detection of DNA adducts formed in cultured cells by benzo(a)pyrene diolepoxide (BPDE), with monoclonal antibodies specific for the BP-deoxyguanosine adduct. *Toxicol Environ Chem* 16:325-339 (1988).
- Beach, A.C. and Gupta, R.C. Human biomonitoring and the <sup>32</sup>P-postlabeling assay. *Carcinogenesis* 13:1053-1074 (1992).
- Booth, E.D., Aston, J.P., van den Berg, P.T.M., Baan, R.A., Riddick, D.A., Wade, L.T., Wright, A.S., and Watson, W.P. Class-specific immunoabsorption purification for polycyclic aromatic hydrocarbon-DNA adducts. *Carcinogenesis* 15:2099-2106 (1994).
- Chen, D.Y. and Dovichi, N.J. Yoctomole detection limit by laser-induced fluorescence in capillary electrophoresis. *J Chromatogr B* 657:265-269 (1994).
- Cosman, M., Ibanez, V., Geactinov, N.E., and Harvey, R.G. Preparation and isolation of adducts in high yield derived from the binding of two benzo[a]pyrene-7,8-dihydroxy-9,10-oxide stereoisomers to the oligonucleotide d(ATATGTATA). *Carcinogenesis* 11:1667-1672 (1990).
- Dickey, C., Santella, R.M., Hattis, D., Tang, D., Hsu, Y., Cooper, T., Young, T.L., and Perera, F.P. Variability in PAH-DNA adduct measurements in peripheral mononuclear cells: implications for quantitative cancer risk assessment. *Risk Analysis* 17:649-656 (1997).
- Edman, L., Mets, U., and Rigler, R. Conformational transitions monitored for single molecules in solution. *Proc Natl Acad Sci USA* 93:6710-6715 (1996).
- Eggeling, C., Fries, J.R., Brand, L., Gunther, R., and Seidel, C.A.M. Monitoring conformational dynamics of a single molecule by selective fluorescence spectroscopy. *Proc Natl Acad Sci USA* 95:1556-1561 (1998).
- Friedberg, E.C., Walker, G.C., and Siede, W. DNA Repair and Mutagenesis. ASM Press, Washington, DC (1995).
- Funk, M., Ponten, I., Seidel, A., and Jernstrom, B. Critical parameters for adduct formation of the carcinogen (+)-*anti*-benzo[a]pyrene-7,8-dihydrodiol 9,10-epoxide with oligonucleotides. *Bioconjugate Chem* 8:310-317 (1997).



- Harlow, E. and Lane, D. Antibodies: A Laboratory Manual. Cold Spring Harbor Laboratory Press, Cold Spring Harbor, NY (1988).
- Hsu, T.M., Liu, T.M., Amin, S., Geactinov, N.E., and Santella, R.M. Determination of stereospecificity of benzo[a]pyrene diolepoxide-DNA antisera with site-specifically modified oligonucleotides. *Carcinogenesis* 16:2263-2265 (1995).
- Kang, D.H., Rothman, N., Poirier, M.C., Greenberg, A., Hsu, C.H., Schwartz, B.S., Baser, M.E., Groopman, J.D., Weston, A., and Strickland, P.T. Interindividual differences in the concentration of 1-hydroxypyrene-glucuronide in urine and polycyclic aromatic hydrocarbon-DNA adducts in peripheral white blood cells after charbroiled beef consumption. *Carcinogenesis* 16:1079-1085 (1995).
- Lam, M.T., Wan, Q.H., Boulet, C.A., and Le, X.C. Competitive immunoassay for staphylococcal enterotoxin A using capillary electrophoresis with laser-induced fluorescence detection. *J Chromatogr A* 853:545-553 (1999).
- Le, X.C., Xing, J.Z., Lee, J., Leadon, S.A., and Weinfeld, M. Inducible repair of thymine glycol detected by an ultrasensitive assay for DNA damage. *Science* 280:1066-1069 (1998).
- Le, X., Scaman, C., Zhang, Y., Zhang, J., Dovichi, N.J., Hindsgaul, O., and Palcic, M.M. Analysis by capillary electrophoresis: laser-induced fluorescence detection of oligosaccharides produced from enzyme reactions. *J Chromatogr A* 716:215-220 (1995).
- Margulis, L.A., Ibanez, V., and Geactinov, N.E. Base-sequence dependence of covalent binding of benzo[a]pyrene diol epoxide to guanine in oligodeoxyribonucleotides. *Chem Res Toxicol* 6:59-63 (1993).
- Poirier, M.C., Santella, R., Weinstein, I.B., Grunberger, D., and Yuspa, S.H. Quantitation of benzo[a]pyrene-deoxyguanosine adducts by radioimmunoassay. *Cancer Res* 40:412-416 (1980).
- Sambrook, J., Fritsch, E.F., and Maniatis, T. *Molecular Cloning: A Laboratory Manual*, 2nd ed. Cold Spring Harbor Laboratory Press, Cold Spring Harbor, NY. 11.31-11.32 (1989).
- Santella, R.M. Immunological methods for detection of carcinogen-DNA damage in humans. *Cancer Epidemiology Biomarkers & Prevention* 8:733-739 (1999).
- Santella, R.M., Perera, F.P., Young, T.L., Zhang, Y.J., Chiamprasert, S., Tang, D., Wang, L.W., Beachman, A., Lin, J.H., and DeLeo, V.A. Polycyclic aromatic hydrocarbon-DNA and protein adducts in coal tar treated patients and controls and their relationship to glutathione S-transferase genotype. *Mutat Res* 334:117-124 (1995).





- Santella, R.M., Lin, C.D., Cleveland, W.L., and Weinstein, I.B. Monoclonal antibodies to DNA modified by a benzo[a]pyrene diol epoxide. *Carcinogenesis* 5:373-377 (1984).
- Seidel, C.A.M., Schulz, A., and Sauer, M.H.M. Nucleobase-specific quenching of fluorescent dyes. 1. Nucleobase one-electron redox potentials and their correlation with static and dynamic quenching efficiencies. *J Phys Chem* 100:5541-5553 (1996).
- Szeliga, J. and Dipple, A. DNA adduct formation by polycyclic aromatic hydrocarbon dihydrodiol epoxides. *Chem Res Toxicol* 11:1-11 (1998).
- Tan, W.G., Carnelley, T.J., Murphy, P., Lee, J., Barker, S., Wang, H., Weinfeld, M., and Le, X.C. Detection of DNA adducts of benzo[a]pyrene using immunoelectrophoresis with laser-induced fluorescence – analysis of A549 cells. *J Chromatogr A*, in press (2001).
- Tao, L. and Kennedy, R.T. On-line competitive immunoassay for insulin based on capillary electrophoresis with laser-induced fluorescence detection. *Anal Chem* 68:3899-3906 (1996).
- Vamosi, G. and Clegg, R.M. The helix-coil transition of DNA duplexes and hairpins observed by multiple fluorescence parameters. *Biochemistry* 37:14300-14316 (1998).
- van Houten, V., Denkers, F., van Dijk, M., van den Brekel, M., and Brakenhoff, R. Labeling efficiency of oligonucleotides by T4 polynucleotide kinase depends on 5'-nucleotide. *Anal Biochem* 265:386-389 (1998).
- Wang, H., Xing, J., Tan, W., Lam, M., Carnelley, T., Weinfeld, M., and Le, X.C. Binding stoichiometry of DNA adducts with antibodies studied by capillary electrophoresis and laser-induced fluorescence. *Anal Chem*, submitted (2001).
- Xing, J.Z., Carnelley, T., Lee, J., Watson, W.P., Booth, E., Weinfeld, M., and Le, X.C. Assay for DNA damage using immunochemical recognition and capillary electrophoresis. In: *Methods in Molecular Biology 162: Capillary Electrophoresis of Nucleic Acids*, Vol. 1: Introduction to the Capillary Electrophoresis of Nucleic Acids (Mitchelson K.R., and Cheng, J. Eds.) pp 419-428. Humana Press Inc., New Jersey (2001).



## Chapter 4: Conclusions and Future Research

### 4.1 Discussion and Conclusions

The objective of this thesis research was to apply the capillary electrophoresis – laser induced fluorescence technique (Le et al., 1998) to the detection of DNA adducts caused by the carcinogen benzo[*a*]pyrene. Analysis of samples containing BPDE adducts produced inconclusive results. Therefore, the main focus of the research was to develop a fluorescent-labeled DNA standard molecule containing a known amount of BPDE adducts to assist in assay development.

Experiments conducted using the fluorescent BPDE-modified oligonucleotide standard were able to explain some of these preliminary results as well as provide additional information. Binding characteristics of different BPDE-DNA antibodies were compared, and 8E11 appeared to give the best result in terms of binding and specificity. It would therefore be the most appropriate antibody for use in future studies. Useful information about optimizing sample preparation procedures, incubation parameters, and electrophoresis conditions was also obtained. This information has since been utilized to improve the DNA damage assay for BPDE adducts. The standard has also been used as a fluorescent probe to investigate binding stoichiometry of BPDE-DNA antibodies (Wang et al., 2001) and to develop competitive immunoassays for detection of BPDE adducts (Tan et al., 2001). The design of the standard will allow easy substitution of different types of DNA damage for future studies.

The capillary electrophoresis DNA damage assay combines specific recognition with high sensitivity, minimal sample preparation, and fast analysis times (<5 minutes per run). It also requires relatively small amounts of DNA and very few reagents. These advantages combined with the potential for automated analysis using commercial capillary electrophoresis instruments suggest that it may be suitable for use in studies of DNA damage in human populations. However, considerable research would be necessary to address the issues associated with using biomarkers in epidemiological studies



(Toniolo et al., 1997). These include: validation of the method through intra- and inter-laboratory comparisons; sample collection, processing and storage techniques; adduct persistence and stability; interpretation of results from surrogate tissues; and epidemiological design issues using biomarkers. Nevertheless, the technique improves upon many of the shortcomings of existing methods and may provide a solid foundation for this type of environmental health research.

DNA repair is an important mechanism in defense against cancer development. The ability to detect DNA damage and repair at clinically and environmentally relevant levels of exposure will help to clarify some questions that remain about low level toxic effects. Currently, it is assumed that molecular mechanisms such as DNA repair behave similarly at high or low level exposures to carcinogens. This assumes the absence of any practical thresholds of effect in these processes. By analyzing these processes directly in human samples, this debate can potentially be resolved. Even if thresholds are not discovered, zero exposure in the environment is an idealistic, unattainable goal. By analyzing very low level human exposures to environmental contaminants in relation to cancer incidence, safe levels of exposure, i.e. no detectable increase in cancer, are likely to be discovered (Hrudey and Krewski, 1995). It is certain that the high sensitivity of this new method will allow better understanding of interindividual susceptibility to DNA adduct formation. This information will need to be considered in risk management decisions, regarding the extent to which the susceptible portion of the population should be protected from exposure to environmental contaminants. These potential outcomes may require the development of new methods for quantitative assessment of human cancer risk from environmental exposure to carcinogens. Human biomonitoring using techniques such as the capillary electrophoresis DNA damage assay will potentially be a vital component of these new initiatives.





## 4.2 Future Research

There are many potential projects that may be pursued to expand on the results of this research. These topics include further work with the fluorescent DNA damage standards as well as continued development of a biomarker for exposure to benzo[*a*]pyrene based on the capillary electrophoresis DNA damage assay.

1. The BPDE-DNA standard should be re-synthesized to improve its performance by addressing the concerns outlined in Chapter 3. This may include synthesis of oligonucleotides with stereospecific BPDE adducts.
2. The DNA damage standard design may be applied to other forms of DNA damage, including oxidative damage or other chemical carcinogens.
3. By using the fluorescent BPDE-DNA standard, the parameters of the DNA damage assay should be investigated further in an attempt to improve the results. Alternatively, the standard may be used to explore other options for quantifying BPDE adduct levels in DNA samples, including CE-based competitive immunoassay methods using the standard as a fluorescent tracer molecule (Tan et al., 2001).
4. Once the best method of measuring BPDE adducts is established, the technique should be validated with DNA samples from cells treated with varying doses of benzo[*a*]pyrene as well as DNA from human samples (lymphocytes or other tissues). After intralaboratory validation of the assay, it should be compared to other techniques to assess its strengths and weaknesses regarding application to human biomonitoring studies.





### 4.3 References

- Hrudey, S.E. and Krewski, D. Is there a safe level of exposure to a carcinogen? *Environ Sci Tech* 29:370A-375A (1995).
- Le, X.C., Xing, J.Z., Lee, J., Leadon, S.A., and Weinfeld, M. Inducible repair of thymine glycol detected by an ultrasensitive assay for DNA damage. *Science* 280:1066-1069 (1998).
- Tan, W.G., Carnelley, T.J., Murphy, P., Lee, J., Barker, S., Wang, H., Weinfeld, M., and Le, X.C. Detection of DNA adducts of benzo[*a*]pyrene using immunoelectrophoresis with laser-induced fluorescence – analysis of A549 cells. *J Chromatogr A*, in press (2001).
- Toniolo, P., Boffetta, P., Shuker, D.E.G., Rothman, N., Hulka, B., and Pearce, N. (eds). *Application of Biomarkers in Cancer Epidemiology: IARC Scientific Publications No. 142*. International Agency for Research on Cancer, Lyon, France, 1997 (318 pp).
- Wang, H., Xing, J., Tan, W., Lam, M., Carnelley, T., Weinfeld, M., and Le, X.C. Binding stoichiometry of DNA adducts with antibodies studied by capillary electrophoresis and laser-induced fluorescence. *Anal Chem*, submitted (2001).

















University of Alberta Library



0 1620 1492 0407

**B45434**